From Past to Present: Impacts of Fire on Amazonian Forests

Submitted by **Laura BARBOSA VEDOVATO**, to the University of Exeter as a thesis for the degree of Doctor of Philosophy in Geography, August 2022.

I certify that all material in this thesis which is not my own work has been identified and that any material that has previously been submitted and approved for the award of a degree by this or any other University has been acknowledged.

Laura B. Vedovato

(Signature) ……

Cite as:

Vedovato, L.B., 2022. From Past to Present: Impacts of Fire on Amazonian Forests. PhD thesis, University of Exeter, Exeter, UK.

Abstract

Amazonian forests have exceptional biodiversity with the highest species richness on Earth, providing vital ecosystem services that regulate carbon and hydrological cycles both regionally and globally. Despite rainforests being a naturally fire-free system, increasing evidence has shown that fires existed in Amazonian forests before European colonization, where its ignition depended on a combination of drought and human activity. Nowadays, anthropogenic actions, such as land-use and land-cover changes, associated to global climate change, increasingly transform these forests into a more fire-prone environment. Fire brings several impacts to tropical forests, transforming these forests into a carbon source, altering forest dynamics, microclimate and forest structure. Despite studies on the impacts of fire on carbon dynamics in Amazonian forests, there is still a knowledge gap in how historical fires impact the current forest dynamics, especially over increased frequency of droughts, and how modern fires affects the vertical canopy structure of primary and secondary forests and their ability to recover from fires. The aim of this thesis is to investigate the impacts of historical and recent fires on current carbon dynamics and forest structure.

In chapter 2, I investigate the effects of historical fires on the current response of forests to drought. For this, I used soil pyrogenic carbon (PyC) as a proxy of historical fires and field-based biomass estimates across the Amazon Basin spanning drought and non-drought years. My results show a strong positive correlation between soil PyC and soil fertility, clay and silt, and a negative correlation between soil PyC and wood density and sand. Furthermore, I found that forests with low concentrations of soil PyC were more impacted by drought. These findings support the hypothesis that soil PyC increases soil fertility and soil water holding capacity, affording higher resistance to drought, whilst also favouring the establishment of species associated with historical disturbances such as fire and drought.

In chapters 3 and 4, I focus on the impacts of recent fires on primary and secondary forests, respectively. Chapter 3 investigates the effects of fire and fire reoccurrences on the canopy structure of primary forests. I used a range of forest structure attributes from airborne lidar data across the Brazilian Amazon. My findings show that forests

that experienced repeated fires experience greater changes after fire and need longer to recover.

In chapter 4, I used lidar data to analyse the impacts of fire on the forest structure of secondary forests. The results show that fires negatively affect canopy structure of secondary forest in early and later successional stages, however, forests in later successional stage have lower potential to recover forest structure after fire than early successional stages.

Overall, the results of this thesis show that the impacts of fire on Amazonian forests affect carbon dynamics and storage, as well as altering forest structure and many related ecosystem services. Impacts caused by fire can be irreversible or may take many decades to fully recover, leaving traces behind after burns which happened centuries ago. My results indicate that forest conservation and management policies should be implemented to avoid fires and protect the long-term future of Amazonian forests.

Acknowledgements

I would like to thanks CAPES, my sponsor in Brazil, for the opportunity to develop this research at the University of Exeter, which added uncountable knowledge and experience in my life over the last few years. This work was also supported by the UK Natural Environment Research Council (NERC NE/N011570/1), CAPES Science without Borders (PVE 177/2012) and SilvaCarbon Fund.

I express my great gratitude to my supervisors Ted Feldpausch and Luiz Aragão. I thank you for all your valuable knowledge that you shared with me and for all the support you have given, especially in the hard moments. Our conversations were always inspiring and helped me in my journey to become a better scientist.

I thank the Sustainable Landscape project and EBA project for their availability of airborne lidar data, which made a considerable part of my research possible. Thank you to forestsplot network and all researchers involved on this, which make possible this fantastic dataset of Amazonian inventory plots.

I am very grateful for all my colleagues and field assistants that helped me during my fieldwork campaigns. Thank you to my supervisor Luiz Aragão for the company on these adventurous field campaigns in Alta Floresta-MT and Tapajós-PA, where we shared many good moments! Thank you Henrique Cassol for the assistance in Alta Floresta and Viola Heinrich for the assistance in Tapajós, and all the local field assistants who were always full of good energy and left really good memories from all these field campaigns! By the way, I am sorry for all the heavy bags full of soils that you help me to carry! Thanks to Erika Berenguer for all the assistance with the logistics in Tapajós and for allowing me to sample soil in your plots. A big thank you to Lola, Carlos (Xarazinho) and Fernanda Santos for all your support on my field campaign in Caxiuanã. I had such great moments and learned a lot by your side in this amazing part of the Amazonian forest! Thank you to all my field assistants in Caxiuanã, whom without I could have not imagined to finish this campaign.

A big thank you to Lidiany Carvalho and Danilo Almeida who gave me incredible support on my PhD journey with so many pieces of constructive advice, and also for the great non-academic conversations whilst sharing a coffee or a beer! Thank you to all the Brazilian and aggregate community - Luciana, Fabio, Thais, Jefferson, Dani,

Paulo, Fernanda, Mateus, Carol, Gustavo, Rosalia, Julieth, Michael and Rosie - for all the good moments shared and bringing a little bit of Brazil to everyday life in Exeter. Thanks also to the Capoeira Society which welcomed me to their group and did not allow me to forget how to “gingar”! A special thank you to my boyfriend and my favourite person, David. Thank you for celebrating each little victory with me and also for holding my hand every time I thought this journey was unreachable. Having you by my side gave me strength to keep going until now. Finally, I thank my family for always supporting my choices, even when it meant crossing an ocean to live apart for years, in a place that I have never been and where I didn’t know anyone. Thank you for believing in me and for sending your love throughout my PhD journey.

Some of the many people that helped me throughout my field campaigns. Many thanks!

This thesis is dedicated to the memory of my grandfather,
Alberto Vedovato,
who was an example of strength and perseverance to me.

Table of Contents

List of Tables

List of Figures

Abbreviations

^{14}C	Carbon-14
ACD	Aboveground Carbon Density
ADE	Amazon Dark Earth
AGB	Aboveground biomass
AGC	Aboveground carbon
AICc	corrected Akaike Information Criterion
AMS	Accelerator Mass Spectrometry
BP	Before Present
Ca	Calcium
CHIRPS	Climate Hazards Group InfraRed Precipitation with Stations
CHM	Canopy Height Model
CO_2	Carbon Dioxide
CWD	Cumulative Water Deficit
DBH	Diameter at Breast Height
DEM	Digital Model of Elevation
DSM	Digital Surface Model
DTM	Digital Terrain Model
ES	Early Successional
GEDI	Global Ecosystem Dynamics Investigation
GLMM	Generalized Linear Mixed Effects Model
GPS	Global Positioning System
HyPy	Hydrogen Pyrolysis
K	Potassium
LAD	Leaf Area Density
LAHV	Leaf Area Height Volume
LAI	Leaf Area Index
Lidar	Light Detection and Ranging
LS	Later Successional
MCWD	Maximum Cumulative Water Deficit
Mg	Magnesium
MRT	Mean Residence Time

OC	non-PyC fraction of Organic Carbon
P	Phosphorus
PCA	Principal Component Analysis
PyC	Pyrogenic Carbon
SLA	Specific Leaf Area
SMA	Standardised Major Axis regression
SOC	Soil Organic Carbon
TOC	Total Organic Carbon
YSLF	Years Since Last Fire

Chapter 1: General Introduction

National Forest of Tapajós, PA, Brazil

1.1 Amazonian forests

The Amazon forest spans approximately 6 million km^2, and represents the largest and most biodiverse of global tropical forests, containing about a quarter of all global terrestrial species (Field *et al.*, 1998). Tropical forests provide many ecosystem services such as controlling precipitation regimes (Salati & Vose, 1986; Avissar & Werth, 2005; Langenbrunner *et al.*, 2019) and regulating the global carbon cycle. Tropical forests store 55% of the carbon found globally in forests and contribute to the carbon sink at approximately 2.4 ± 0.4 Pg C yr^{-1} (Pan *et al.*, 2011). Across the Amazon Basin, forests are not uniform, but instead have variable temperature and precipitation regimes, species composition, and physical and chemical soil properties (Fyllas *et al.*, 2009; Quesada *et al.*, 2012). These differences have significant impacts on their carbon cycle. For example, across the large soil fertility gradient from the West (near Andes) to the East, aboveground carbon stocks increase but productivity declines (Quesada *et al.*, 2012). The capacity of tropical forests to store and sequester carbon is, however, in decline because of climate change, land conversion and other anthropogenic influences such as deforestation and fires (Harris *et al.*, 2012; Brienen *et al.*, 2015; Hubau *et al.*, 2020). Understanding the effects of anthropogenic disturbances on tropical forests is important when predicting the future carbon and water cycles, and for conservation planning, which directly and indirectly impacts all ecosystems.

1.2 Primary and secondary forests

Across the Amazon, ~88% of old-growth forests have not experienced clear-cutting in recent history (35 years) and exist as intact or primary forests (MapBiomas, 2021). In contrast, secondary forests, forests which have experienced clearance and regrowth, comprise ~4% of Amazonian forests (Heinrich *et al.*, 2021). Major differences exist between primary and secondary forests in biomass, forest structure and plant function, which I outline in this section.

1.2.1 Biomass and carbon sequestration

Primary forests have higher aboveground biomass (AGB) stocks because these forests are formed by tree species with high wood density, large diameter stems and tall trees (Chave *et al.*, 2005). However, this high AGB stock is unevenly distributed across the Amazon Basin (Quesada *et al.*, 2012). Forests with higher AGB are concentrated in the Eastern region of the Amazon, where soils have low fertility (Quesada *et al.*, 2012) and forests have slower dynamics (Phillips *et al.*, 2004), creating conditions for taller trees (Feldpausch *et al.*, 2011) that hold more biomass (Feldpausch *et al.*, 2012). Soils rich in nutrients may play an important role in explaining the almost double rates of stem turnover in the Western and Central areas compared with the Eastern Amazon (Phillips *et al.*, 2004; Stephenson & van Mantgem, 2005; Aragão *et al.*, 2009).

When tree growth and recruitment exceed tree mortality, forests act as a net aboveground carbon sink, having the ability to convert about 15% of anthropogenic CO_2 emissions into biomass (Phillips et al. 2008). However, a long-term declining trend of carbon accumulation has been observed in recent decades (Brienen *et al.*, 2015; Hubau *et al.*, 2020) when compared to the 1990s, the rate of net increase in aboveground biomass has declined by one-third (Brienen *et al.*, 2015). This is because growth rates have levelled off at the same time as an increase in the mortality rate, leading to a shorter carbon residence time (Brienen *et al.*, 2015). Tree mortality is mainly driven by the interaction between species traits and the environment, which results in physiological failure or structural damage that causes death (Franklin *et al.*, 1987; McDowell *et al.*, 2018). Tree death caused by physiological failures is related to senescence, stress caused by light competition and moisture, or hydraulic failure due to water transport difficulties (McDowell, 2011; Rowland *et al.*, 2015). Tree mortality caused by structural failure has been more dominant in Western regions of Amazonia, where soils are more fertile, and trees invest more in growth than wood structure (Chao *et al.*, 2009). Growth rates are an important factor when predicting tree death, with faster-growing species having a higher risk of death (Esquivel-Muelbert *et al.*, 2020). Tree species with slower growth rates tend to have higher wood density, investing in defence and structure and consequently are expected to have lower rates of mortality (Coelho de Souza *et al.*, 2016).

In the Brazilian Amazon, secondary forests are mainly located in the South-East region and span the Arc of Deforestation (Smith *et al.*, 2020). Regrowth of secondary forests is highly dependent on climatic conditions, having slow carbon accumulation with intense dry seasons and lower annual rainfall (Poorter *et al.*, 2016). The historical land use of secondary forests also determines their regrowth rate, with the intensity of land use, frequency and duration of land degradation and type of management practices interfering in the recovery of these areas (Jakovac *et al.*, 2021). Secondary forests growing on abandoned cropland have faster carbon accumulation rates than those growing on abandoned pastures (Fearnside & Guimaraes, 1996). Secondary forest regrowth in areas that experienced a high number of slash-and-burn cycles or shifting cultivation, in contrast, have the slowest rates of carbon accumulation (Jakovac *et al.*, 2015; Heinrich *et al.*, 2021). The rate of carbon accumulation also changes between successional stages. Aboveground biomass accumulation rates in young secondary forests (≤ 20 years) are 5.9 ± 0.8 Mg ha^{-1} $year^{-1}$, while in older secondary forests (> 20 years) this rate decreases to 2.3 ± 0.3 Mg ha^{-1} $year^{-1}$ (Requena Suarez *et al.*, 2019). The rate of AGB accumulation likely decreases with succession because later successional stage forests have lower productivity. Moreover, AGB is one of the slowest attributes to fully recover in secondary forests, because it is predominantly driven by large trees (Poorter *et al.*, 2016; Poorter *et al.*, 2021). Despite this, Amazonian secondary forests had a substantial carbon stock of 294 Tg in 2017 (Heinrich *et al.*, 2021). However, secondary forests are vulnerable to droughts and fire, which leads to increased mortality rates in these forests and consequently carbon emissions to the atmosphere (Berenguer *et al.*, 2018b; Rappaport *et al.*, 2018).

1.2.2 Forest structure

Besides different AGB stocks and rates of AGB gain, primary and secondary forests also have differences in canopy structure. Primary forests normally have higher mean canopy heights and also fewer canopy gaps than secondary forests (Almeida *et al.*, 2016; Sato *et al.*, 2016). The tallest trees in Amazonia are found in primary forests. However, their distribution is not equal, driven instead by wind, light availability, precipitation and temperature (Gorgens *et al.*, 2021). Leaf area index (LAI) is also higher in primary forests because of a more complex canopy structure with more

vertical strata than secondary forests (Chazdon & Pearcy, 1991; Feldpausch *et al.*, 2005; Brando *et al.*, 2014). Primary forests also present a less dense understory, except in canopy gaps, because greater shade levels produced by higher LAI in these forests are not suitable for the establishment of shade-intolerant pioneer species that grow in the understory (De Frenne *et al.*, 2021). These pioneer species are more dominant, however, in secondary forests in early successional stages. This results in different canopy structures as pioneer species become replaced by later successional species. Not all secondary forests follow the same successional pathway, but it is typically linked to the previous land-use and locality (Mesquita *et al.*, 2001; Jakovac *et al.*, 2021). Over succession, canopy structure may change and later successional stage forests begin to become more similar to primary old-growth forests (Poorter *et al.*, 2016).

1.2.3. Functional composition

Primary and secondary forests also possess different species composition that present different functional strategies. A spectrum of functional traits exists within trees, as species trade-off between fast growth rates and high survival rates (Salguero-Gómez *et al.*, 2016), including resistance to fire and drought (Brando *et al.*, 2012; Rowland *et al.*, 2015; Barros *et al.*, 2019; Bittencourt *et al.*, 2020). Tropical forests support a wide range of functional strategies as species adapt to a range of conditions. In primary forests, a wide diversity of functional strategies exists as species partition their environmental niche to avoid competition (Ricklefs, 1977; John *et al.*, 2007; Oliveira *et al.*, 2019). Functional strategies are not limited to the overall life history strategy, but also exist at the organ level, including the leaf economic and wood economic spectrum (Wright *et al.*, 2004; Chave *et al.*, 2009). Fast growing species typically have low wood density and acquisitive leaves with high specific leaf area, low herbivory resistance and short leaf longevity (Wright *et al.*, 2004; Chave *et al.*, 2009). Soil nutrient availability is an important determinant of where species are found along the leaf and wood economic spectra (Coomes *et al.*, 2009; Ordoñez *et al.*, 2009; Quesada *et al.*, 2012; Bartholomew *et al.*, 2022). Given the gradient in soil nutrients across the Amazon Basin, the nutrient-rich soils of the West typically support more acquisitive species with a faster life-history strategy, whilst the nutrient-poor East

supports more conservative strategies that favour survival (Ordoñez *et al.*, 2009; Quesada *et al.*, 2012). Consequently, there is a gradient in plant functional traits across the Amazon Basin, with higher wood density and lower specific leaf area (SLA) in the nutrient-poor East compared with the nutrient-rich West. Functional traits of trees that are adapted to low nutrient availability are also typically traits that promote greater drought and fire resistance (Pellegrini *et al.*, 2021). Consequently, forests in the East Amazon are more likely to be pre-adapted to deal with these emerging stresses than species with a faster life-history strategy in the West Amazon.

In secondary forests, a filtering of plant functional traits occurs because of their more extreme environment. In the highly open canopies of secondary forests, functional strategies are restricted to those that favour growth over survival, as conservative strategies that favour survival are quickly outcompeted. Pioneer species are typically found towards the more acquisitive end of the plant economics spectrum, growing fast and optimising the use of the readily available resources, such as high photosynthetic capacity to optimise the use of light (Wright *et al.*, 2004) and traits that allow them to compete for nutrients, such as nitrogen-fixation (Batterman *et al.*, 2013). As succession occurs in secondary forests, the canopy begins to close and light in the understory becomes more limiting. Therefore, more shade-tolerant, conservative species can establish as they can compete more effectively for light in a darker environment (Denslow *et al.*, 2019). As a consequence of the shift in community composition, there is a shift in the community average of plant functional traits with secondary forest succession, with wood density increasing and specific leaf area decreasing (Poorter *et al.*, 2021). Given the link between more conservative traits and resistance to drought and fire, later successional stage secondary forests may be more able to resist these stresses.

1.3 Fires in the Amazon

1.3.1 Historical fires

The historical fire regime of the Amazon has been identified through ^{14}C radiocarbon dating of charcoal using an Accelerator Mass Spectrometry (AMS). The pattern of fire occurrence in the last millennium can even affect wetlands, and there are still trees

surviving from these historical fire events (McMichael *et al.*, 2012; Power *et al.*, 2012). The origin of these historical fires is associated with climatic variation and/or land use in Pre-Columbian times (Denevan, 1992; Bush & Silman, 2007). Many of these areas were occupied by humans as evidenced by domesticated tree species, artefacts, and Anthropogenic Dark Earth soil (*Terra Preta de Índio*) (Clement, 1999; Petersen *et al.*, 2001; Neves *et al.*, 2003; Neves *et al.*, 2004; de Oliveira *et al.*, 2020).

Evidence suggests that past human activities influenced the floristic composition and structure of Amazonian forests (de Oliveira *et al.*, 2020). Levis *et al.* (2017) found a significantly higher abundance and richness of domesticated species in South-Western Amazonian forests, followed by North-Western, Southern and Eastern Amazonia. Forests closer to archaeological sites or rivers also have a richer assemblage of domesticated species than forests elsewhere (Figure 1.1). Up to 50% of the variation in the abundance, relative abundance, richness and relative richness of domesticated species in southwestern and eastern regions can be explained exclusively by human influence (Levis *et al.*, 2017).

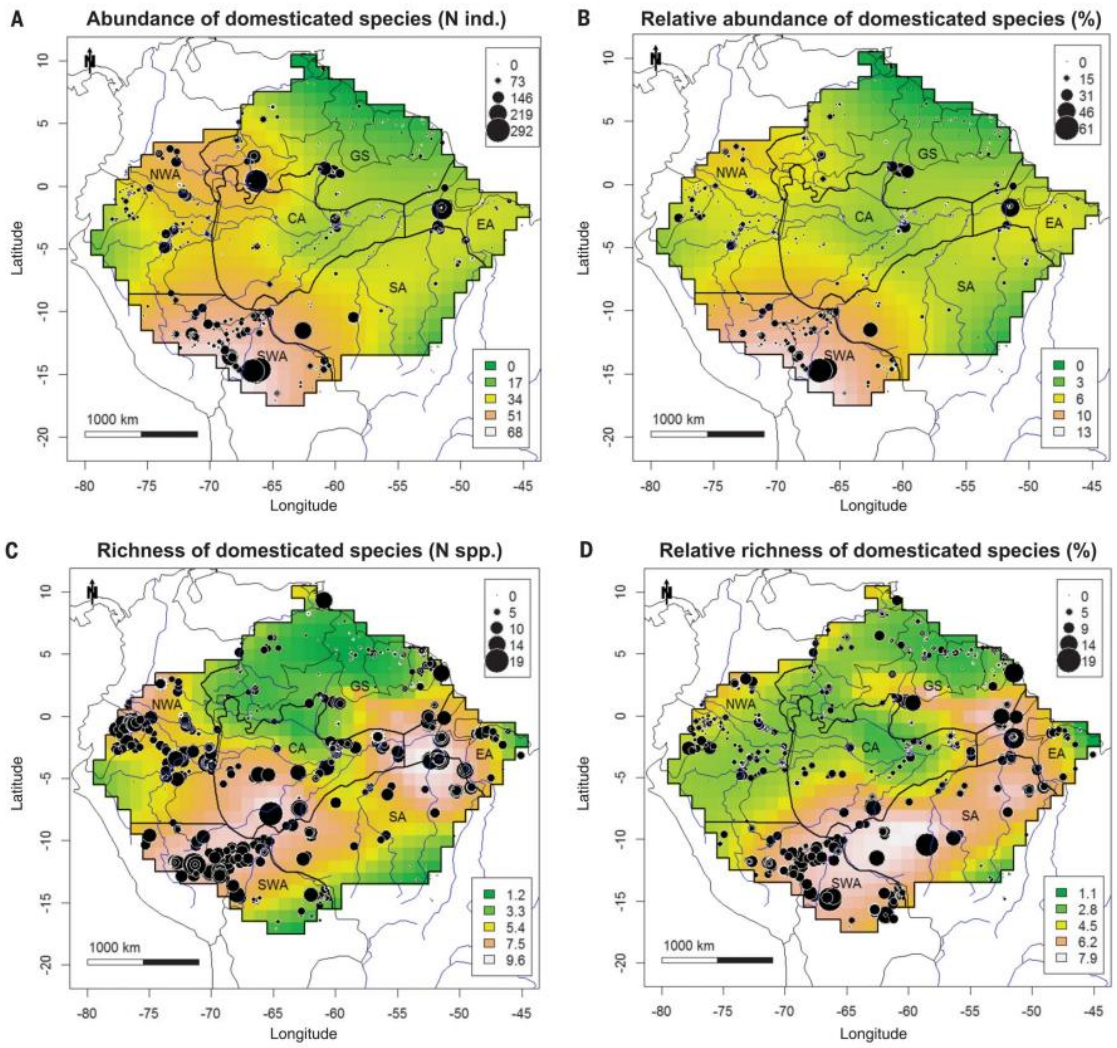

Figure 1.1. Spatial variation of 85 domesticated species across Amazonia. (A to D) Maps showing (A) the spatial variation of the total number of individuals of domesticated species (abundance) per hectare (ha), (B) the relative abundance of domesticated species, (C) the total number of domesticated species (richness) per plot, and (D) the relative richness of domesticated species in lowland plots in six geological regions of Amazonia (NWA, northwestern Amazonia; SWA, southwestern Amazonia; SA, southern Amazonia; CA, central Amazonia; GS, Guiana Shield; and EA, eastern Amazonia). Black circles show the observed values of absolute abundance (A) and relative abundance (B), ranging from 0 to 292 individuals of domesticated species per 1 ha and 0 to 61% of the total number of individuals, and the observed values of absolute richness (C) and relative richness (D), ranging from 0 to 19 domesticated species per plot and 0 to 19% of the total number of species. The white-green background shows the interpolation of the observed values (in percent) in each plot modeled as a function of latitude and longitude on a 1°-grid cell scale by use of loess spatial interpolation.

Source: Levis et al. (2017)

Soil charcoal dated in the Amazon is concentrated between 2,700 and 500 years BP Goulart et al. (2017), with the oldest charcoals found in Eastern Amazonia (Belterra, Pará) with 7,759-7,585 cal years BP and the most recent in central Amazonia (Careiro, Amazonas) with 472-311 cal years BP (Goulart *et al.*, 2017). In another study, Santos *et al.* (2000) performed soil charcoal dating in central Brazilian Amazon and found the ages of charcoal vary between 130 to 2,400 years, but mostly between 1,200 and 1,400 years BP. These charcoal dating have been associated with human occupation, mainly following the course of rivers and with dry periods during the Holocene in the Amazon region (Sanford *et al.*, 1985; Denevan, 1996; Pessenda *et al.*, 1998; Neves *et al.*, 2003; Neves *et al.*, 2004). In a more recent study across Amazonia, fire history also spans 11,500 cal years BP, showing a peak in fire records preceding the Columbian Encounter (Feldpausch *et al.*, 2022) (Figure 1.2). Charcoal radiocarbon dating analysis shows that at some sites the maximum fire return time interval was shorter than the time since last fire, suggesting that in the last ~800 years these forests had gone a longer period without fire occurrences than in the past 2,000-3,500 years (Feldpausch *et al.*, 2022).

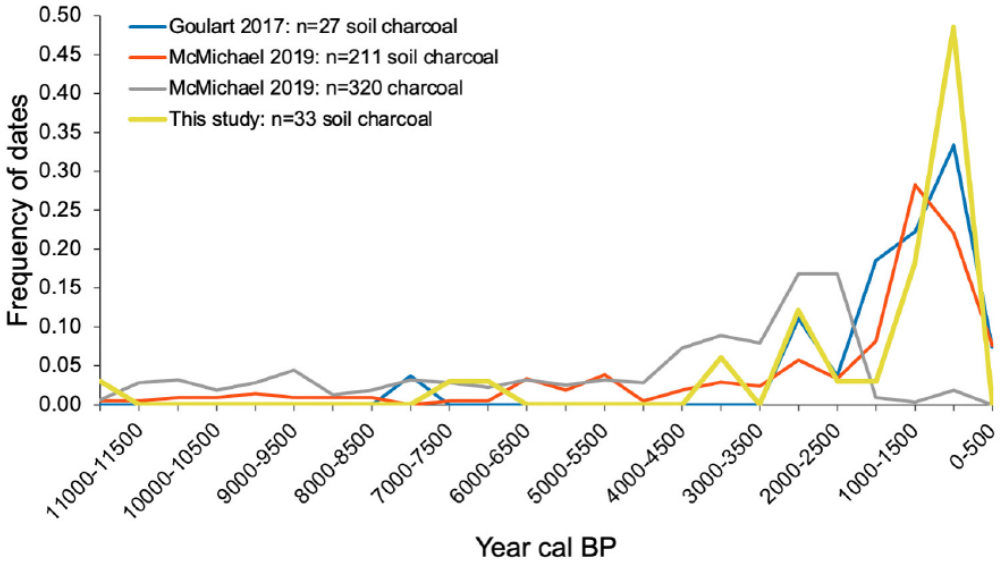

Figure 1.2. Frequency of dates from charcoal and soil charcoal by years calibrated before present (BP) in fraction of total dates per study from Goulart *et al.* 2017, compilations by McMichael and Bush, 2019, and Feldpausch, 2022.

Source: Adapted from Feldpausch *et al.* 2022

The use of fire in the Amazon as a tool for forest management and domestic use was very common for the first human civilizations (Denevan, 1992). Fire escaping from the controlled boundaries and spreading through the forest (Sanford *et al.*, 1985) had become very frequent throughout the Basin (Zarin *et al.*, 2005; Balch *et al.*, 2008) and has left a considerable amount of charcoal and pyrogenic carbon in the soil (Pivello, 2011; Koele *et al.*, 2017; da Silva Carvalho *et al.*, 2018).

Despite historical fires causing tree mortality, damage to vegetation and reductions in carbon stocks, fire may also increase forest productivity by producing pyrogenic carbon (PyC), which increases soil fertility, improves water holding capacity, decreases aluminium toxicity and improves cations exchange capacity in the soil (Glaser *et al.*, 2000; Glaser *et al.*, 2001). Therefore, initial slow forest regeneration may be compensated later by higher forest productivity that owes to the effects of soil PyC (Glaser *et al.*, 2002; Cheng *et al.*, 2008).

Pyrogenic carbon is a thermochemically altered (pyrolysed) carbon originated from biomass and fossil fuel burning that has incomplete combustion of organic matter (Bird *et al.*, 2015). It is produced at temperatures between 400˚C to 600˚C (Miranda *et al.*, 1993; Saiz *et al.*, 2014; Saiz *et al.*, 2015) and it can be found in the atmosphere, soils, sediments, ice, terrestrial water bodies and the oceans (Schmidt & Noack, 2000). Since there has been enough oxygen on Earth to sustain a combustion process, PyC has been produced, which is recorded to up 420 Myr ago (Scott & Glasspool, 2006). Due its recalcitrant characteristic, PyC has a mean residence time (MRT) in a range of 700 to 9,000 years (Lehmann *et al.*, 2008). However, as PyC is formed by high temperatures and depends on existing biomass, it could also be interpreted as a proxy for fire severity. Some research shows that PyC is a dominant component in the global carbon cycle (Preston & Schmidt, 2006; Lehmann *et al.*, 2008; Bird *et al.*, 2015) and can represent more than 30% of total soil organic carbon (SOC) (Reisser *et al.*, 2016). Moreover, PyC can act as an important proxy of past fire disturbances (Rehn *et al.*, 2021).

In Amazonia, there is a large soil fertility gradient (higher in the west near the Andes) that affects carbon stocks and forest productivity (Quesada *et al.*, 2012). Despite this knowledge, it is not yet known whether PyC can contribute to the large basin-scale variation in forest productivity. Currently, PyC has been mainly studied in areas of

Anthropogenic Dark Earth and biochar (deliberate production of PyC) additions in agriculture.

A study from southern Amazonia found that PyC can significantly and positively affect soil fertility but found no relationship with species richness. In areas with high concentrations of PyC in the soil, such as in Anthropogenic Dark Earth, there was significantly higher biomass and species composition. There is also a positive correlation between PyC and clay content in soils and a negative correlation with soil sand content. Therefore, soil clay content and forest aboveground biomass can contribute to explaining the PyC content of soils (Oliveira, 2017).

There have been few studies of the spatial distribution of PyC in the Amazon. Koele et al. (2017) analysed 37 plots across the Amazon Basin and estimated a PyC stock of 1.10 Pg over 0-30 cm soil depth (1.44 Mg PyC ha^{-1}), and 2.76 Pg over 0-100 cm soil depth (3.62 Mg PyC ha^{-1}). When analysed by depth, they found a gradient in the average concentration of PyC, with the highest concentration of PyC situated in the surface layers, with the values of 0.76 g kg^{-1} for the 0-5 cm depth, 0.63 g kg^{-1} for the 5-10 cm depth, 0.52 g kg^{-1} for the 30-50 cm depth, 0.41 g kg^{-1} for the 50-100 cm depth and 0.28 g kg^{-1} for 150-200 cm depth (Figure 1.3).

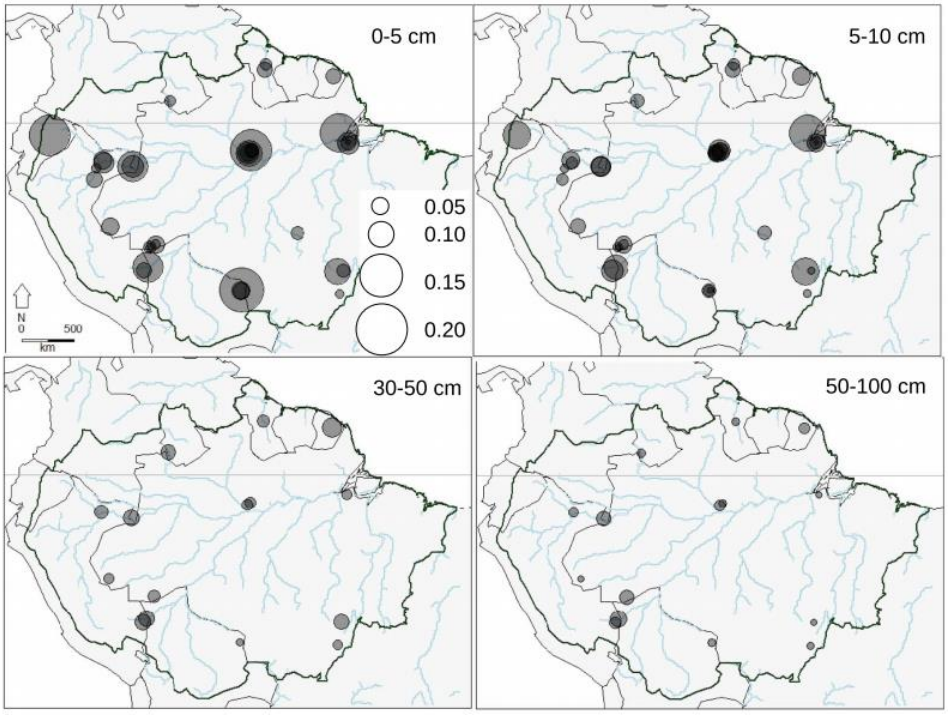

Figure 1.3. Spatial variability of PyC in 0–5 cm, 5-10 cm, 30-50 cm and 50-100 cm, in 37 one hectare forest plots, with no known recent fire or anthropogenic disturbance, sampled in the Amazon Basin. Points are scaled to the amount of PyC in percentage. Symbols are semi-transparent to allow visualization when overlapping.
Source: Koele et al. (2017)

Information on PyC stocks throughout the Amazon Basin acts as another metric of past fires, and together with charcoal radiocarbon dating, it will help to identify the occurrence and effects of the last fire disturbance, contributing to a better understanding of the functional and structural dynamics of the Amazonian forest. Greater knowledge of post-fire effects can improve estimates of the future of the carbon sink and the ability of forests to respond to future fire events. For example, if the long-term carbon sink is partially driven by recovery from past disturbance or PyC fertilization, then the strength of CO_2 fertilization effects on the carbon sink may be overestimated.

1.3.2 Recent fires

Tropical forests are not a fire-prone environment since they have high annual precipitation and closed canopies leading to a humid understory. Therefore, most fires in these forests are from anthropogenic sources that are mainly related to activities

such as land use changes. Because of the high humidity, fires in tropical forests are primarily understory fires and predominantly occur during severe droughts (Alencar *et al.*, 2006), when dry litter and dry accumulated woody biomass on the ground act as fuel and carry fire. These fires can weaken trees by charring stems, leading to post-burn tree mortality (Balch *et al.*, 2011). Consequently, canopy gaps are created, generating a drier microclimate that transforms the forest into an environment that is more susceptible to future fire disturbances. Tree species in tropical rainforests are poorly adapted to fire with thin bark, low wood density and small diameter trees being at greater risk of mortality (Brando *et al.*, 2012).

Recent fires are become more frequent and are closely related to deforestation and the increasing frequency and intensity of droughts in Amazonia (Silva Junior *et al.*, 2019). Between 1998 and 2020 the number of fires in the Brazilian Amazon increased 74% (INPE, 2021). Forest degradation and fragmentation are also strongly linked to fire occurrences because they generate a drier microclimate (Bullock *et al.*, 2020; Silva Junior *et al.*, 2020b). During the 2015/2016 drought in Amazonia, the extension of burned forest areas in the Brazilian Amazon reached 9,246 Km^2 which represented ~ 25% of all burned areas in that period (Silva Junior *et al.*, 2019). Forests affected by fires store 25% less biomass than adjacent unburned forests even 31 years after the fire event (Silva *et al.*, 2018). Another study in Eastern Amazonia found that five years after fire, forests still have 23% less biomass stocks than unburned areas (Sato *et al.*, 2016). Delayed losses of biomass driven by tree mortality are estimated to occur from 3 to 8 years after the fire (Barlow *et al.*, 2003b; Berenguer *et al.*, 2021), but can persist for at least three decades, as a result of mortality of large trees (> 50 cm DBH) with high wood density (Silva *et al.*, 2018). The increase in the rate of fires in the last decade has led to uncertainties in carbon emission estimates, since the gross emissions by fire during drought years (989 ± 504 Tg CO_2 $year^{-1}$) correspond to more than half of the emissions from old-growth forest deforestation (Aragão *et al.*, 2018).

In addition to the negative impact on biomass stocks in Amazonian forests, fire can also affect the vertical structure of the forests. However, few studies have addressed this impact on Amazonian forests and are restricted in spatial coverage (Almeida *et al.*, 2016; Sato *et al.*, 2016; Rappaport *et al.*, 2018). In the Rio Negro basin, burned forests had 16% lower maximum height and 166% more gap fractions than surrounding unburned areas (Almeida *et al.*, 2016). Meanwhile, in western Amazonia,

forest height after fires was not able to recover within 10 years (Sato *et al.*, 2016). The length of time for the recovery of the vertical canopy structure after fire still needs to be explored further to assess whether these patterns extend to the whole of Amazonia. Leaf area index (LAI) is another attribute that decreases with fire (Brando *et al.*, 2014), allowing an increase in solar radiation and, consequently, a drier and hotter understory. These changes in the understory microclimate transform the forest to become more susceptible to fire reoccurrences, arresting the succession process in these forests (Mata *et al.*, 2022). Therefore, fire impacts can lead to long-term changes in carbon stocks and forest structure (Rappaport *et al.*, 2018; Silva Junior *et al.*, 2018).

1.4 Drought in Amazonian forests

The frequency of drought events in Amazonian forests is increasing and has been estimated to reoccur on average each 5 years (Panisset *et al.*, 2018). Droughts can be caused by natural processes related to changes in sea surface temperature, e.g., the Atlantic Multidecadal Oscillation, the El Nino Southern Oscillation and the Pacific Decadal Oscillation (Marengo & Espinoza, 2016; Aragão *et al.*, 2018). However, changes in patterns of large-scale atmospheric circulation caused by anthropogenic action such as land-use and land-cover changes may exacerbate the intensity of droughts (Spracklen & Garcia-Carreras, 2015; Llopart *et al.*, 2018). Climate change is predicted to increase the frequency, intensity, and length of droughts in Amazonia (Malhi *et al.*, 2008; Bonini *et al.*, 2014). The carbon sink of Amazonian forests diminishes during droughts as photosynthesis and net productivity decrease, and tree mortality caused by the direct effect of droughts and by the indirect effect of understory fires increases (Phillips *et al.*, 2010; Brando *et al.*, 2014; Gatti *et al.*, 2014; Rowland *et al.*, 2015; Bonal *et al.*, 2016).

In the extreme drought of 2015/2016, 46% of the Brazilian Amazon biome was under severe hydric stress, which led to a decrease in the photosynthetic capacity and changes in canopy structure (Anderson *et al.*, 2018). In 2005, western Amazonia experienced a strong water deficit which resulted in a decline in canopy structure and moisture. Despite the gradual recovery in total rainfall in the following years, these attributes did not fully recovery within 4 years, suggesting the reoccurrence of drought in Amazonia will lead to persistent changes in forest structure (Saatchi *et al.*, 2013).

Another drought in 2010 also negatively impacted growth rates in Amazonian forests (Feldpausch *et al.*, 2016).

Large trees are more affected in growth and mortality rates during droughts than smaller trees (Phillips *et al.*, 2010; Bennett *et al.*, 2015; Rowland *et al.*, 2015). This higher sensitivity of large trees to drought is likely driven by greater vulnerability to hydraulic stress (Ryan *et al.*, 2006; McDowell, 2011; Rowland *et al.*, 2015; Bittencourt *et al.*, 2020), higher radiation and evaporative demand on exposed crowns (Roberts *et al.*, 1990; Nepstad *et al.*, 2007). The mortality of these large trees can cause great negative impacts on carbon storage (Rowland *et al.*, 2015), and because they play important roles in forests as keystone species (Lindenmayer *et al.*, 2012). The loss of the large trees can thus cause changes to the microenvironment, soil nutrient availability, local hydrological regimes, food abundance in form of fruits, seeds, flowers, foliage and nectar for several organisms (Lindenmayer *et al.*, 2012). Large tree mortality also opens gaps in the canopy, leading to a dry understory and consequently an increase in the susceptibility of these forests to fire. This increase in drought frequency then also leads to an increase in fire occurrence, with consequences for future forest dynamics and climate change.

1.5 Forest monitoring using field measurements and remote sensing

1.5.1 Field measurements

Field measurements are used to quantify carbons stocks, forest structure and wood volume. Overall, these measurements are made in a delimited sample of the forest, the forest plot (e.g. 1 ha), where all living trees, palms and lianas are censused by measuring their diameter at breast height (DBH), which typically corresponds to 1.3 m from the ground (Phillips *et al.*, 2009b). Tree attributes including DBH, tree height, wood density and taxonomic information are measured and used to calculate several plot-level metrics such as the number of individuals or stems (n ha^{-1}) – stem density; total basal area of all stems (m^2 ha^{-1}); wood volume (m^3 ha^{-1}); and the total aboveground live biomass (Mg ha^{-1}), the AGB (Souza & Soares, 2013). These data measured in the field, especially AGB, are used in regression models, spatial interpolation techniques and in combination with remote sensing datasets to upscale

its spatial distribution to larger areas. In general, AGB data is obtained by allometric AGB equations and from destructive sampling methods. The destructive sampling method is considered the most accurate approach (Lu *et al.*, 2016), whereby trees are felled and cut, the wet weight is estimated, and then a subset is dried and weighed to convert to dry biomass (Soares *et al.*, 2011). From this highly laborious approach, it is possible to derive allometric regression equations for AGB estimation from individual tree attributes such as DBH, crown diameter and total tree height (Soares *et al.*, 2011). However, allometric regressions are specific to their environmental conditions from their reference data (Lu *et al.*, 2016), such as forest and soil types.

Frequent forest recensuses, usually in permanent plots (Phillips *et al.*, 2009b; Davies *et al.*, 2021), allow investigation of temporal changes in species composition, forest structure, wood volume and biomass (Souza & Soares, 2013). Some metrics usually analysed refer to growth, recruitment, mortality and net change rates, which are often calculated in terms of biomass or carbon in ecological studies (Phillips *et al.*, 2009a). Forest plots are not just important for understanding biomass and forest structure, but can also reveal important information about soil, other components of carbon budget and species interactions. The infrastructure generated by permanent research plots also provides a platform for detailed functional trait studies (Davies *et al.*, 2021; ForestPlots.net *et al.*, 2021; Malhi *et al.*, 2021).

1.5.2 Remote sensing

Forests can also be monitored by a range of remote sensing technologies, including passive and active technologies. One increasingly common active remote sensing technology is Light Detection and Ranging (lidar). I focus on this technology here as it is the basis of this thesis.

Lidar was developed after World War II and evolved quickly in 1960 with the invention of the laser system (Carter *et al.*, 2012; Hassebo, 2012). The first aim of lidar was to topographically map and develop a Digital Model of Elevation (DEM) with a high level of accuracy in areas that were difficult to access (Wagner *et al.*, 2004; Giongo *et al.*, 2010). In forest applications, lidar can provide accurate measurements of forest structure and carbon stocks over large areas (Lu, 2006; Stark *et al.*, 2012; Rappaport *et al.*, 2018), allowing the evaluation of forest changes after environmental

disturbances (Andersen *et al.*, 2014; Leitold *et al.*, 2018). Lidar is a laser scanning technology and works by emitting sheaves of laser (generally in near-infrared band - 0.9 to 1.1 μm) directed to the surface, computing the distance between the sensor and the target (Lefsky *et al.*, 2002). Lidar sensors are coupled to inertial navigation systems and global positioning system (GPS) receivers on airborne platforms, to record data across large areas (van Leeuwen & Nieuwenhuis, 2010) (Figure 1.4).

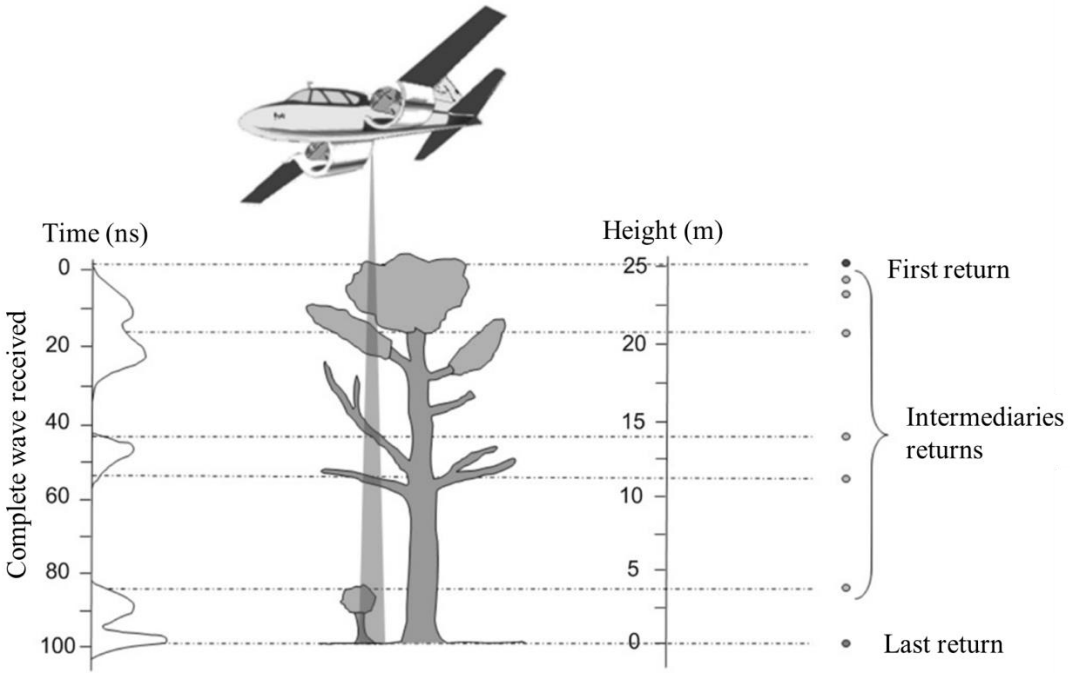

Figure 1.4. Principles and components of an airborne handling system.
Source: Adapted from Giongo *et al.* 2010.

Lidar sensors have two main data processing possibilities. The first is discrete-return, which is when the return signal identifies one or a small number of major peaks representing objects in the laser path. Most studies of forests in Amazonia use the discrete return method with small footprints. The second type is known as full-waveform, which records and reconstructs the entire reflected signal (Lefsky *et al.*, 2002; Ullrich & Pfennigbauer, 2011). This method can provide a more complete three-dimensional representation of the forest canopy (Ullrich & Pfennigbauer, 2011; Anderson *et al.*, 2016), but also demands higher computational power and generates a large volume of data due to its greater complexity (Anderson *et al.*, 2016). New tools are being developed to facilitate the processing of full-waveform lidar data (Zhou & Popescu, 2019). Moreover, recently, a satellite-based full-waveform lidar system has been placed in orbit, developed specifically for forest and ecosystem studies - the

Global Ecosystem Dynamics Investigation (GEDI). GEDI will allow understanding of vertical canopy structure variations to advance rapidly in the coming decades (Dubayah *et al.*, 2020).

Many studies have used lidar to monitor forest structure dynamics in the Amazon e.g. (Andersen *et al.*, 2014; Leitold *et al.*, 2018; Dalagnol *et al.*, 2019; de Almeida *et al.*, 2020; Moura *et al.*, 2020), but few studies have addressed the impacts of fire on canopy structure (Almeida *et al.*, 2016; Sato *et al.*, 2016; Rappaport *et al.*, 2018). To generate models to estimate AGB from lidar, it is common to use reference data from permanent forest plot inventories. With these data, it is possible to calibrate regression models between AGB and lidar return point metrics, normalized by the DEM (Andersen *et al.*, 2014; Longo *et al.*, 2016; Silva *et al.*, 2017). Longo *et al.* (2016) calibrated their model using 407 plots across the Amazon Basin, comprising old-growth areas and areas disturbed by fire and selective logging. Their research comprised several lidar overflights, conducted with similar parameterization, e.g., the minimum point return (4 return points m^{-2}), avoiding inconsistency and tendency in biophysical parameters models (Silva *et al.*, 2017). Besides the use for AGB estimations, the ability of lidar to penetrate the canopy allows the generation of high resolution topographic maps and accurate estimates of vegetation height, cover and structure (Lefsky *et al.*, 2002). From the lidar point cloud, it is possible to extract several metrics from the canopy model, such as average height, percentiles and standard deviation (d'Oliveira *et al.*, 2014). From the interpolation of first and last returns, the digital surface model (DSM) and digital terrain models (DTM) are generated. When subtracting the DTM from the DSM, a canopy height model (CHM) is produced (Leitold *et al.*, 2015). Several metrics can be extracted from the CHM providing information about, for example, canopy gaps fractions, maximum and mean canopy height, canopy roughness, among others (Stark *et al.*, 2012; Andersen *et al.*, 2014; d'Oliveira *et al.*, 2014; Longo *et al.*, 2016). Although these metrics are very useful to describe forest structure, other more sophisticated analysis can better describe forest structure (Lefsky *et al.*, 2002). The leaf area index (LAI) and leaf area density (LAD) can be obtained from transmission rates of pulses (or light energy) through the volumetric units of the canopy (Stark *et al.*, 2012; Tang *et al.*, 2012; Detto *et al.*, 2015). The LAI provides information on the ratio of canopy leaf area per unit ground surface area (m^2 m^{-2}) (Wilson, 1959), while the LAD represents the vertical

distribution of LAI as subcomponents of the height strata ($m^2\ m^{-3}$) (de Almeida *et al.*, 2019b). Lidar technology is, therefore, a powerful tool capable of providing detailed information about the vertical canopy structure, AGB and changes in structure over time and after forest disturbances.

1.6 Outline chapters

The overall aim of this thesis is to investigate the effects of past and recent fires on the dynamics and structure of Amazonian forests. For this, I use both field-based and remote sensing methodologies. I combine data on soil fertility, soil pyrogenic carbon, forest inventory data, satellite data and airborne lidar data across the Amazon Basin, revealing how the world's largest tropical forest responds to historical and recent fires.

This thesis is divided into 5 chapters (Figure 1.5). This chapter, **chapter 1**, outlines our current understanding of primary and secondary Amazonian forests and their response to fire and drought. In particular, I focus on biomass and forest structure as these are the main themes of my thesis. I also compare field-based and remote sensing methodologies for forest monitoring as these are techniques I employ in my thesis.

My empirical research is presented in chapters 2-4. In **chapter 2**, I aim to evaluate whether fires have left a legacy on soil and vegetation, which may affect how forests now respond to droughts. In this chapter I use an Amazon-wide, long-term plot network ranging from 1981 to 2017, spanning drought and non-drought years, and soil fertility and pyrogenic carbon data. More specifically, I investigate how net aboveground carbon, including its components (gain and loss), varies with soil pyrogenic carbon concentration and how this moderates the response of aboveground carbon to drought.

Chapters 3 and 4 of my thesis focus on the impacts of recent fires on Amazonian forests. In **chapter 3**, I aim to investigate the impacts of recent fires and their reoccurrence on biomass and the vertical canopy structure of primary forests across Amazonia. I use 110 airborne lidar sites covering unburned and burned areas, burned between 2001 and 2018. A range of lidar metrics is used to evaluate changes in forest structure caused by fire, the impact of fire reoccurrence and the potential for recovery.

I also compare forests with low and high carbon stocks to test whether they experience different responses to fire.

In **chapter 4**, I focus on analysing the impact of recent fires on the vertical canopy structure of secondary forests across the South-Eastern region of the Brazilian Amazon. For this study, I use 20 airborne lidar sites, which covered unburned and burned secondary forests. In this chapter, I use lidar metrics to evaluate how secondary forest successional stage influences the impact of fire on forest structure and its subsequent recovery.

Finally, **chapter 5** synthesises the overall findings of this thesis and draws recommendations derived from this body of research.

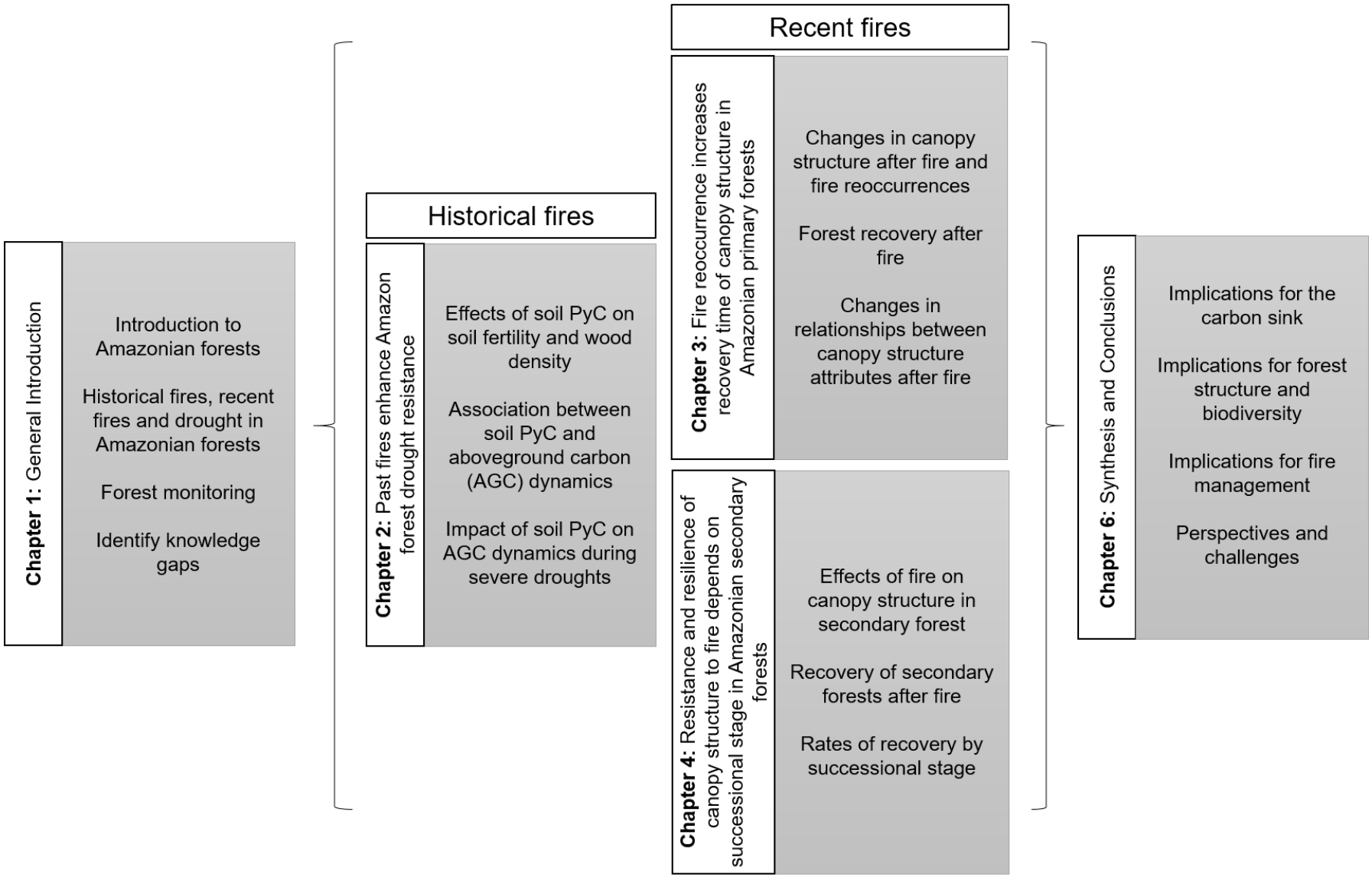

Figure 1.5. Conceptual diagram of the specific aims of each chapter. Each box represents a chapter as indicated in each box.

Chapter 2: Past fires enhance Amazon forest drought resistance

Soil, charcoal, and soil PyC sampling in a field campaign in Alta Floresta, MT, Brazil

This chapter was submitted to **Frontiers in Forests and Global Change** journal as Laura B. Vedovato, Lidiany C. S. Carvalho, Luiz E.O.C Aragão, Michal Bird, Oliver L. Phillips, Patrícia Alvarez, Jos Barlow, David C. Bartholomew, Erika Berenguer, Wendeson Castro, Joice Ferreira, Filipe M. França, Yadvinder Malhi, Beatriz Marimon, Ben Hur Marimon Júnior, Abel Monteagudo, Edmar A. Oliveira, Luciana O. Pereira, Aline Pontes-Lopes, Carlos A. Quesada, Camila V. J. Silva, Javier E. Silva Espejo, Marcos Silveira, Ted R. Feldpausch.

2.1 Abstract

Drought and fire reduce productivity and increase tree mortality in tropical forests. However, fires also produce pyrogenic carbon (PyC), which persists *in situ* for a long time, and represents a legacy of past fires, potentially improving soil fertility and water holding capacity, and/or favouring establishment and stimulating growth of fire and drought-associated tree species. Using an Amazon-wide, long-term plot network, in forests without known recent fires, integrating site-specific measures of forest dynamics, soil properties and a unique soil PyC concentration database, we investigate how PyC is correlated with physicochemical soil properties, wood density, aboveground carbon (AGC) dynamics and affects forest resistance to severe drought. We found that forests with higher concentrations of soil PyC had both higher soil fertility ($p<0.001$) and lower wood density ($p<0.001$). Soil PyC is not associated with AGC dynamics in non-drought years. However, during extreme drought events, forests with higher concentrations of soil PyC experience lower reductions in AGC gains (woody growth and recruitment), with this drought-immunising effect increasing with drought severity. Forests with a legacy of past fires are therefore more likely to continue to grow and recruit under increased drought severity. Forests with high soil PyC concentrations (third quartile) have 3.8% greater AGC gains under mean drought, but 33.7% greater under the most extreme drought than forests with low soil PyC concentrations (first quartile), offsetting losses of up to 0.68 Mg C $ha^{-1}yr^{-1}$ of AGC under extreme drought events. This suggests that past fires have legacy effects on current forest dynamics, by altering soil fertility and/or favouring establishment of earlier successional tree species capable of faster growth during droughts. Therefore, mature forest that experienced fires centuries or millennia ago may have greater resistance to current short-term droughts.

2.2 Introduction

Despite the long-standing view that tropical rainforests are fire-free systems, there is increasing evidence that fires existed in Amazonian forests before European colonization (Richards, 1973; Erickson, 2008). Fires in these wet environments depend on the combination of drought and ignition from human activity (Bush *et al.*, 2008; França *et al.*, 2020). Pre-Columbian fires were widespread and, in some areas,

recurrent, with return intervals of hundreds of years (Sanford *et al.*, 1985; Feldpausch *et al.*, 2022). These fires mostly spanned 7,000 to 250 years before present (BP), with an increase in fire frequency ~1,500 to 500 years BP (Sanford *et al.*, 1985; Santos *et al.*, 2000; Goulart *et al.*, 2017). Fires today are associated with deforestation and droughts (Silva *et al.*, 2020; Silveira *et al.*, 2020) and increased 74% in 2020 compared to 1998 in the Brazilian Amazon (INPE, 2021). Fragmented forests are at a greater risk of fire, especially in El Niño years, because fire spreads from forest edges to the interior of forests (Silva Junior *et al.*, 2018; Silva Junior *et al.*, 2020a). However, the long-term legacy of these fires on soil and vegetation remains unclear.

Forest fires produce pyrogenic carbon (PyC) which can act as an important proxy of past forest fire disturbances (Rehn *et al.*, 2021). PyC is formed through the incomplete combustion of biomass (Bird *et al.*, 2015). Some PyC can be lost as aerosols during burning (Bird *et al.*, 2015) and through decomposition and erosion from steep slopes (Rumpel *et al.*, 2006; Bird *et al.*, 2015; Coppola *et al.*, 2019). However, the remaining PyC is highly recalcitrant and can persist in the environment for millennia, including in soil (Bird *et al.*, 2015). In the Amazon, there is a large stock of soil PyC (1.1 Pg in the top 30 cm alone) as a result of long-term PyC accumulation produced mostly by historical fires (Koele *et al.*, 2017). A well-known example of long-term PyC accumulation and amendment of soil fertility are the Amazon Dark Earth soils (ADE, Anthrosols or *Terra Preta de Índio*), which are rich in PyC because of historical indigenous land management with fire and, as a result of this, have higher fertility than adjacent areas (Glaser, 2007; de Oliveira *et al.*, 2020).

Fire can alter soil physicochemical properties. In addition to producing ash that can have a positive short-term effect on soil fertility, PyC produced by fires can also have positive long-term effects (Glaser *et al.*, 2002), e.g., decreasing aluminium toxicity and improve cation exchange capacity via surface carboxylic groups on aromatic backbones, increasing soil organic carbon and water holding capacity because of the porous structure of PyC (Glaser *et al.*, 2002). These changes potentially alleviate soil water deficits during drought events and improve soil fertility. Furthermore, forests rich in soil PyC (Amazon Dark Earth) have higher productivity (Aragão *et al.*, 2009) and can allocate more carbon towards tree growth than forests in adjacent areas (Doughty *et al.*, 2014).

In recent decades, Amazonian forests have experienced an increase in drought frequency and severity (Lopes *et al.*, 2016; Paredes-Trejo *et al.*, 2021). Under future climate scenarios this trend will continue to increase greenhouse gas concentrations (Duffy *et al.*, 2015). Forest dynamics play an important role in determining whether the Amazon acts as a net carbon sink, with drought events reducing the carbon sequestration capacity of the forest (Brienen *et al.*, 2015; Hubau *et al.*, 2020). In 2005, the mega-drought experienced by Amazonian forests caused an estimated carbon loss over the entire basin at a rate of 0.3 Pg C yr^{-1} (Yang *et al.*, 2018). Furthermore, during the 2010 drought, the Amazon forest experienced a net biomass loss of 1.95 Mg ha^{-1} yr^{-1}, driven by an increase in biomass mortality and a decrease in biomass productivity (Feldpausch *et al.*, 2016). However, the response to drought events can vary according to soil properties and plant functional traits such as wood density. Forests growing on more fertile soils and with lower wood density species which also experience faster tree turnover (Quesada *et al.*, 2012), are often more vulnerable to severe drought (Feldpausch *et al.*, 2016; Greenwood *et al.*, 2017) and consequently, more vulnerable to fire (Berenguer *et al.*, 2021). After fire events in Amazonian forests, severe structural and compositional changes frequently occurs, with early successional tree species with low wood density favoured for establishment (Barlow & Peres, 2008; Berenguer *et al.*, 2018b). Fire can affect forest carbon dynamics for over a decade (Sato *et al.*, 2016; Silva *et al.*, 2020), but it is unclear if it leaves a legacy impact on forest carbon dynamics over much longer periods, either through changes induced in the soil by PyC or by selection for species and traits associated with fire and drought.

Here, we evaluate whether historical fires have left a legacy on soil and vegetation that affect how, over the past four decades, Amazonian forests have responded to drought. Historical fires in this chapter refer to fires that occurred any time prior to satellite records (i.e. before 1985). The aims of this research are: i) to understand how soil PyC concentration is associated with physicochemical soil properties and tree wood density, ii) to determine whether there is an association between soil PyC and aboveground carbon (AGC) dynamics, iii) to understand whether forests with higher soil PyC concentrations and/or more favourable soil physicochemical properties, change AGC dynamics during severe droughts. We hypothesised that soil PyC as a proxy or legacy of past fires might influence Amazonian forests in three non-exclusive

ways, by: (1) improving soil fertility, tending to accelerate the turnover in Amazonian forests, (2) increasing water holding capacity, potentially conferring a higher resistance to droughts and (3) favouring the establishment of species in a long-term succession, associated with past fire and drought disturbances. In this chapter, we define resistance as the capacity of the forest to maintain carbon gains rates during drought events.

2.3 Methods

2.3.1 Forest dynamics

We used forest dynamics data of 95 plots encompassing 432 censuses from a published dataset plus data obtained via ForestPlots.net (Hubau *et al.*, 2020; ForestPlots.net *et al.*, 2021) (Figure 2.1). Censuses took place between 1981 and 2017, including drought and non-drought periods. Plot size ranged from 0.25 ha to 9 ha, with a mean size of 1.14 ha and total plot area of 108 ha. Census interval ranged from 4 months to 5.6 years, and plots have been monitored for an average of 15 years each. For each census interval we calculated Aboveground Biomass (AGB) gains through growth and recruitment, AGB losses through mortality and AGB net change as the difference between AGB gains and AGB losses. Wood density used to calculate AGB is available on ForestPlots.net dataset and is derived from a global wood density database (Lopez-Gonzalez *et al.*, 2011). AGB rates were transformed into Aboveground Carbon (AGC) stocks using the ratio 2:1 (IPCC, 2006). We excluded from the analysis censuses with an interval length longer than twice the mean value of all censuses (> 5.77 years), since long intervals are less likely to be able to detect any effects of drought. All plots are in mature lowland forest (< 1500 m above sea level), without known recent fire disturbances or selective logging and represent a climatic and edaphic variation gradient across the Amazon Basin.

2.3.2 Soil Pyrogenic Carbon and Non-PyC fraction of Organic Carbon

Soil samples were collected from the same plots as the forest inventory data (Figure 2.1) at depths of 0-5, 5-10, 10-20 and 20-30 cm as part of past studies (Koele *et al.*, 2017; Quesada *et al.*, 2020) and this study. In plots ≥ 1 ha we sampled a minimum of

5 different locations across the plot, and in plots < 1 ha we sampled 3 locations. Then, we combined the samples in each plot by depth to result in one sample per plot per depth. For each sample, we measured the total organic carbon (TOC), pyrogenic carbon (PyC), and non-PyC fraction of the organic carbon (OC). The hydrogen pyrolysis technique (HyPy) (Ascough *et al.*, 2009) was used to quantify the PyC fraction of TOC, which represents stable polycyclic aromatic carbon with a ring number of > 7 (Meredith *et al.*, 2013). However, there is potentially more PyC that is not quantified by this technique since PyC produced by forests fires includes a variable fraction of PyC with an aromatic ring size of < 7 that is not quantified by the technique. The non-PyC fraction of organic carbon (OC) is the difference between TOC and PyC and will include low temperature PyC not quantified by HyPy (if present).

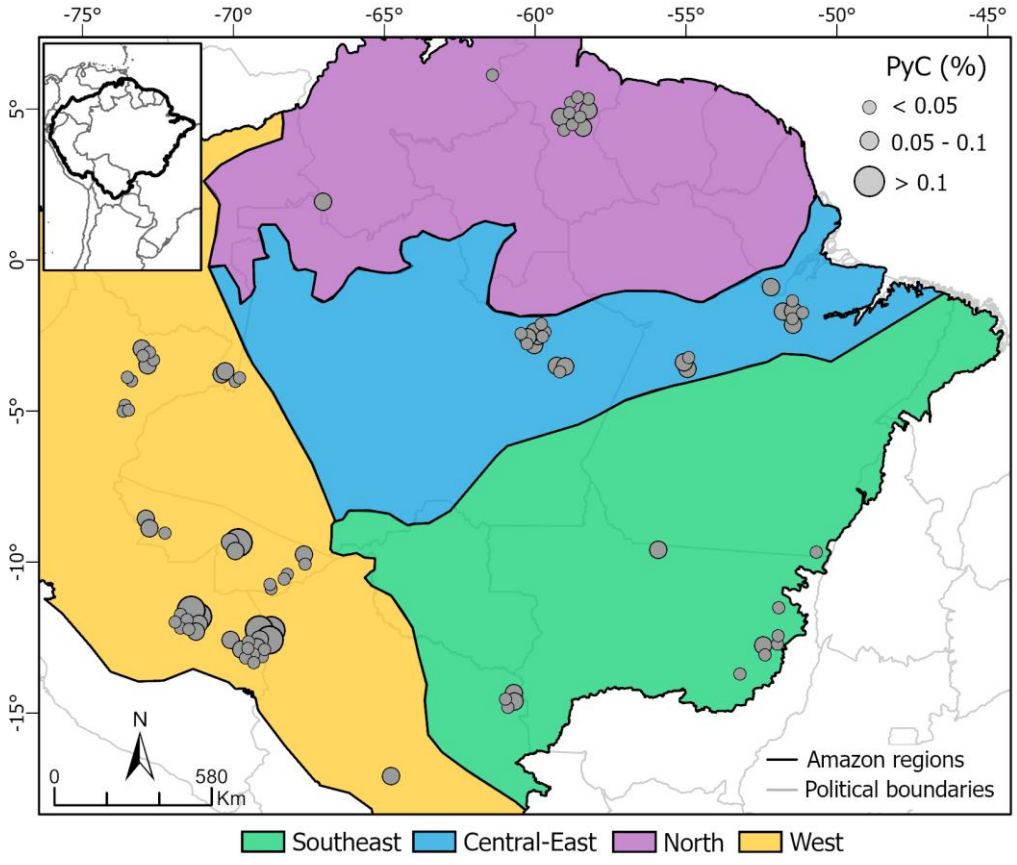

Figure 2.1. Spatial distribution of the plots analysed. Note that locations are approximate and displayed to reduce overlapping points where multiple plots are sampled. The size of grey dots is proportional to the mean concentration of PyC in the 0-30 cm interval at each site. Amazon regions are defined following Feldpausch *et al.* (2011).

We calculated the weighted mean for all depths to estimate the PyC and non-PyC OC concentrations in the soil surface (0-30 cm). The statistical analyses use continuous values; for Figure 2.4, we assigned each plot to one of two PyC classes based on the PyC median distribution: “Low” - values smaller than 0.048% and “High” - values equal or higher than 0.048%.

2.3.3 Maximum Cumulative Water Deficit anomaly

The Maximum Cumulative Water Deficit (MCWD) is a well-established metric to indicate water stress in forests (Aragão *et al.*, 2007), based on studies that show the average evapotranspiration (E) of lowland moist tropical forests is approximately 100 mm per month (da Rocha *et al.*, 2004; von Randow *et al.*, 2004). Consequently, if the monthly precipitation (P) is lower than 100 mm, the forest enters a state of water deficit (WD), which can accumulate over time (CWD). To calculate CWD, we used monthly precipitation data from Climate Hazards Group InfraRed Precipitation with Stations (CHIRPS) from January 1981 until December 2017 (Funk *et al.*, 2015). The following rule was applied to calculate the CWD per plot (p) for each month (n), using the evapotranspiration fixed at 100 mm month^{-1}:

$$\text{If } WD_{n-1(p)} - E_{(p)} + P_{n(p)} < 0;$$

$$\text{then } WD_{n(p)} = WD_{n-1(p)} - E_{(p)} + P_{n(p)};$$

$$\text{else } WD_{n(p)} = 0 \qquad (2.1)$$

The most negative CWD value among all months in each calendar year was taken as the MCWD. Subsequently, we calculated MCWD for each census interval, which refers to the most negative CWD during the census interval. The mean annual MCWD from 1981 to 2017 for each plot was used as the baseline to compute MCWD anomalies (Z-score) for each census interval, normalized by the standard deviation (σ). Censuses with anomalies ≤ -1.65 were classified as severe drought events, based on a confidence level of 90% (Aragão *et al.*, 2018).

2.3.4 Physicochemical soil properties

Soil physicochemical data derived from plot samples were provided by ForestPlots.net (ForestPlots.net *et al.*, 2021). We used data for surface (0-30 cm) soil including soil texture (silt, clay, sand fractions), total P, pH and exchangeable cations (K, Mg, Ca). The soils samples were all analysed following the protocol described in Quesada *et al.* (2010).

All soil fertility variables were centred, scaled and condensed into one axis using a principal component analysis (PCA) using the R package *FactoMineR* (Husson *et al*., 2016). The first eigenvalue explained 73.3% of the variance and was used as a single soil fertility variable in the analysis, visualized using the R package *factoextra* (Kassambara & Mundt, 2017) (SI Figure 2.1, SI Table 2.1).

2.3.5 Data Analysis

To evaluate the relationship between soil PyC and soil fertility, OC, wood density and soil texture we used Pearson's correlation test. We applied a natural log transformation to soil PyC, soil fertility and OC to meet assumptions for data normality.

We applied a generalized linear mixed effects model (GLMM) to evaluate the relationship between soil PyC and AGC gain, loss and net change. To account for census replication per plot and for regional differences across the Amazon Basin, we used the plot code nested in plot clusters as a random intercept effect in the models, with a fixed slope. The plot clusters refer to plot codes that are located within the same local group and are represented by the same three first letters of the plot codes (Lopez-Gonzalez *et al.*, 2011).

To evaluate the effects of soil PyC on the change in AGC dynamics with drought severity, we filtered our database to only include censuses classified as severe drought (MCWD anomalies ≤ -1.65σ) (Feldpausch *et al.*, 2016). In this analysis, we also applied a GLMM using the same random effect cited above. Soil PyC, severe MCWD anomalies, OC, soil fertility, wood density and interaction between variables were used as predictors to evaluate differences in AGC dynamics according to drought severity. We applied a square-root transformation of AGC loss, and a log transformation of soil PyC and MCWD anomalies to ensure a normal distribution of

fitted residuals. All variables were standardised to allow comparisons between model outputs. We applied a backwards stepwise selection procedure and selected the best models according to the lowest corrected Akaike Information Criterion (AICc) values using the *MuMIn* package (Barton, 2020). To evaluate spatial autocorrelation which could bias the models' coefficients, we used the models' residual to plot spline correlograms with 95% confidence interval based on 1,000 bootstrap resamples using *spline.correlog* function of the package *ncf* (BjØrnstad & Falck, 2001). In order to understand whether the effects of soil PyC were driven by organic carbon soil amelioration, we re-ran the models with OC instead of soil PyC. All GLMM models were performed using the *lme4* package (Bates *et al.*, 2018). All statistical analyses were conducted using R statistical software version 4.0.3 (R Core Team, 2020).

2.4 Results

2.4.1 Soil PyC, physicochemical soil properties and wood density

Soil PyC was significantly correlated with all measured variables including soil fertility, OC, wood density and soil texture as percentage of sand, clay and silt. We found highly significant positive correlations between soil PyC with soil fertility (PCA axis-1) ($r = 0.49$, $p<0.001$), OC ($r=0.30$, $p=0.003$), clay ($r=0.52$, $p<0.001$) and silt ($r=0.34$, $p=0.002$), and a negative correlation between soil PyC with wood density ($r= -0.33$, $p<0.001$) and sand ($r= -0.6$, $p<0.001$) (Figure 2.2).

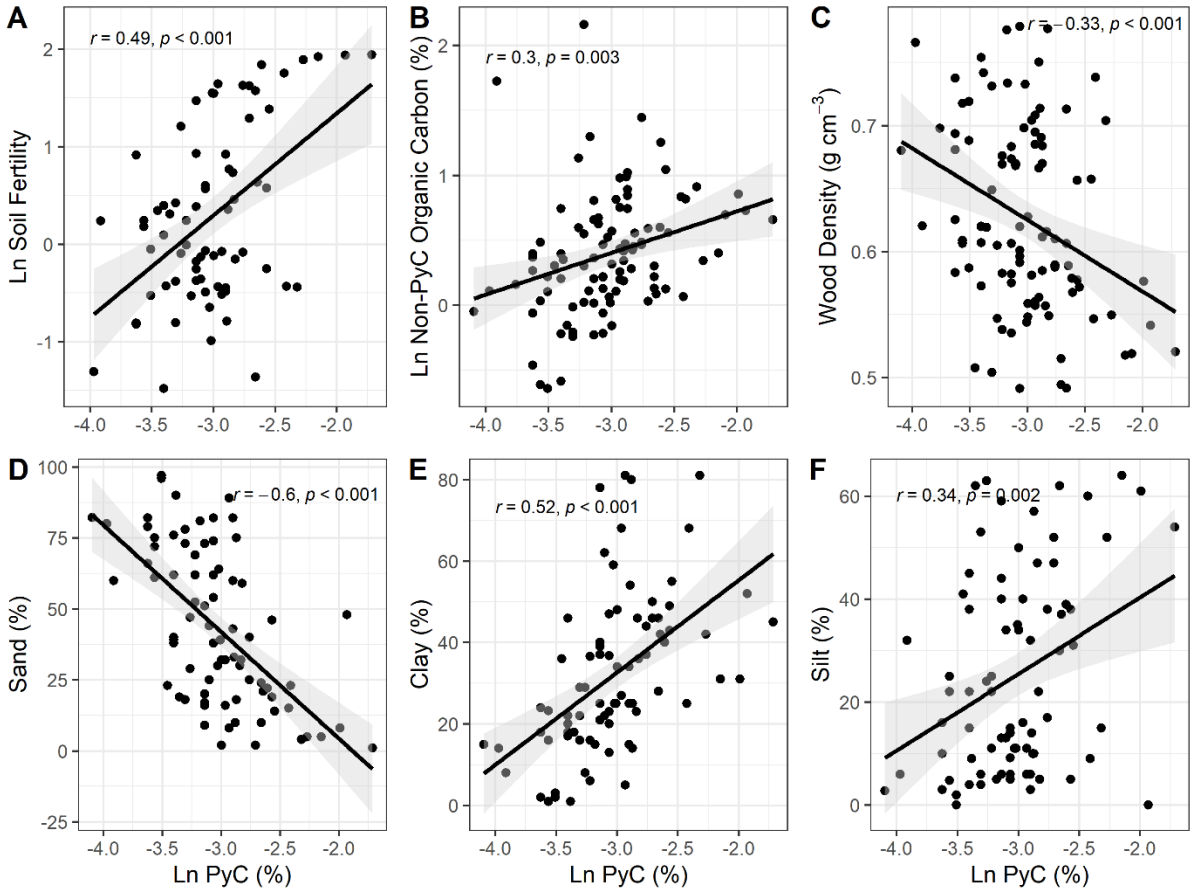

Figure 2.2. Relationship between soil PyC, physicochemical soil properties and wood density. (A) Soil fertility (log scale), (B) Organic Carbon (log scale) (%), (C) Wood Density (g cm^{-3}), (D) Sand (%), (E) Clay (%), (F) Silt (%). Shading denotes 95% confidence intervals of the linear models. Soil PyC is log transformed.

2.4.2 Soil PyC and AGC dynamics across all census

Our results showed no significant relationship between soil PyC with AGC gain, AGC loss or AGC net change (Figure 2.3, SI Table 2.2). There was no significant autocorrelation in the model residuals and thus no spatial bias in the model results (SI Figure 2.2).

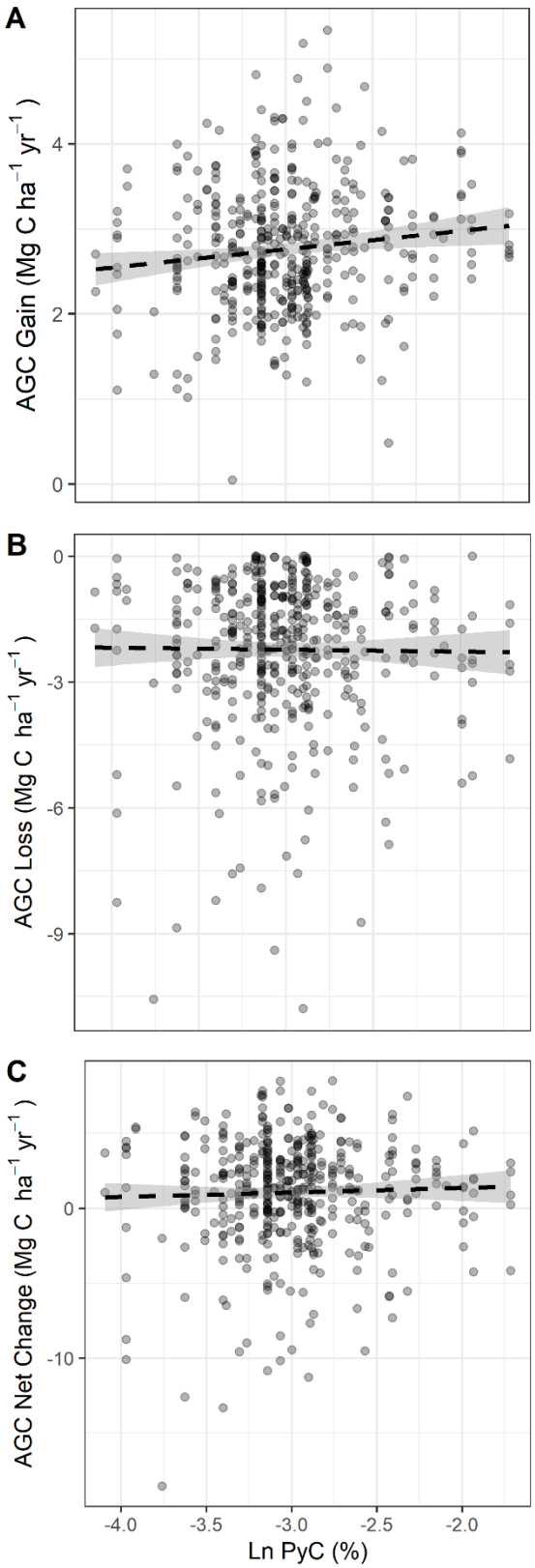

Figure 2.3. Relationship between AGC dynamics with PyC (log-scale) for (A) AGC gains, (B) AGC losses and (C) AGC net change. Dashed lines represent non-significant relationships between variables and the shading denotes the 95% confidence interval from our GLMM.

2.4.3 Soil PyC effects on AGC dynamics with drought severity

To investigate the effect of PyC on AGC dynamics during drought events, we selected only censuses that had experienced a severe drought (i.e., MCWD anomalies ≥ 1.65σ). Soil PyC, MCWD anomalies, OC, soil fertility, wood density, and interactions between variables were used as predictors to evaluate AGC dynamics with drought severity (SI Table 2.3). The best models selected to explain AGC dynamics based on AICc values are reported in Table 2.1. Spline correlograms of the best models show no significant spatial autocorrelation in the model residuals (SI Figure 2.3). Wood density and the interaction of soil PyC with MCWD anomalies were significant predictors of AGC gains (i.e., woody productivity) during severe droughts. Our results show lower rates of AGC gains in forests with greater wood density. We also found a significant interaction between soil PyC and MCWD anomalies on AGC gains ($p=0.041$), with the slope between AGC gains and MCWD anomalies increasing with soil PyC (Table 2.1).

We found a difference in AGC gains between low and high soil PyC forests (i.e., forests with PyC concentrations lower or greater than the median, respectively) to increase with drought severity, as AGC gains significantly declined at a greater rate in low soil PyC forests compared with high soil PyC forests (Figure 2.4). We compared events around the mean MCWD anomaly (~ -2σ, $p<0.046$) and the most severe MCWD anomaly (~ -4.3σ, $p<0.001$) for forests with the first quartile of observed soil PyC concentration (0.038%) to forests with the third quartile of observed soil PyC concentration (0.056%), which is ~1.5 times greater. Our models suggest that forests with the third quartile of observed soil PyC concentrations have 3.8% greater AGC gains under mean drought conditions, but 33.7% greater under the most extreme drought conditions compared with forests with the first quartile of observed soil PyC concentrations. These results may translate to a difference in the gain of 0.68 Mg C $ha^{-1}yr^{-1}$ during a most extreme drought.

The best model to explain AGC losses also included WD and the interaction between soil PyC and MCWD anomalies. However, the effect size was not significantly different from zero. We could not explain any of the variance in AGC net change during severe droughts with the tested variables (Table 2.1). We also found the non-PyC OC had no

significant effect to explain AGC gain and loss with drought severity when tested instead of soil PyC (SI Table 2.4).

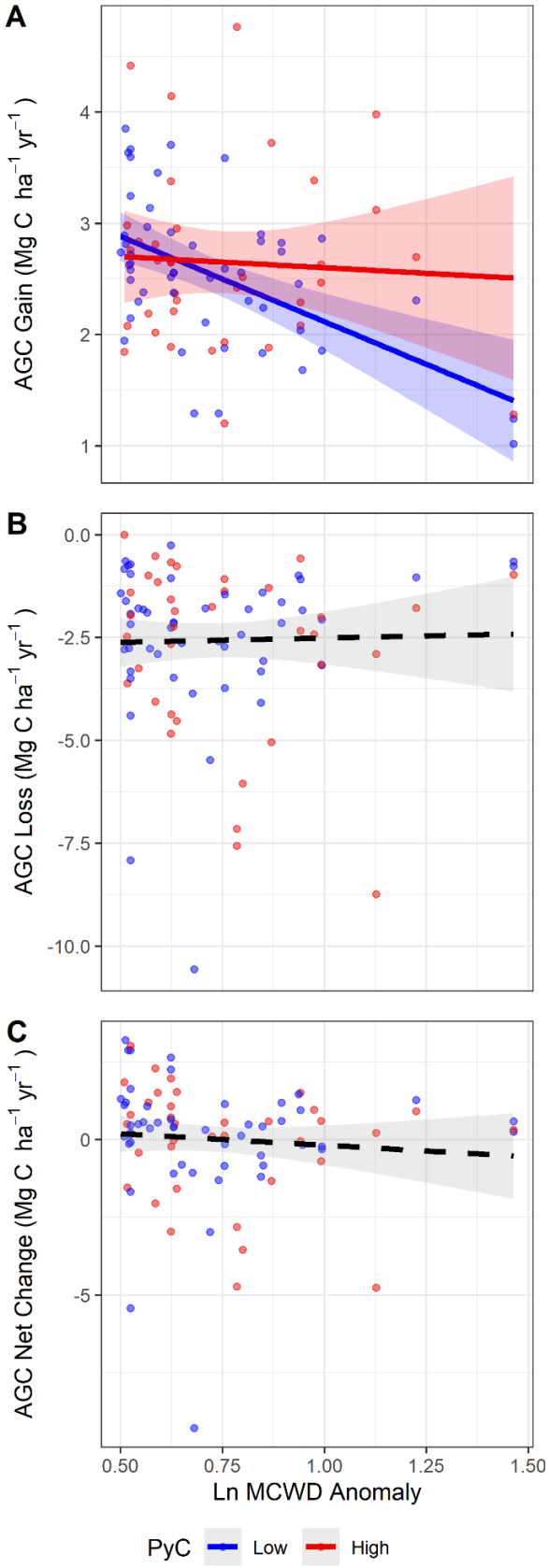

Figure 2.4. The relationship between soil PyC and (A) AGC gains, (B) AGC losses and (C) AGC net change with drought severity (MCWD anomaly). Blue lines and dots represent plots classified as low percentage of PyC in soil (<0.048%) and red as high percentage of PyC in soil (≥ 0.048%). Solid lines represent significant relationships between MCWD anomalies and AGC dynamics, whilst different slopes between blue and red lines represent a significant interaction between soil PyC and MCWD anomaly in the best model ($p<0.05$). Dashed lines represent non-significant relationships between variables. Shading denotes the 95% confidence interval. The MCWD anomaly is log transformed.

Table 2.1. Parameter estimates for the selected models explaining AGC (gain, loss and net change) during severe droughts ($\sigma \leq -1.65$).

	Intercept	MCWD Anom	PyC	WD	PyC:MCWD Anom	Plot code: Plot cluster	Fixed effect (marginal) R^2	Total (conditional) R^2
AGC gain	2.55 ± 0.09***	-0.071 ± 0.08	0.1 ± 0.08	-0.25 ± 0.11*	0.18 ± 0.08*	0.49	0.21	0.73
AGC loss	1.48 ± 0.07***	0.06 ± 0.06	-0.01 ± 0.07	-0.15 ± 0.08	0.12 ± 0.07	0.35	0.08	0.49
AGC net change	0.18 ± 0.20	-	-	-	-	0.00	0.00	0.00

Note: Coefficient estimates ± SE are presented for each fixed effect. Total (conditional) R^2 represents the total variation explained by the model and is partitioned into the variation explained by the fixed effects (marginal R^2) and fixed plus random-effects (conditional R^2). Asterisks represent the significance level of each variable: *p<0.05; **p<0.01; ***p<0.001.

2.5 Discussion

Drought drives major reductions in the rate of biomass growth and increases in tree mortality across Amazonia (Feldpausch *et al.*, 2016; Aleixo *et al.*, 2019), but the effect of past disturbances on modulating forest responses to drought were largely unknown. This is the first study to analyse the effects of soil PyC, acting as a proxy of past fire legacies on AGC dynamics in Amazonian forests. Overall, we found that soil PyC does not have a significant effect on rates of AGC dynamics (Figure 2.3, SI Table 2.2).

However, under severe droughts, the drought impact on AGC gains is significantly greater in forests with low soil PyC compared to those with high soil PyC (Figure 2.4, Table 2.1). This pattern, though, did not affect the overall AGC net change during severe droughts. Our results also show that soil PyC is positively correlated with soil fertility and soils with higher clay and silt content (Figure 2.2 –A, E, F). Moreover, we found a negative correlation between soil PyC and tree wood density (Figure 2.2 –C). Our research highlights the potential importance of past fire legacies on forest soils and long-term forest succession a basis for further investigations of repercussions of past fires across Amazonia.

2.5.1 Soil PyC, soil physicochemical properties and wood density

Our findings indicate that soil PyC is associated with increased soil fertility (Figure 2.2-A). Studies of ADE and biochar (PyC) addition indicate that PyC can improve soil fertility via several mechanisms (Glaser *et al.*, 2001; Czimczik & Masiello, 2007). PyC has a polycyclic aromatic structure and can persist in the environment for centuries to millennia (Bird *et al.*, 2015). Therefore, PyC can reduce aluminium toxicity, increase cation exchange capacity, and improve water holding capacity (Glaser *et al.*, 2001; Czimczik & Masiello, 2007). The ADE are historical indigenous lands where fire was frequently used as a land-management tool. Covering only 3% of Amazonia (McMichael *et al.*, 2014), these small-scale areas (e.g., 0.5-300 ha in size) (Paz-Rivera & Putz, 2009) are more fertile and richer in soil PyC than adjacent areas (Glaser *et al.*, 2002; Liang *et al.*, 2006; Glaser, 2007). The mean concentration of soil PyC across six ADE plots was 0.18% (range = 0.03-0.34%) (Oliveira et al 2022, in press), representing a 3.5 fold greater mean soil PyC concentration compared to the non-ADE soils (range = 0.01-0.18%) sampled in this study. As ADE soils were intentionally formed by indigenous populations by burning discarded organic and inorganic matter, there is expected to be higher concentrations of PyC in these areas. In non-ADE soils, we found the effect of PyC to rise with its concentration. Even though soil PyC concentrations in non-ADE soils are lower when compared to ADE soils, in the low fertile soils of the Amazon, soil PyC still had effects on these forests. Higher concentrations of soil PyC in non-ADE areas are likely related to more recent and/or frequent fires; however, since we do not have information on charcoal dating in these

areas, it remains uncertain. On the other hand, it is likely that the concentrations of soil PyC found in non-ADE soils have a long-term effect on soil fertility and/or indicates changes in species composition. Our study highlights the impact of soil PyC-associated changes in soil fertility for non-ADE soils representing the remaining 97% of the Amazon Basin, where we found a positive correlation between PyC and soil fertility.

We quantified total resistant PyC, representing PyC produced *in situ* by local fires and PyC that may have been deposited by aeolian transport from remote fires. The aerosol-derived PyC is derived semi-continuously from ancient to modern fires and fluxes have recently been estimated (fossil fuel + biomass burning) at approximately 6 kg km^{-2} yr^{-1} in Amazonia (Coppola *et al.*, 2019). Given this rate, it would still take approx. 27,000 years to accumulate the estimated store of 1.1 Pg (0-30 cm) of PyC in the Amazon Basin from aerosol deposition alone (Koele *et al.*, 2017). This suggests that the majority of the PyC analysed derives from ancient local fires. Whilst, atmospheric transport, over centennial-scales, may also have been important, and these processes combined may have improved soil fertility over time.

Soil texture is a key determinant of soil fertility. There is a large range of physical and chemical soil properties across the Amazon Basin that vary according to gradients of pedogenic development, where nutrient pools are lowest in the most weathered soils (Quesada *et al.*, 2010). We found the same pattern for soil PyC, with soil PyC concentration negatively correlated with soil sand content (Figure 2.2-D), occurring in highly weathered soils. Due to macropore predominance, sandy soils are more aerated and, consequently, destabilise PyC through high rates of oxidation and potentially greater rates of vertical translocation (Major *et al.*, 2010). On the other hand, soils that suffered less weathering and, consequently, have more clay and silt, showed a positive association with PyC (Figure 2.2-E, F) because of lower PyC oxidation rates. Our results corroborate other studies showing that soils with > 50% clay content have significantly more PyC (Reisser *et al.*, 2016). Moreover, clay-rich soils present more opportunities for organo-mineral interactions, helping to stabilise PyC (Sørensen, 1972; Six *et al.*, 2002; Reisser *et al.*, 2016).

We also found a negative correlation between wood density and soil PyC (Figure 2.2-C). A previous large-scale fire experiment has already shown that tropical soft-wood trees are at greater risk of death from fire, in part because tree species with low wood

density are less likely to close wounds postfire (Balch *et al.*, 2015). Moreover, wood density had an important effect on tree survival rates in areas burned repeatedly, where increasing wood density by 0.8 g cm^{-3} can enhance survival probability by 15% (Brando *et al.*, 2012). Note that only one previous work has investigated the relationship between soil PyC and wood density and did not find a significant tendency (Massi *et al.*, 2017). However, it included fewer than half the number of plots used in our study.

It is well established that wood density is negatively correlated with soil fertility (Baker *et al.*, 2004; Quesada *et al.*, 2012). We found a strong correlation between soil PyC and soil fertility (Figure 2.2-A), and other previous studies have shown soil PyC can increase soil fertility as discussed previous in this section. Despite not being able to separate the origin of soil PyC (aerosol deposition or local produced) in our analyses, we hypothesise that forests with high soil PyC concentrations added by aerosol deposition are more likely to have low wood density. This may be because soil PyC can increase soil fertility, leading to forests with fast stem turnover (Quesada *et al.*, 2012). Meanwhile, forests with high concentrations of locally produced soil PyC may have experienced past fire disturbances *in situ*. Low wood density in these forests with high concentrations of soil PyC may be an indicator of disturbance and an earlier successional state, rather than merely changes in soil fertility.

Whilst we found correlations between soil PyC and soil fertility, soil texture and tree wood density, we were unable to directly test causal relationships in this study and these results should therefore be interpreted with caution. It should be noted that the highest concentration of soil PyC were found in the West Amazon that also has the most fertile soils, the lowest sand content and the lowest stand-level wood density (Quesada *et al.*, 2012).

2.5.2 Soil PyC effects on AGC dynamics across all census

Our results do not show an effect of soil PyC on AGC dynamics when analysed across all census intervals. This result may be related to low concentrations of soil PyC found in the majority of the plots analysed in this study. A study from eastern and southern Amazonia showed that biomass and forest composition had legacy effects in forests on or near ADE soils with high soil PyC and a history of ancient fires, which in general

presented higher aboveground biomass (de Oliveira *et al.*, 2020). It is likely that soil PyC has a greater effect at high concentrations since the effect of PyC on soil fertility and water holding capacity is likely to be small at the concentrations found in this study (Glaser *et al.*, 2002; Glaser, 2007). Moreover, disturbances in ADE are likely to be much greater (de Oliveira *et al.*, 2020) and therefore they may still have differences in species composition and traits that would not have persisted in forest that were less disturbed.

2.5.3 Effects of soil PyC on AGC dynamics in relation to drought severity

Drought events can occur because of natural processes that are related to changes in sea surface temperature, e.g., Atlantic Multidecadal Oscillation, El Niño Southern Oscillation and Pacific Decadal Oscillation (Marengo & Espinoza, 2016; Aragão *et al.*, 2018). However, anthropogenic actions such as land-use and land-cover changes and greenhouse gas emissions may exacerbate the intensity of droughts by changing patterns of large-scale atmospheric circulation (Spracklen & Garcia-Carreras, 2015; Llopart *et al.*, 2018). Drought events in the Amazon are becoming more frequent, prolonged and intense and as a result of both globally and locally driven climate change (Malhi *et al.*, 2008; Dubreuil *et al.*, 2012; Bonini *et al.*, 2014). Amazonian forests are vulnerable to drought, which causes biomass losses and reducing forest productivity, enough to temporarily reverse a large multi-decadal carbon sink into mature forest biomass (Phillips *et al.*, 2009a; Feldpausch *et al.*, 2016; Anderson *et al.*, 2018; Gatti *et al.*, 2021).

Our results show that during extreme droughts events, forests with greater soil PyC have significantly greater rates of AGC gain compared to forests with lower soil PyC, with this difference increasing with drought severity (Figure 2.4). These results may be driven by the capacity of soil PyC to hold more water in the soil (Glaser *et al.*, 2002; de Melo Carvalho *et al.*, 2014), alleviating the effects of severe droughts, and allowing trees to continue to grow under drought conditions. This significant difference on AGC gains during drought events in forests with higher soil PyC compared to lower soil PyC, may also be related to soil fertility, since forests with high concentrations of soil PyC are also more fertile soils. The drought immunisation response is associated with the PyC fraction of TOC and not the non-PyC fraction of the organic carbon, since we

found no significant effect of OC on changes in AGC gains and losses with drought severity. This indicates that the responses we found are potentially related to past fire effects on soil and vegetation (Quesada *et al.*, 2012).

Some studies have shown that during extreme droughts, undisturbed forests can lose more AGC than forests disturbed by past fires (Brando *et al.*, 2014; Berenguer *et al.*, 2021). Since undisturbed forests have trees with higher wood density than those in disturbed forests, the death of few large trees in an undisturbed forest can cause a greater amount of carbon loss than in disturbed forests (Brando *et al.*, 2014; Berenguer *et al.*, 2021). Therefore, our results may demonstrate that forests with a stronger history of fires, here identified by high concentrations of soil PyC, can be more resistant to current drought events since they may have lower overall biomass resulting from an establishment of long-term successional species, and consequently not showing a significant reduction of biomass growth during drought events.

In contrast to finding a significant effect of PyC on AGC gains, we were unable to explain any of the variance in AGC losses (Table 2.1). Berenguer *et al.* (2021) found that forests increase the carbon loss rates for up to 3 years after a drought, and consequently, forest inventories taken in the first year after a drought may not detect the full drought impact on tropical vegetation. Since many of our census intervals did not capture 3 years of post-drought dynamics, we may be failing to capture any effect of PyC on long-term carbon losses. Moreover, high spatial and temporal heterogeneity in tree mortality may prevent a signal from being detected in this study (Johnson *et al.*, 2016; Pugh *et al.*, 2020). Many of our plots were small (≤ 1 ha) or had short census intervals (< 2 years), making it difficult to estimate AGC losses precisely. Much larger datasets may be needed to separate a trend from the large natural variance in tree mortality. Despite an increase in AGC gains, we are not able to detect an increase in AGC net change. Since spatial variation in carbon stocks depends more on losses than gains (Johnson *et al.*, 2016; Hubau *et al.*, 2020; Pugh *et al.*, 2020) the caveats outlined above are also likely to hold true for the AGC net change data.

2.5.4 Implications for the future of Amazonian forests

It is critical to understand the impacts of past fire events on contemporary forest dynamics. Our results highlight the importance of understanding past fire regimes

when predicting how species composition and carbon storage will change as a result of drought events. Our results suggest past fires may influence current forest dynamics by altering soil fertility and/or establishing earlier successional tree species. A major shift in the frequency and intensity of fires and droughts has occurred this century, bringing large uncertainties for future predictions of the carbon cycle (Aragão *et al.*, 2007; Aragão *et al.*, 2018; Silva Junior *et al.*, 2019). This increase in fire represents a new fire regime for the Amazon (Aragão *et al.*, 2018; Silveira *et al.*, 2020). These fires bring several impacts to tropical rainforests such as changes in forest structure, species composition and carbon dynamics (Sato *et al.*, 2016; Prestes *et al.*, 2020; Silva *et al.*, 2020; Pontes-Lopes *et al.*, 2021). Forests that burned 30 years ago still have ~25% less aboveground biomass than unburned forests (Silva *et al.*, 2018), showing these impacts can persist over decades. From our analysis using soil PyC as a proxy and/or legacy of past fires, it is possible that forests which burned centuries ago may still not have recovered to their pristine state but instead continue to exhibit some attributes associated with recently disturbed or secondary forests (Berenguer *et al.*, 2018b; de Oliveira *et al.*, 2020; Heinrich *et al.*, 2021). Our study, however, suggests that mature forests that experienced fires centuries or millennia ago have greater resistance to short-term droughts, as consequence of past fires. Further studies and experiments are needed to identify whether the effects of PyC on fertility and/or water holding capacity drive the patterns we observe, or whether PyC simply acts as a proxy of past fires.

Chapter 3: Fire reoccurrence increases recovery time of canopy structure in Amazonian primary forests

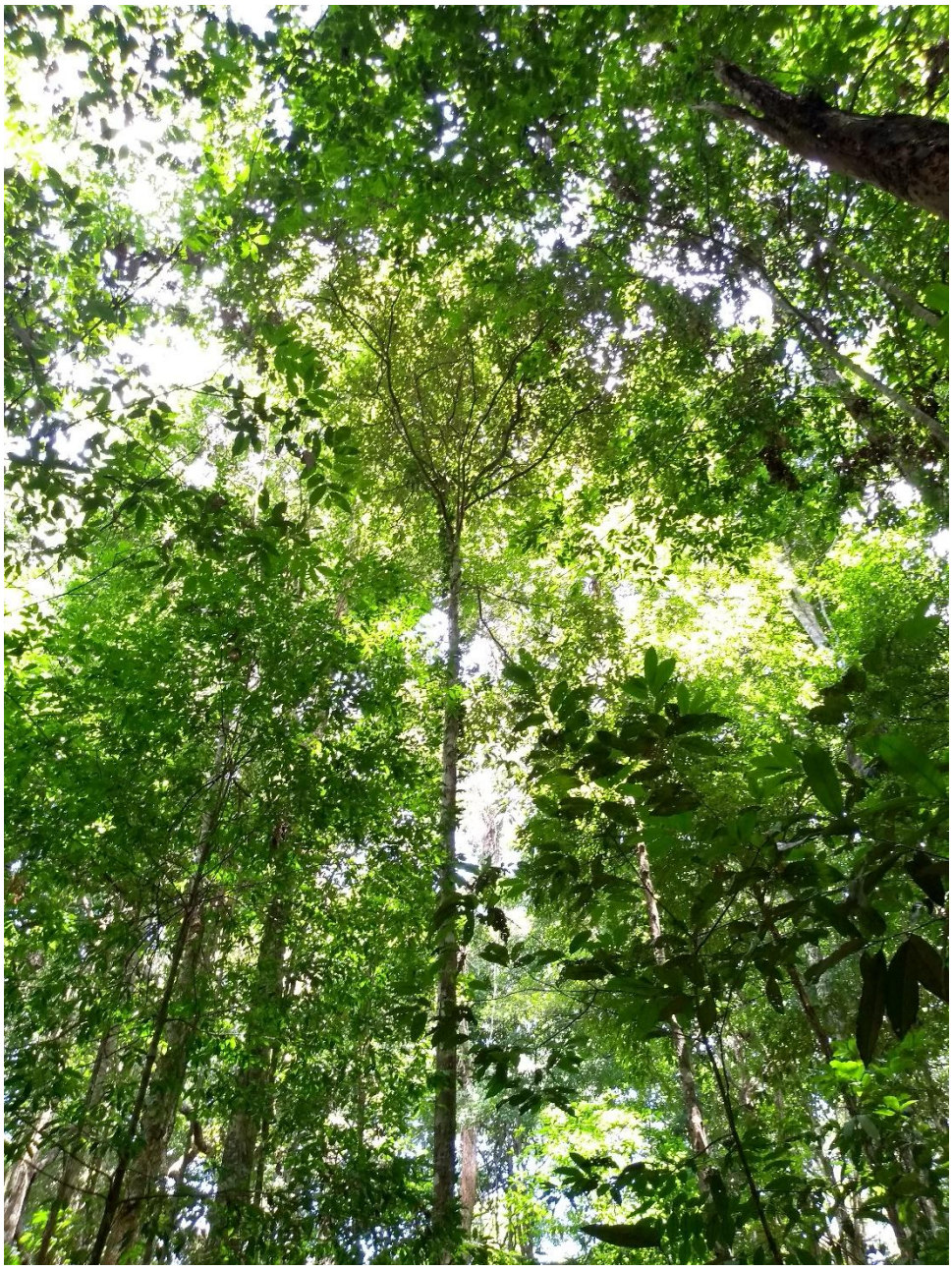

National Forest of Caxiuanã, PA, Brazil

This chapter is in preparation for submission to **Remote Sensing of Environment** or a related journal as Laura B. Vedovato, Ted R. Feldpausch, Danilo Roberti Alves de Almeida, Aline Pontes-Lopes, Celso H. L. Silva Júnior, David Bartholomew, Ricardo Dalagnol, Mauro Assis, Eric B. Gorgens, Carlos A. Silva, Ruben Valbuena, Luiz E. O. C. Aragão (in prep). Fire reoccurrence increases recovery time of canopy structure in Amazonian primary forests.

3.1 Abstract

Fire frequency has increased in recent decades in Amazonian forests, bringing changes to forest structure and impacting the global carbon balance. To date, the effects of fire have largely been assessed by ground-based *in situ* measurements and remote sensing data collected from passive sensors. We used airborne light detection and ranging (lidar), an active remote sensing technology, with the ability to penetrate the forest canopy and provide detailed information of the vertical forest profile, to analyse post-fire changes in forest structure. We utilised 110 airborne lidar transects across the Brazilian Amazon which spanned unburned and burned areas. The MODIS burned area product (MCD64A1) was used to detect burned areas from 2001 to 2018 and to calculate the years since the last fire (YSLF) occurrence and fire reoccurrences. Then, we calculated canopy structure and aboveground carbon density (ACD) metrics to analyse the impact of fire by years since last fire (YSLF) and fire reoccurrence on forest structure. Our results show ACD, maximum and mean canopy height did not recover to unburned state after ten YSLF in areas with repeated fire events. The leaf area index (LAI) and roughness also did not recover after ten YSLF within areas which had a single fire event. Overall, repeated fires degrade the canopy structure further and increase the time needed for forests to recover to the pre-burned state. Changes in canopy structure creates conditions that increase the likelihood of further fire events reoccurring before full recovery. Fire mitigation actions are needed to avoid increasing losses in carbon stocks, reducing biodiversity, and affecting regional climate and hydrological cycles.

3.2 Introduction

Wildfires in moist, closed-canopy *Terra Firme* Amazonian forests are estimated to have been rare events before European colonisation, with median intervals of fire return of 450 years in some forests (Feldpausch *et al.*, 2022). However, the frequency of fires in Amazonia has increased, especially in the last few decades, with an increase of 74% in 2020 compared to 1998 (INPE, 2021). These forest fires are mainly associated with anthropogenic activities (Pausas & Keeley, 2009) and are more frequent during drought years (Alencar *et al.*, 2006; Gatti *et al.*, 2014; Anderson *et al.*, 2018; Aragão *et al.*, 2018). During drought, the dry litter and dry wood debris on the

forest floor act as fuel for these understory fires, with slow-moving ground fire heating stems and weakening the non-fire adapted tree species, which can ultimately cause these trees to die.

Tree mortality is high after fires and can persist for decades with delayed mortality of large trees, greatly reducing carbon stocks (Kauffman, 1991; Barlow *et al.*, 2003b; Haugaasen *et al.*, 2003; Silva *et al.*, 2018). Consequently, forest structure is likely to be affected considerably. However, little is known how vertical forest structure is altered by fire and its ability to recover over time.

In the short-term, fire causes a 36-74% increase in mortality for trees ≥10 cm diameter at breast height (DBH) and increased mortality of larger trees (DBH >50 cm) up to 3 years after fire (Kauffman, 1991; Barlow *et al.*, 2003b; Haugaasen *et al.*, 2003). Tree mortality creates canopy gaps and decreases mean height and biomass of the forests. Losses of the largest trees will also reduce the maximum height, create particularly large gaps and reduce biomass storage (Dalagnol *et al.*, 2019). Moreover, forests affected by fires have been shown to store approximately 25% less biomass than adjacent unburned plots even after 31 years (Silva *et al.*, 2018). Only recently, studies have revealed a decrease in leaf area index (LAI) and canopy height in burned forest, which are accentuated with fire reoccurrences; however, these studies have been limited to a floodplain of the Rio Negro in Amazonas, central Amazonia and an experimentally burned forest site in Mato Grosso, southern Amazonia (Brando *et al.*, 2014; Balch *et al.*, 2015; Almeida *et al.*, 2016).

Fire and the reoccurrence of fire affects the long-term recovery of Amazonian forests by killing 76% of saplings and leading to rapid growth of early successional tree species (Haugaasen *et al.*, 2003). However, in areas severely burned the growth of aggressive bamboo and grasses seems to inhibit seedling regeneration (Haugaasen *et al.*, 2003). In a study in Brazil's Pará State, there was no, or little, recovery in forest structure and floristic composition nine years after a single fire event, with species that are common in unburned forest being rare or totally absent in the burned forest (Barlow & Peres, 2008). Fire reoccurrence further affects forests, potentially turning closed-canopy primary forests to more open forests dominated by short-lived pioneer species (Barlow & Peres, 2008). During a drought year, forests that experienced repeated fires had the majority of trees killed, the canopy cover reduced by half, and invasive grasses became dominant (Balch *et al.*, 2015). Forest areas that burned multiple times within

a decade had up to 94% less aboveground carbon than unburned forests (Longo *et al.*, 2016). Fire also reduces biomass accumulation in regrowing secondary forests (forests deforested and allowed to regrow) (Zarin *et al.*, 2005; Feldpausch *et al.*, 2007), with forests burned five or more times having >50% reduction in carbon accumulation (Zarin *et al.*, 2005). Therefore, the reoccurrence of fire further increases greenhouse gas emissions beyond those emitted from single forest fire events (Fearnside, 2012; Vasconcelos *et al.*, 2013).

The exclusive use of ground-based *in situ* measurements and remote sensing data collected by passive sensors are not able to detect subtle changes in canopy structure caused by fire. Consequently, the use of these techniques in combination with light detection and ranging (lidar) is recommend to obtain more accurate results when estimating changes in canopy structure (Goetz *et al.*, 2015). Lidar can provide a detailed vertical forest profile from which it is possible to estimate canopy height, openness, spatial heterogeneity, leaf area index (LAI) and other metrics related to forest structure (van Leeuwen & Nieuwenhuis, 2010; Stark *et al.*, 2012; Almeida *et al.*, 2016). These metrics are useful to better assess changes in forest dynamics and ecology beyond carbon stocks and sequestration.

Few studies have used lidar to evaluate forest degradation by fire in Amazonia (Almeida *et al.*, 2016; Longo *et al.*, 2016; Sato *et al.*, 2016; Rappaport *et al.*, 2018). A study in the Rio Negro floodplain in Amazonia found that seasonally flooded forests experienced greater damage than surrounding unflooded forests four years after burning; burned unflooded forests had 12% lower maximum height, 134% more open canopies and 166% higher gap fraction when compared to unburned areas, while the differences in flooded forests were even bigger (44%, 1282% and 206%, respectively) (Almeida *et al.*, 2016). In western Amazonia, lidar measurements indicated that forest height and biomass of burned areas had not recovered 10 years after burning (Sato *et al.*, 2016). A study in southern Amazonia found that forest structure varied with fire severity and frequency, with forests with a history of one, two and three or more fires having 54%, 25% and 8% of aboveground carbon density (ACD), respectively, when measured a year after burning (Rappaport *et al.*, 2018).

These studies provide clear evidence of the profound changes in ACD and long-term effects of fire on Amazonian forests, with several studies providing estimates by region

and forest type. However, there is a major gap in understanding the effects of fire reoccurrence on canopy structure and the time required for burned forests to return to their unburned state or whether they can totally recover. This research aims to investigate, the changes in canopy structure and its recovery after single and repeated fires across the Brazilian Amazon. More specifically, we address the following research questions: (i) how fire and fire reoccurrence change canopy structure, (ii) how long does canopy structure take to recover following fires, (iii) how do repeated fires affect this recovery and (iv) how fire changes the relationship between canopy structure attributes in primary forests.

3.3 Methods

3.3.1 Study area and lidar data

To address our questions, we selected 110 airborne lidar collections from the more than 900 lidar data available across the Brazilian Amazon, collected by the Sustainable Landscape project (Sustainable-Landscapes, 2016) and Improving Biomass Estimation Methods for Amazon (EBA) project (EBA, 2016), with both datasets having a minimum point density of 4 points m^{-2}. The lidar data were collected between 2016 and 2018 and span primary forests in different climates and soil types (Figure 3.1). The selection of the lidar data was based on the criteria that within the lidar transect there was primary forests unburned and burned. Moreover, we applied a negative buffer of 60 m around the primary forests boundaries and excluded all patches of unburned and burned areas smaller than 1 ha to avoid using any area that does not represent the core of a mature forest.

To identify mature forest within the lidar data, we used the land use and land cover classification data from MapBiomas collection 5 (MapBiomas, 2021). Then, we used burned area data from the MODIS, MCD64A1 product, with a monthly temporal resolution and a spatial resolution of 500 m (Giglio, 2015) which overlapped the primary forests within the lidar sites to identify the burned areas. For our purposes, we obtained the burned area product from 2001 to 2018 and combined it annually. For each pixel of burned area we computed how many years had passed since the last fire before the airborne lidar flight date (YSLF), and the number of fire reoccurrences.

We classified the forests according to the number of fire reoccurrences, as either single burned (B1) or repeated burned (B2+) forests. This methodology allowed us to analyse the effects of fire in mature forest for up to 17 years since burning.

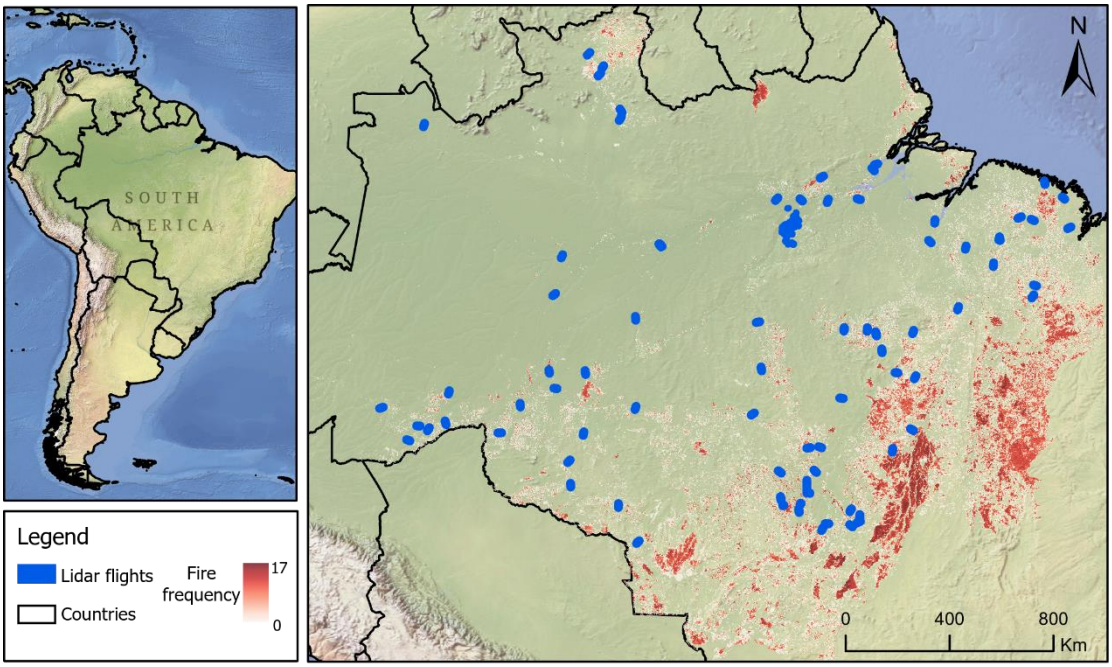

Figure 3.1. Study area. The blue areas represent the lidar sites used in this study. Black lines represent country limits. Red colours represent frequency of fire, with darker red showing higher fire frequency.

3.3.2 Lidar metrics

We measured a range of lidar metrics for the selected unburned and burned areas. The lidar data were pre-processed following de Almeida *et al.* (2019b). From the normalised cloud points, we extracted the Canopy Height Model (CHM) at 1 m-grid spatial resolution and then calculated the following metrics: Aboveground Carbon Density (ACD), maximum canopy height, mean canopy height, canopy roughness, and canopy openness at 5 m, 10 m and 15 m height. The ACD was calculated at a spatial resolution of 50 m following equation S7-supporting information in Longo *et al.* (2016) which uses the mean top canopy height. The maximum and mean height were obtained by aggregating the 1 m-grid CHMs to a 10 m-grid, getting the maximum and the average values respectively. Roughness was obtained by the standard deviation divided by the mean height resulting from the 1 m-grid to 10 m-grid aggregation. The openness at 5 m, 10 m and 15 m represents the fraction of pixels below 5, 10 and 15

m, respectively (de Almeida *et al.*, 2020). In addition to CHM derived metrics, we used metrics derived from the Leaf Area Density profile (LAD), which is the area of leaves found at each height interval per volume of canopy (m^2 m^{-3}) (de Almeida *et al.*, 2019b). From the LAD we extracted the Leaf Area Index (LAI), which is the sum of LAD values obtained along the profile, the Understory LAI, which corresponds to the sum of LAD values from 1 m to 5 m from the ground and the Leaf Area Height Volume (LAHV), which is the sum of the products of height and mean LAD at that height for each 1 m height interval *i* in the LAD profile (Eq. 3.1). All metrics extracted by LAD were also calculated at 10 m of spatial resolution. These metrics were developed by de Almeida *et al.* (2019a).

$$LAHV = \sum (i \times LAD_i) \quad (3.1)$$

where *i* (*i*= 1,2,3, …, maximum height) is the height within the canopy, and LAD_i is the horizontal mean of leaf area densities at that respective height.

We consider each delimitation of burned and unburned areas within the lidar site as individual samples. As each sample has multiple pixels, we calculated the average for each sample by generating bootstrap estimates, resampling 50 observations with replacement across 10,000 iterations. We considered the unburned mature forest inside each transect as the reference value for the lidar metrics. In transects with more than one unburned sample, we used the mean value between the bootstrap results from these samples. Then, we calculated a relative delta between burned and unburned areas sampled for each lidar transect (Eq. 3.2).

$$\Delta_{LM_{rel}} = ((BA_{LM} - UB_{LM})/UB_{LM}) * 100 \quad (3.2)$$

Where LM correspond to the different lidar metrics used in this study, BA is the value of the lidar metric for the burned area sampled, and UB is the value of the lidar metric for the unburned area sampled. Use of relative delta values helps to minimise the regional differences between locations of the lidar transects, to account for variance explained by the regions.

3.3.3 Data Analysis

To visualise the distribution of lidar metrics across the three different treatments of unburned, burned in a single event and burned in multiple events, we ran a principal

component analysis (PCA) using the R package *FactoMineR* (Husson *et al.*, 2016). We grouped the years since the last fire (YSLF) into 3 classes: 0-3, 4-9 and 10+ years to visualise the differences over time. For this analysis, we used the absolute values of each lidar metric centred and scaled to their unit variance.

The standardised major axis regression (SMA) from the package *smatr* (Warton *et al.,* 2012) was used to test for relationships among the lidar metrics. The ACD, Openness at 5 m, Openness at 10 m and Understory LAI were squared root transformed and Roughness was natural log transformed. Sidak adjusted p-values were used to account for multiple pairwise comparisons. We compared the intercept and slope of these relationships between different lidar metrics using Wald tests. Additionally, we tested for bivariate relationships between fire reoccurrence groups.

To evaluate differences between the fire reoccurrence groups (B1 and B2+), we used the Mann-Whitney U test for non-normal distributed data and the *t*-test for the normal distributed lidar metrics data. We used the same tests to evaluate if the relative delta values for each metric are significantly different from zero in each treatment analysed (Reoccurrences and YSLF groups).

Different regions of Amazon have different biomass stocks (Feldpausch *et al.*, 2012) and forest structure (Feldpausch *et al.*, 2011) resulting from different soil types, precipitation, tree species composition, amongst others, which may affect the recovery after fire (De Faria *et al.*, 2021; Heinrich *et al.*, 2021). Therefore, we classified our samples in “Low” and “High” biomass stock, using the median value (64 Mg C ha^{-1}) calculated in all unburned areas sampled. To analyse the effect of different biomass stocks on forest recovery, we also tested for significant differences in each lidar metric across all group treatments, using the Mann-Whitney U test for non-normal distributed data and *t*-tests for normally distributed data.

To evaluate the effects of YSLF and fire reoccurrence on each lidar metric, we applied linear models including the variable biomass stock as a predictor. To test for the effect of larger regional spatial differences, we also applied equivalent linear mixed effect models using the *lme4* package (Bates *et al.*, 2018), using regions defined by Heinrich *et al.* (2021) as a random effect with a random intercept and a fixed slope. To improve the predictive power, we used the continuous value of the YSLF variable in the models rather than groups.

3.4 Results

3.4.1 Post-fire changes on canopy structure

Our results show that fire has negative impacts on canopy structure. The metrics ACD, maximum and mean height, LAI and LAHV had significant negative delta values, showing a decrease in these metrics when forests area burned ($p<0.001$). Meanwhile, openness at 5 m, 10 m and 15 m, and roughness had significant positive delta values, indicating higher openness and roughness in burned forests ($p<0.001$; Table 3.1). Understory LAI was the only metric that did not have significant differences between unburned and burned forests in the first 3 years after burning (Table 3.1, Figure 3.2, and SI Figure 3.1).

Table 3.1. Parameter estimates ± standard error of linear models for the delta values of the canopy metrics analysed using as predictors: years since last fire (YSLF), Reoccurrences groups (B1 and B2+), Biomass groups (Low and High), and interaction between YSLF and Reoccurrences groups. Significance level: *p<0.05; **p<0.01; ***p<0.001.

	Intercept	YSLF	Reoccurrences	Biomass	YSLF:Reoccurrences	R^2
Δ ACD	-24.98 ± 3.62***	1.63 ± 0.42***	-14.42 ± 5.14**	7.24 ± 3.44*	-0.88 ± 0.80	0.11
Δ Maximum H.	-8.54 ± 1.68***	0.5 ± 0.2*	-5.56 ± 2.39*	2.10 ± 1.60	-0.46 ± 0.38	0.06
Δ Mean H.	-16.01 ± 2.38***	1.08 ± 0.28***	-11.11 ± 3.38**	4.64 ± 2.27*	-0.14 ± 0.53	0.11
Δ Openness 5m	93.56 ± 13.47***	-8.3 ± 1.58***	24.40 ± 19.16	-3.14 ± 12.84	1.48 ± 3.01	0.08
Δ Openness 10m	50.04 ± 7.59***	-3.94 ± 0.89***	23.89 ± 10.80*	-0.51 ± 7.24	0.97 ± 1.7	0.08
Δ Openness 15m	19.84 ± 4.31***	-2.40 ± 0.50***	12.98 ± 6.14*	13.4 ± 4.11**	1.17 ± 0.96	0.1
Δ Roughness	33.18 ± 4.82***	-3.15 ± 0.56***	16.80 ± 6.86*	-4.89 ± 4.6	-1.64 ± 1.08	0.13
Δ LAI	-21.25 ± 2.87***	1.82 ± 0.34***	-3.64 ± 4.04*	6.41 ± 2.72	-0.16 ± 0.63	0.11
Δ Understory LAI	-4.33 ± 5.06	0.17 ± 0.5	17.62 ± 7.12*	4.63 ± 4.81	0.087 ± 1.11	0.02
Δ LAHV	-26.82 ± 3.68***	2.17 ± 0.43***	-12.09 ± 5.18*	8.03 ± 3.5*	-0.69 ± 0.81	0.13

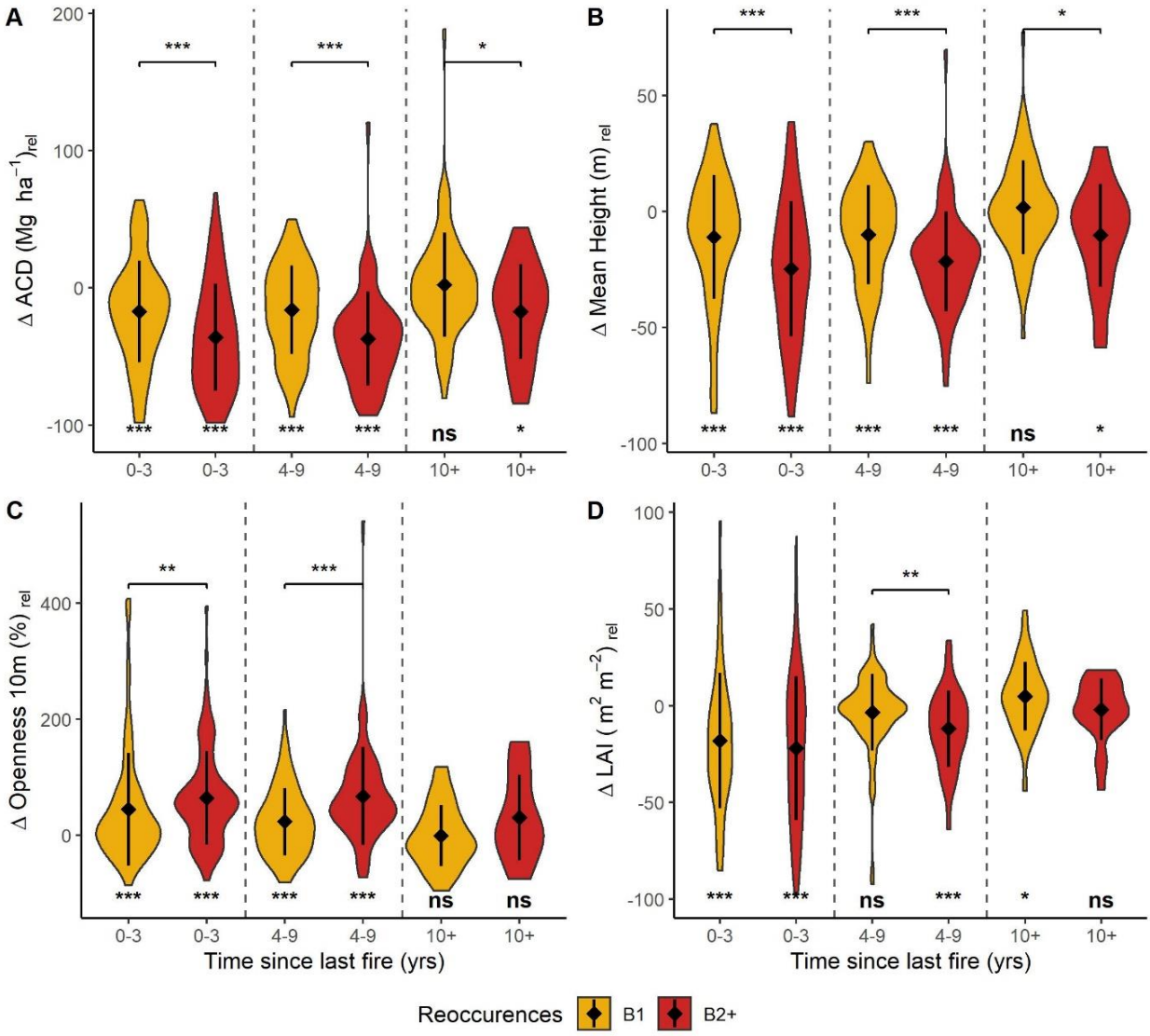

Figure 3.2. Violin plots for the canopy metrics (A) ACD, (B) Mean Height, (C) Openness at 10m and (D) LAI. Yellow violins represent areas with single fire event and red violins represent areas with repeated fire events. Significance levels on the bottom of the violin represent significant difference from 0 (unburned state) and significant levels on top of violins represent significant difference between reoccurrences groups. Groups without brackets had no significant difference. Significance level: *p<0.05, **p<0.01, ***p<0.001; ns, non-significant difference.

Our PCA analysis showed the overall structure of recently burned forests (0-3 YSLF) differs from unburned forests (Figure 3.3 -A). We also evaluated the effects of fire on canopy metrics separating forests with low (ACD < 64 Mg C ha^{-1}) and high (ACD ≥ 64 Mg C ha^{-1}) carbon stocks. The effect of fire significantly changed between low and

high carbon stock forests, with greater differences in ACD, mean height, and LAHV in low carbon stock forests ($p<0.05$), but reduced differences in low carbon forests for openness at 15 m ($p<0.01$; Table 3.1). When we included region in the model as a random effect, the effect of carbon stock was not significant for any metric except openness at 15 m (SI Table 3.2), indicating that our results are driven by differences in biomass between regions rather than within regions.

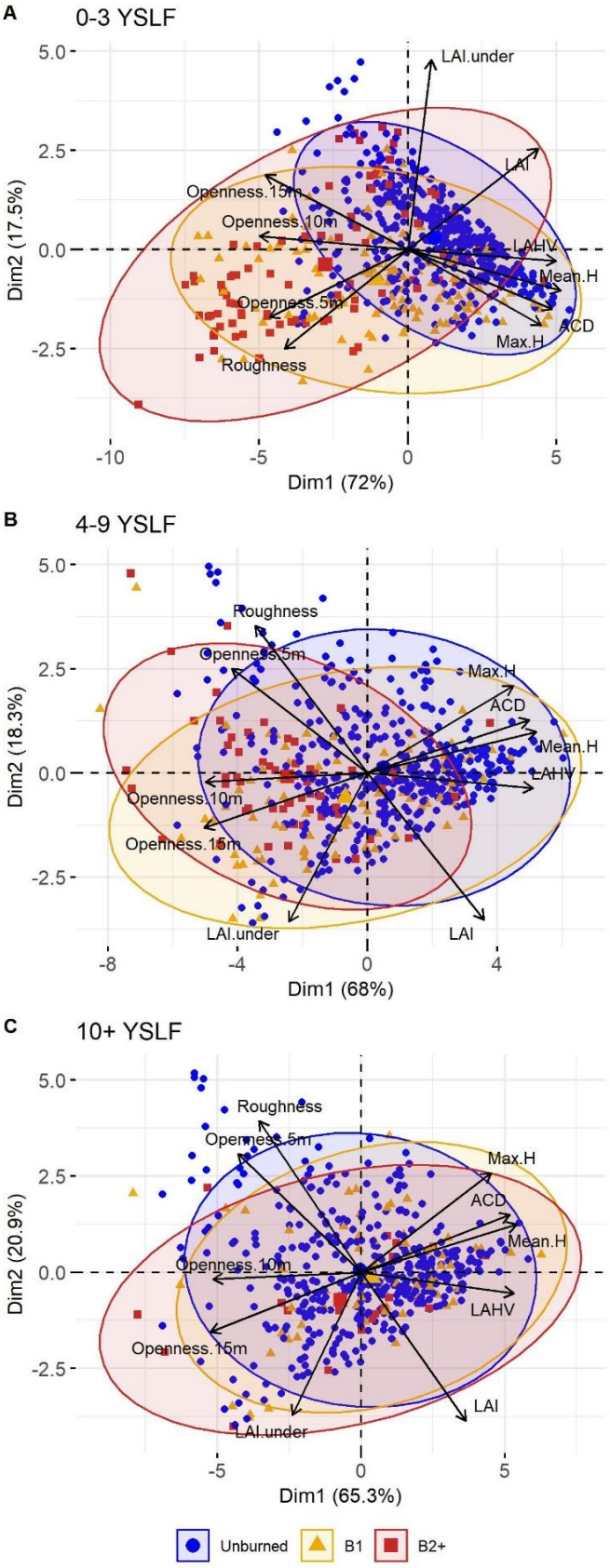

Figure 3.3. Principal Component Analysis for the different YSLF groups A) 0-3 YSLF, B) 4-9 YSLF and C) 10+ YSLF. Ellipses represent the 95% data distribution for Unburned (blue), single fire event (yellow) multiple fire events (red). Percentage values

in parentheses represent the proportion of variance explained the respective axis dimension. For weighting of each variable on each dimension, see SI Table 3.1.

3.4.2 Impacts of repeated fires on canopy structure

Our results show that the reoccurrence of fire increased changes in canopy structure (Table 3.1; Figure 3.2, Figure 3.3-A). We found the reoccurrence of fire significantly explained changes in all metrics ($p<0.05$) analysed except for openness at 5 m ($p>0.05$; Table 3.1).

When focusing on recently burned areas, the 0-3 YSLF group, repeated fires had significantly greater impacts on canopy structure than one fire event for all metrics ($p<0.05$), except LAI, roughness and openness at 5 m (Figure 3.2; SI Figure 3.1). The PCA analysis also showed that burned forests are more variable in overall canopy structure and that this variance increases when the forest burns more than once (Figure 3.3-A). Overall, forest that experienced repeated fires are more dissimilar from unburned forests than those that experienced a single fire event.

3.4.3 Recovery after single and repeated fires

All canopy metrics significantly changed over time after the last fire event ($p<0.05$), except for understory LAI. Over time ACD, maximum and mean height, LAI and LAHV increased after fire, and openness at 5 m, 10 m and 15 m and roughness decreased (Table 3.1). However, the interaction between YSLF and fire reoccurrence did not significantly explain changes in the canopy structure, showing the rate of recovery does not depend on the number of fires experienced. These relationships held even when accounting for regional differences across Amazonia (SI Table 3.2).

We also analysed canopy recovery after fire by YSLF groups (Figure 3.2). Our results showed a trend whereby the violin plots became more similar to forests in an unburned state as YSLF increased. However, this recovery after fire was not consistent for all metrics. For example, in areas with single fire events, the metrics LAI and roughness became similar to an unburned state after 4-9 YSLF; however, in the 10+ YSLF group these metrics were again significantly different from an unburned forest, but now with higher LAI and lower roughness (Figure 3.2-D; SI Figure 3.1-B). This recovery pattern

was consistent across the combined canopy structure as indicated by greater convergence of the fire reoccurrence groups in PCA analysis with YSLF. As the time since the last fire event increases, we find greater overlap in the PCA, with only forests that experienced multiple fire events (B2+) showing a wider spread at 10+ YSLF.

We also compared recovery between forests with low and forests with high carbon stocks by YSLF groups. We found that ACD, mean and maximum canopy height have the same responses. In low carbon stock forests, these metrics did not recover to the unburned state even after 10+ YSLF when they had repeated fire events ($p<0.05$, SI Figure 3.2). In high carbon stocks forests, these metrics recovered to the unburned state in the 4-9 YSLF group if only a single fire event occurred. Areas with multiple fire events still had significantly lower values than unburned forests for ACD, mean and maximum canopy height ($p<0.001$). Also, areas with multiple fire events in forests with high carbon stocks had significantly lower values of ACD, mean and maximum canopy height when compared to forests that had single fire events in 4-9 YSLF group ($p<0.001$; SI Figure 3.2-A,C). Overall, the response of the metrics shows that forests with low carbon stocks take longer time to achieve the unburned state than forests with high carbon stocks, especially in areas that suffered repeated fires. Moreover, these low carbon forests present more significant differences between single and repeated fire events in the metrics analysed (SI Figure 3.2).

3.4.4 Changes in relationships between canopy structure attributes after fire

We analysed the relationship between canopy metrics using standardised major axis regression (SMA) and how these were affected by repeated burning. All metrics were significantly related among them, except by maximum height vs roughness, openness at 5 m vs understory LAI and roughness vs understory LAI (Table 3.2, SI Table 3.3). We also found that fire changed the relationship between all metrics, except by ACD vs mean height and LAI vs roughness, meaning the impacts of fire is not equal on all components of the vertical canopy structure of the forest (Table 3.2, SI Table 3.3). However, the effect of burning on these relationships varied depending on number of fire reoccurrences and the group of YSLF. We found that 44% of the 45 relationships analysed showed significant differences between single fire and unburned forests in the first 3 years after the fire. However, this rose to 80% of the relationships when the

forest burned more than once. In the first 3 years, 69% of relationships were different between single and repeated burns. Over time, we found that the relationships recovered, with only 0% and 24% of relationships of single and repeated fires, respectively, differing from unburned forests more than 10 years after the fire, and only 13% of relationships differing between single and repeated fires (SI Table 3.4).

In particular, the relationship between canopy openness (5 m, 10 m and 15 m) with ACD and LAHV persists between single and repeated burns with ACD and LAHV decreasing in repeated burns. In single burned forests, we find the difference increased in the period 4-9 years after fire to 56% of the relationships, indicating an uncoordinated recovery of forest structure metrics. Overall, relationships between forest structure metrics recover with time, but take longer to recover in areas with repeated fires.

Table 3.2. Summary of standardised major axis regression between lidar metrics for different treatments and YSLF groups. Significance level: *p<0.05, **p<0.01, ***p<0.001; ns, non-significant relationships. The grey box denotes invalid correlations where x and y variables are the same.

Bivariate relationship (y vs x -axis)		Treat.	Intercept			Slope			r^2			p			Difference in slope and elevation						
			YSLF			YSLF group			YSLF group			YSLF group			Treat.	YSLF group					
			0-3	4-9	10+	0-3	4-9	10+	0-3	4-9	10+	0-3	4-9	10+		0-3		4-9		10+	
																B1	B2+	B1	B2+	B1	B2+
ACD	Mean H.	Unb.	0.29	0.29	0.29	0.48	0.48	0.48	0.98	0.98	0.98	***	***	***	Unb.	ns	ns	ns	ns	ns	ns
		B1	0.15	0.21	0.20	0.49	0.48	0.48	1.00	1.00	1.00	***	***	***	B1		**		ns		ns
		B2+	0.32	0.23	0.13	0.48	0.49	0.49	0.99	0.99	1.00	***	***	***	B2+						
	Open 10m	Unb.	14.09	14.09	14.09	-12.39	-12.39	-12.39	0.63	0.63	0.63	***	***	***	Unb.	***	ns	**	***	ns	**
		B1	15.61	12.87	13.93	-14.69	-10.42	-12.30	0.86	0.86	0.79	***	***	***	B1		***		ns		*
		B2+	13.92	12.28	11.78	-12.57	-9.70	-9.12	0.94	0.86	0.85	***	***	***	B2+						
	LAI	Unb.	0.45	0.45	0.45	2.06	2.06	2.06	0.20	0.20	0.20	***	***	***	Unb.	ns	**	**	ns	ns	ns
		B1	1.29	-3.85	-0.96	2.47	2.82	2.36	0.55	0.40	0.14	***	***	**	B1		***		***		ns
		B2+	1.88	0.75	-4.94	1.59	1.54	3.08	0.66	0.46	0.32	***	***	**	B2+						
Mean Height	Open 10m	Unb.	28.67	28.67	28.67	-26.05	-26.05	-26.05	0.69	0.69	0.69	***	***	***	Unb.	**	ns	***	***	ns	**
		B1	31.41	26.28	28.43	-29.94	-21.71	-25.58	0.87	0.87	0.79	***	***	***	B1		*		ns		*
		B2+	28.65	24.60	23.87	-26.62	-19.70	-18.78	0.95	0.86	0.87	***	***	***	B2+						
	LAI	Unb.	-0.03	-0.03	-0.03	4.34	4.34	4.34	0.24	0.24	0.24	***	***	***	Unb.	ns	***	**	*	ns	ns
		B1	2.24	-8.41	-2.58	5.03	5.84	4.91	0.55	0.39	0.14	***	***	**	B1		***		***		ns
		B2+	3.23	1.01	-10.79	3.32	3.18	6.40	0.67	0.45	0.32	***	***	**	B2+						
Open. 10m	LAI	Unb.	1.08	1.08	1.08	-0.16	-0.16	-0.16	0.36	0.36	0.36	***	***	***	Unb.	ns	**	***	ns	ns	*
		B1	0.96	1.64	1.15	-0.16	-0.28	-0.18	0.59	0.36	0.18	***	***	***	B1		*		**		ns
		B2+	0.96	1.23	1.67	-0.13	-0.17	-0.30	0.65	0.37	0.44	***	***	**	B2+						

Correlation coefficient (r^2) and significant value (p) for SMA analysis and slope. The metrics showed are Aboveground Carbon Density (ACD), Mean height (Mean H.), Openness at 10 m (Open 10m), and Leaf Area Index (LAI). The treatment groups (Treat.) are unburned (Unb.), single fire event (B1) and repeated fire events (B2+).

3.5 Discussion

The impacts of fire on forests can persist for decades, causing losses to biomass stocks and altering canopy structure (Almeida *et al.*, 2016; Sato *et al.*, 2016). These effects are intensified by the reoccurrence of fire (Rappaport *et al.*, 2018). However, uncertainties remain regarding how fire affects the vertical canopy structure of forests and their ability to recover. We showed that fires have negative impacts on canopy structure, with areas that experienced repeated burns and/or have lower biomass stocks more affected. This indicates that fire reoccurrence exacerbates the effects of burning and low carbon stock forests are less resistant. The reoccurrence of fires also slows recovery of the forests, with some metrics such as ACD, mean and maximum height not recovering for more than a decade. Fire can degrade forests for long periods because canopy structure is highly complex.

3.5.1 Impacts of single and repeated fires on Amazonian forests

Biomass stocks decrease following a fire event and these changes are more accentuated with repeated fires (Rappaport *et al.*, 2018). Our findings, spanning areas across the Brazilian Amazon show that areas burned once had 23% less ACD than an unburned area in the first three years after the fire event, but in areas that had repeated fires this difference increases to 54%. This impact of repeated fires on ACD is still present even after 10 years since the last fire event (i.e., 18% less ACD than unburned areas), indicating a long-term carbon loss. Previous studies in southern Amazonia show that forests burned once, twice and 3 times lost 46%, 75% and 93% of ACD compared to an intact forest, respectively, when measured one year after fire (Rappaport *et al.*, 2018). Our results show lower values compared to this study which is possibly explained by the different time lag since the last fire event and indicating forest recovery.

Our observed losses in ACD are likely driven by tree mortality and branch fall. In a burning experiment in the southern region, tree mortality in a forest that burned annually for 3 years was only 16% greater than in areas that burned once, and this mortality was mostly restricted to trees with <20 cm DBH (Balch *et al.*, 2011). However, large diameter trees were also shown to die following drought-induced fires when burned annually for 3 to 6 years (Brando *et al.*, 2014). Since large diameter trees store

~25% of carbon in Amazonian forests (Clark *et al.*, 2019), their mortality could represent the additional ACD loss that we observed when forests experienced multiple burns.

Fire typically kills smaller trees after single fire events, but can also kill large trees if repeated fire events occur (Brando *et al.*, 2014). The loss of large trees is particularly important when considering canopy structure since they can create large gaps in the forest canopy, decreasing forest height and increasing canopy roughness (Dalagnol *et al.*, 2019). A study in central Amazon found 166% more opening at 15 m even 3 to 4 years after a fire, in a forest that underwent only one known fire event (Almeida *et al.*, 2016). In our analysis, we found forest areas with repeated fires increase canopy gaps at 5 m height up to 88% more than forests with a single burn in the first 3 years after fire. In the 4 to 9 years since last fire, this difference decreased to 51%. Moreover, when we analysed gaps at 10 m height, we found areas with repeated fires had 29% more gaps than areas with single burn. Canopy openings increase light penetration in the sub-canopy which accelerates recovery, but also favours the establishment of lianas that could halt seedling growth (Schnitzer *et al.*, 2000; Gerwing & Vidal, 2002). Furthermore, the increase in canopy openings can make forests more susceptible to subsequent fire disturbances, since with more light penetration, the canopy and ground tend to become drier, creating a positive feedback cycle (Balch *et al.*, 2008; Le Roux *et al.*, 2022). In drier conditions fire probability and intensity increases, and consequently, mortality rates, especially in extreme drought years (Aragão *et al.*, 2007; Brando *et al.*, 2014; Aragão *et al.*, 2018).

Canopy openings that emerge after fire-induced tree mortality are likely to decrease the mean and maximum height of the forest. We observe this tendency in our results, where repeated fires decrease mean and maximum heights by 8% and 12%, respectively when compared to unburned forests, after 10 years since the last fire. In western Amazonia, Sato *et al.* (2016) also found significantly greater mean height in unburned areas than in burned areas after 4 and 9 years from the fire event. Moreover, in central-east Amazonia in a multi-temporal study, mean height of burned areas was significantly lower than the unburned areas 2.5 and 3.5 years since the last fire (Pontes-Lopes, 2021), which aligns with our findings and indicates burned forests are shifting to shorter forests.

The changes in forest structure caused by fire also impacts the distribution of leaves, branches and tree recruitment (Brando *et al.*, 2012; Balch *et al.*, 2015; Pontes-Lopes, 2021). Our findings show significant differences in forest understory in areas with repeated fire events, where in 4-9 YSLF events the understory LAI increased 28% compared to unburned forests and 5% compared to areas that burned once. Almeida *et al.* (2016) evaluated the forest understory in upland forest of the Rio Negro Basin, using a similar metric used in this study, the LAD from 1-4 m, where they found an increase of 52% of LAD 1-4 m compared to the pre-burned state within 3-4 years before the fire. The lower values in our study may be related to regional differences, since our study spans areas across the whole of the Brazilian Amazon. An increase in understory LAI indicates that understory vegetation can respond to greater light availability following canopy opening and remains resilient to multiple burning events, indicating a potential for regrowth even after repeated burns.

Although the burned dataset MCD64A1 has a coarse spatial resolution that brings uncertainties about the overlapping areas within the lidar transects, our results were consistent with the literature, with repeated fires intensifying the forest disturbances (Balch *et al.*, 2011; Brando *et al.*, 2014; Rappaport *et al.*, 2018). However, it is likely that there is a considerable underestimation in the extent of burned areas since the coarse resolution of the product is not suited to detect small fires, especially understory fires. If detected, these data would potentially increase the certainty of the effects of fire on the vertical structure of tropical forests.

3.5.2 Forest recovery following fire events

Studies across different regions of Amazonia show the effects of fire on forest structure can persist for many years (Almeida *et al.*, 2016; Sato *et al.*, 2016; Rappaport *et al.*, 2018; Silva *et al.*, 2020). Forests can recover low-density biomass quickly, since after a fire, tree species with faster growth and low wood density thrive (Berenguer *et al.*, 2018b) under post-fire conditions of high irradiance and soil enriched by ash from burning (Glaser *et al.*, 2002). However, this fast growth does not always lead to a recovery to the biomass stock of non-burned forests. Our results showed that areas burned multiple times were not able to recover ACD within 10 years since last fire, presenting 19% less ACD than unburned forests. In western Amazonia, biomass

stocks decreased by 7% 10 years after the fire event (Sato *et al.*, 2016). Our higher values are likely driven by the effects of fire reoccurrences and regional differences. Overall, these results show that ACD can take more than one decade to fully recover from fire.

Besides ACD, other important canopy structure attributes are also affected by fire and can take decades to fully recover, having impacts on microclimate and forest functioning (De Frenne *et al.*, 2021). In our analysis, maximum and mean height of the forests were not able to recover within one decade after the last fire event if they suffered repeated burns, indicating that these forests shift to shorter forests for more than a decade. However, canopy openings at 5 m, 10 m and 15 m fully recovered within the first 9 years since fire in areas with single and repeated fires. The closure of the canopy over time is likely related to the growth of understory vegetation. The understory growth is driven by reduced competition for light that emerges after canopy LAI is reduced, supporting greater leaf growth in the understory and transformed into a dense environment (Laurance *et al.*, 2006b). In a forest that suffered only one known fire, LAI reduced 10% compared to 3-4 years before fire (Almeida *et al.*, 2016). Our results show a similar pattern in areas of repeated fires with reductions of 12% compared to the unburned state. Changes in LAI and understory LAI may affect biodiversity promoting species typical of disturbed habitats and reducing habitat available for those species associated with microclimatic and ecological conditions in undisturbed environments.

The ability to recover may be affected by repeated burns if successive burns reduce resilience. However, we found no interaction between recovery and fire reoccurrence, indicating that forests can still recover even after multiple burns if they are given sufficient time in a fire-free state. Whilst we find the potential for forests to recover, multiple burns create a micro-climate where the forest becomes drier and fire ignition is more likely to occur. Re-burning is more likely with fragmentation (Armenteras *et al.*, 2013; Silva Junior *et al.*, 2020a; Driscoll *et al.*, 2021) and the large-scale increase in fire (74% in 22 years) across Amazonia (INPE, 2021). Where the forests continue to re-burn, it is unlikely they will fully recover.

3.5.3 Effects of fire: low versus high carbon stocks forests

Across Amazonia, forests differ in dynamics and carbon stocks because of contrasting climatic and edaphic characteristics of each region (Phillips *et al.*, 2008; Feldpausch *et al.*, 2011; Feldpausch *et al.*, 2012; Quesada *et al.*, 2012). Forests with higher carbon stocks typically have taller trees, tree species with higher wood density and are found on low fertility soils, while forests with low carbon stocks are mostly formed by shorter trees, tree species with lower wood density and likely on high fertility soils, with a resultant fast turnover (Baker *et al.*, 2004; Feldpausch *et al.*, 2011; Quesada *et al.*, 2012). We found that forests with low carbon stocks take longer to achieve the unburned state, especially when suffering from multiple fire events, compared to forests with high carbon stocks. Since forests with low carbon stocks are likely to have more tree species with low wood density, they are also more vulnerable to fire (Berenguer *et al.*, 2021), increasing mortality rates in the following years after fire. This may alter canopy structure and leave the forest prone to other fire events. On the other hand, forests with high carbon stocks are more likely to have tree species with high wood density, which are more resistant to fire (Brando *et al.*, 2012), and consequently have higher rates of survival after fire. Small trees with low wood density have the potential for greater short-term impacts by fire, but they also have greater potential to recover carbon stocks and canopy structure within 10 years.

3.5.4 Holistic recovery of the canopy

A full recovery of the canopy depends on the recovery of all attributes of the canopy, as it provides suitable microclimate and other conditions for several species to survive, e.g. epiphytes, arboreal animals, insects, etc (Lindenmayer & Laurance, 2017; Parra-Sanchez & Banks-Leite, 2022). Although all aspects of forest canopy structure that we measured were shown to be able to recover, different components of forest structure recover at different rates, creating differences in bivariate attribute relationships after fire. Our results consequently indicate that the holistic structure of the canopy does not completely recover after fire. This pattern is intensified in forests that experienced repeated fires with relationships not recovering even after more than a decade. As a result, highly specialised species that may depend on a fully intact canopy for survival may be vulnerable or not return for many years after fire, especially if forests burn

more than once. Conservation of these species is likely to be dependent on preventing fire.

Shifts in attribute relationships after fire will also affect our ability to estimate other attributes of forest structure. Metrics, e.g. biomass, are frequently predicted from canopy height model when using lidar data (Asner & Mascaro, 2014; Longo *et al.*, 2016; Rappaport *et al.*, 2018). However, we found shifts in the relationships between lidar metrics when forests are burned, which means these predictions should not be used for burned areas or should be re-calibrated. Moreover, these shifts persist for more than a decade, indicating that it is vital to know the history of fire when using lidar to predict attributes from lidar metrics.

3.6 Conclusion

Our study that spans the Brazilian Amazon shows post-fire changes to forest canopy structure can persist over decades. Fire impacts not only ACD stocks but also several attributes in the vertical profile of forests that are important to recreate microclimate and ecological conditions essential for long-term forest recovery. Repeated fires have a greater impact on forest structure and increase the time needed to recover to the pre-burned condition. Forests with high carbon stocks are more resistant to fires, but their slower growth rates mean they are less resilient than forests with lower carbon stocks. Different components of canopy structure recover at different rates, causing a decoupling of relationships between metrics that can persist for more than a decade. Whilst some Amazonian forests can recover following fires, fires create conditions that increase the likelihood of further fire re-occurring before full recovery. A drier and hotter climate under climate change and increasing deforestation and fragmentation may further exacerbate the risks of fire reoccurrence, generating a positive feedback cycle where forests have insufficient fire-free time for full recovery.

Chapter 4: Resistance and resilience of canopy structure to fire depends on successional stage in Amazonian secondary forests

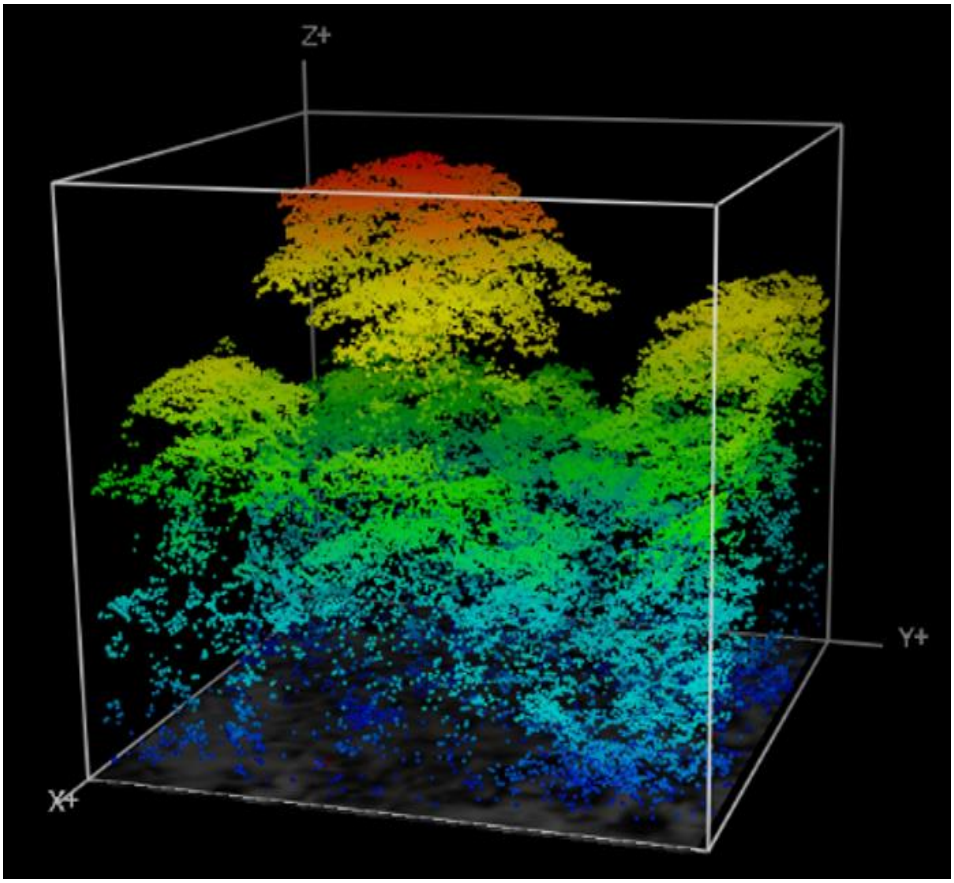

This chapter is in preparation for submission to **Forest Ecology and Management** or a related journal as Laura B. Vedovato, Luiz E. O. C. Aragão, Danilo Roberti Alves de Almeida, Aline Pontes-Lopes, Celso H. L. Silva Júnior, David Bartholomew, Ricardo Dalagnol, Mauro Assis, Eric B. Gorgens, Carlos A. Silva, Ruben Valbuena, Ted R. Feldpausch (in prep.) Resistance and resilience of canopy structure to fire depends on successional stage in Amazonian secondary forests. Forest Ecology and Management.

4.1 Abstract

Secondary forests in the Amazon are important carbon sinks, biodiversity reservoirs, and connections between forest fragments. However, increasing fire frequency threatens their regrowth. In this study, we investigate the impacts of fire on vertical canopy structure of secondary forests of different successional stages and their ability to recover after fire. We used 20 airborne lidar sites across the South-East Amazonian region, which covered both unburned and burned secondary forests. We calculated the following canopy metrics: maximum and mean canopy height, openness at 5 m and 10 m, canopy roughness, leaf area index (LAI) and leaf area height volume (LAHV). Fire negatively affects canopy structure of secondary forests in early successional (ES) and later successional (LS) stages. We only found one instance, in roughness in LS forests, when unburned and burned forests did not significantly differ. In the overall means for each metric, forests in ES stages were less resistant to fire, but more resilient in their post-fire regrowth than LS stage forests. Six out of seven canopy attributes studied showed some potential to recover after fire, but recovery rates were highly variable, taking 12-70 years and were typically faster in ES stages. The greater sensitivity of ES forests likely owes to a drier microclimate due to more pre-existing canopy gaps and their composition and stature, e.g., tree species with traits more vulnerable to fire, and smaller tree sizes with greater exposure to fire. However, the faster recovery in ES stage forests could be due to a greater density of fast-growing, low wood density pioneer species and greater availability of resources such as light and nutrients. Our results indicate that management and policies that mitigate against fire in secondary forests should be implemented to guarantee the success of forest regeneration. These policies are increasingly important as forest succession progresses because of their declining resilience to recover. Mitigation of fires in secondary forests is likely to be critical if they are to continue to provide their wide array of ecological services.

4.2 Introduction

The regrowth of secondary forests on converted land is extensive across the tropics covering 28% of the Neotropics alone (Chazdon *et al.*, 2016). Within Brazil, 56% of all secondary forests are concentrated in the Amazon biome (Silva Junior *et al.*, 2020b).

Tropical secondary forest regrowth plays an important role in climate change mitigation (Chazdon *et al.*, 2016), acting as a carbon sink of 1.6 ± 0.5 Pg C year^{-1} (Pan *et al.*, 2011). Secondary forests also act as important reservoirs of biodiversity, supporting up to 80% of species found in primary forests when reaching 20 years of regrowth (Rozendaal *et al.*, 2019). Furthermore, the conservation value of a secondary forest increases over time (Chazdon *et al.*, 2009; Dent & Joseph Wright, 2009), recovering 2.6% of its species richness and 2.3% of its species composition per year (Lennox *et al.*, 2018). Secondary forests also play an important role in re-establishing connectivity in fragmented landscapes (Metzger, 2003; Uriarte *et al.*, 2016).

Despite tropical forests not being a fire prone environment because of their high humidity, anthropogenic activities combined with severe droughts create conditions for fire ignition, spread, and disturbances in these forests. These are usually understory fires, which weaken the non-fire adapted tree species, causing reductions in the carbon storage and vertical canopy structure of tropical forests. In old-growth forests, fires greatly reduce carbon stocks (Longo *et al.*, 2016; Aragão *et al.*, 2018) decreasing biomass levels by 25% (Silva *et al.*, 2018). Moreover, burning of old-growth forests creates canopy gaps, increases the understory leaf area, and decreases maximum and mean canopy heights (Chapter 3; Almeida *et al.*, 2016; Sato *et al.*, 2016; Pontes-Lopes *et al.*, 2021). The recovery of biomass after fires can take more than a decade in old-growth forests (Chapter 3; Sato *et al.*, 2016; Silva *et al.*, 2018). Although some attributes such as openness and understory leaf area index can fully recover within nine years after the fire event, other canopy metrics such as maximum and mean height, leaf area index (LAI) and roughness can take more than a decade to reach an unburned state (Chapter 3; Almeida *et al.*, 2016). Furthermore, previously burned areas are more susceptible to fire recurrence, especially during drought periods when flammability increases (Alencar *et al.*, 2004). Part of the increase in flammability is driven by changes in the vertical canopy structure of the forest. Since the vertical structure of the forest is responsible for regulating the microclimate in the understory (Ray *et al.*, 2005), changes to it also alter the light availability, temperature and wind in the understory, and determine whether shade tolerant or shade intolerant species recruit (Laurance *et al.*, 2006b).

Secondary forests are even more susceptible to fire events than old-growth forests. Forests with a history of five or more fire reoccurrences accumulate 50% less carbon

than forests without fire or forests that only burned 1 to 2 times (Zarin *et al.*, 2005; Wandelli & Fearnside, 2015). In the Brazilian Amazon, the secondary forest carbon stock could be 8% higher if fire and deforestation were avoided (Heinrich *et al.*, 2021). Although studies of the effects of fire on secondary forest biomass recovery is increasingly widespread (e.g. Zarin *et al.*, 2005; Wandelli & Fearnside, 2015; Heinrich *et al.*, 2021), knowledge is lacking on how fire impacts the vertical structure of secondary forests and whether it can recover.

Old-growth and secondary forests have different forest structures, with secondary forests having shorter trees, more open canopies, lower basal area, and lower maximum diameters (Feldpausch *et al.*, 2005; Berenguer *et al.*, 2018a). Secondary forests typically have lower species richness and a higher density of faster growing tree species with low wood density and higher specific leaf area (Feldpausch *et al.*, 2004; Feldpausch *et al.*, 2005; Berenguer *et al.*, 2018b; Poorter *et al.*, 2021). Primary forests with lower carbon stocks are more vulnerable to canopy structural changes after fire than primary forests with high carbon stocks (Chapter 3). The structure and biomass of secondary forests more closely resembles primary forest with low carbon stocks than those with high carbon stocks. We may therefore expect that secondary forests will respond to fire in a similar manner to primary forests with low carbon stocks. However, secondary forests have different land management histories before becoming secondary forests, which may alter the way that fire impacts these forests and their potential for recovery.

As secondary forests regrow, several attributes associated with plant functioning, species composition, biomass, microclimate and canopy structure recover (Poorter *et al.*, 2021). Secondary forests shift from early successional (ES) stages dominated by light demanding, r-strategy species to later successional (LS) forests with more shade tolerant tree species (Laurance *et al.*, 2006b). The abundance of pioneer species with low wood density and higher specific leaf area, in addition to the dominance of nitrogen-fixing species, declines with secondary succession (Laurance *et al.*, 2006b; Batterman *et al.*, 2013). Meanwhile biomass stocks begin to recover, although at a much slow rate (Steininger, 2000; Jakovac *et al.*, 2021; Poorter *et al.*, 2021). The growth of these trees causes the canopy to increase in height and become less open, changing the microclimate, with the buffering of understory humidity and temperature

increasing (De Frenne *et al.*, 2021). Consequently, LS secondary forests are less prone to burning as they start to resemble primary forests more closely (Chapter 3).

In this landscape-scale study, we evaluated the impact of fires on the canopy structure of tropical secondary forests. Here, we focused on the South-East region of the Brazilian Amazon where secondary forests and fires events are abundant (Smith *et al.*, 2020; Barros-Rosa *et al.*, 2022). We used canopy forest structure metrics derived from airborne lidar data to investigate the resistance of secondary forests in different successional stages to fires and their resilience for regrowth after fire. Here, we defined resistance as the capacity of the forest to remain largely unchanged despite disturbances, and resilience as the capacity of the forest to recover from a disturbance. Specifically, we addressed the following research questions: (i) How does fire impact the canopy structure of secondary forests? (ii) Does this impact differ by successional stage? (iii) Does canopy structure recover after fire? and (iv) Does the rate of forest recovery differ between early (ES) and later successional (LS) stages?

4.3 Methods

4.3.1 Study area and data

Our study spans secondary forests across the South-East region of the Brazilian Amazon (Figure 4.1). Region classification is based on Heinrich *et al.* (2021), which is defined by shortwave radiation, annual precipitation and maximum cumulative water deficit (MCWD). We focus on the South-East region as secondary forests are concentrated in this region and are not uniformly distributed across the Amazon (Smith *et al.*, 2020).

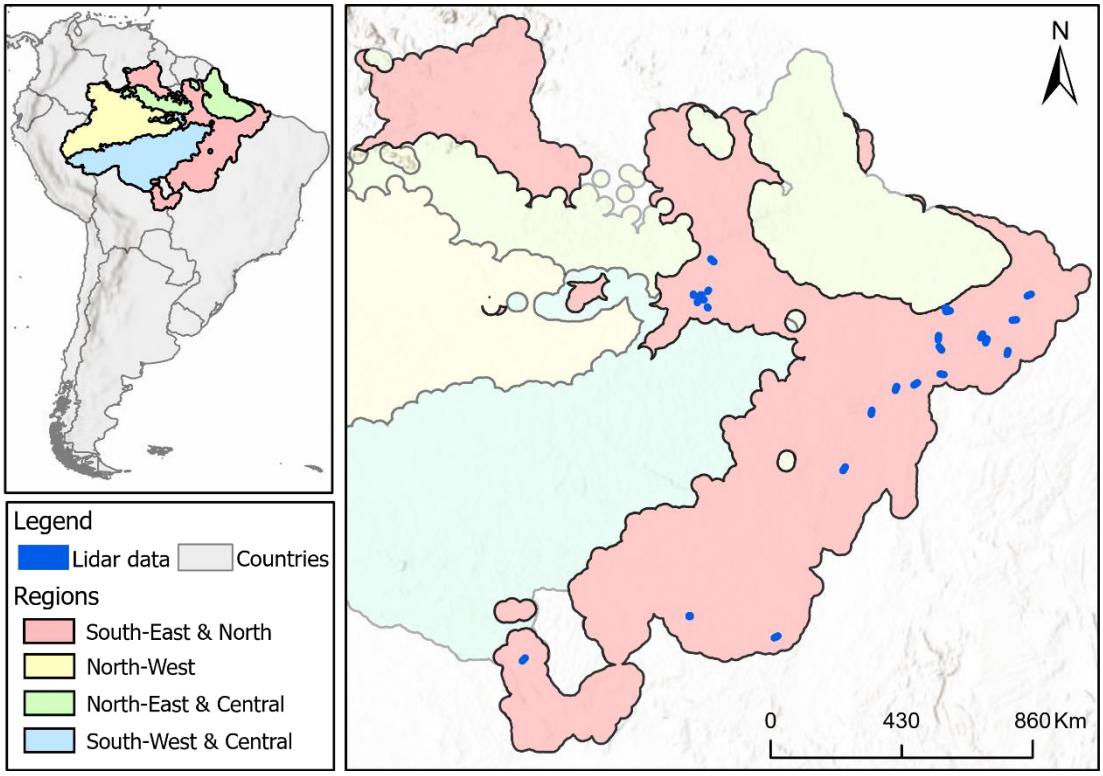

Figure 4.1. The study region with dark blue areas representing the location of lidar flights, red areas representing the South-East & North region, yellow the North-West region, green the North-East & Central region and blue South-West & Central region based on Heinrich *et al.* (2021).

We used 20 airborne lidar sites from the Sustainable Landscape project (Sustainable-Landscapes, 2016) and Improving Biomass Estimation Methods for Amazon (EBA) project (EBA, 2016), which overlapped burned and unburned secondary forests areas within the same site. The used lidar dataset has a minimum point density of 4 points m^{-2}.

To identify areas of secondary forests we used the land use and land cover classification data from MapBiomas collection 5 with spatial resolution of 30 m, which covers the period from 1985 until 2018, allowing analysis of secondary forests of up to 33 years in age (MapBiomas, 2021). We applied a negative buffer of 60 m around our patches of secondary forests and excluded unburned and burned areas smaller than 1 ha to ensure areas represent the core of secondary forests and reduce uncertainty.

To identify the fire events in the lidar surveyed secondary forests, we used the MODIS burned area product (MCD64A1) with a spatial resolution of 500 m (Giglio, 2015) and

overlapped it onto the buffered secondary forests within our lidar sites. As the burned area product has a monthly temporal resolution, we combined it annually from 2001 to 2018, which allowed us to analyse the effects of fire for up 17 years after burning. Then, we calculated for each polygon of burned area how many years have passed since the fire event to the date of the lidar flight. We removed from the analysis areas with repeated fires events because reoccurrence of fire is known to enhance changes canopy structure (Chapter 3; Brando *et al.*, 2014; Balch *et al.*, 2015).

4.3.2 Lidar metrics

We computed several lidar metrics to analyse the vertical structure of unburned and burned secondary forests. The pre-processing of lidar data were executed following Almeida *et al.* (2019). After computing the normalised point cloud, we extracted the canopy height model (CHM) at a spatial resolution of 1 m-grid and we calculated the following metrics: maximum canopy height, mean canopy height, canopy openness at 5 m and 10 m, and canopy roughness. The maximum and mean canopy height values were calculated by aggregating 1 m-grid CHMs to a 10 m-grid, obtaining the maximum and mean values, respectively. Openness at 5 m and 10 m represents the fraction of pixels at heights below 5 m and 10 m, respectively, when aggregating 1 m-grid to 10 m-grid (de Almeida *et al.*, 2020). Roughness was calculated by the standard deviation divided by the mean canopy height resulting from the aggregation of 1 m-grid to 10 m-grid. Besides the CHM-derived metrics, we also calculated metrics derived from the Leaf Area Density (LAD), a voxelized matrix (3D data), which corresponds to the area of leaves found at each height interval per volume of canopy (m^2 m^{-3}) (Stark *et al.*, 2012; Detto *et al.*, 2015; de Almeida *et al.*, 2019b). From the LAD product, we calculated the gridded Leaf Area Index (LAI), which is the sum of LAD along the vertical profile; and the Leaf Area Height Volume (LAHV), which is the sum of the products of height and mean LAD at that height for each 1 m height interval in the LAD profile (Equation 4.1) (de Almeida *et al.*, 2019a). The metrics derived from LAD were also calculated at the 10 m-grid spatial resolution. The use of these metrics allows us to have a detailed information of the vertical distribution of canopy components and detect even subtle differences in the canopy related to fire.

$$LAHV = \sum (i \times LAD_i) \quad (4.1)$$

where *i* (*i*= 1,2,3, …, maximum height) is the height within the canopy, and LAD_i is the horizontal mean of leaf area densities at that respective height.

4.3.3 Early and Later Successional Stage classification

We classified our dataset of secondary forests into early and later successional stages (ES and LS, respectively) by first calculating the mean value of mean canopy height (8.5 m) of all unburned areas inside of each lidar site. Subsequently, we used this threshold to classify the unburned secondary forest polygons as ES stage (average height <8.5 m) and LS stage (average height ≥ 8.5 m) (Figure 4.2). The classification for burned areas followed the same classification as the unburned areas within the same lidar sites, since it is expected they would have the same canopy structure to neighbouring unburned forests if they had not experienced fire.

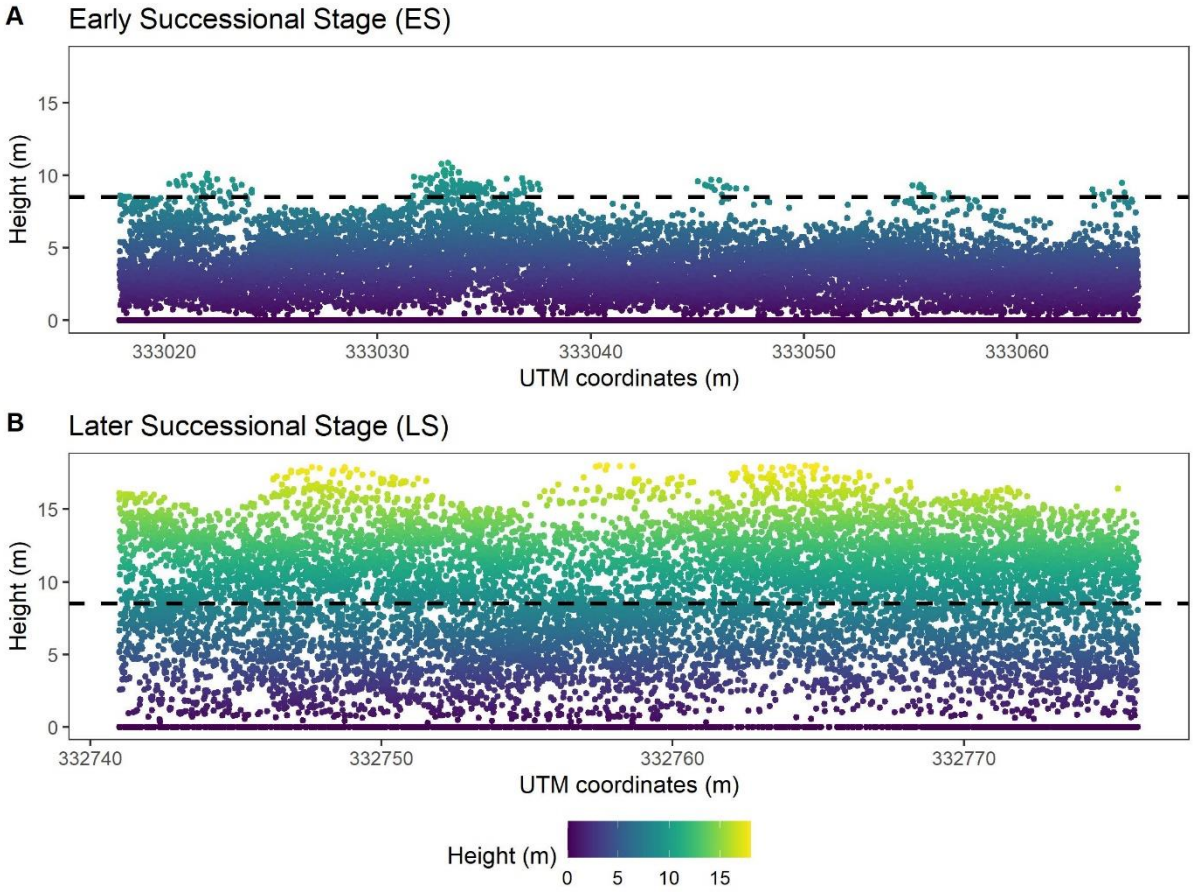

Figure 4.2. Example of (A) early successional stage forest and (B) later successional stage forest. Dashed line represent the height threshold (8.5m) for the classification.

We adopted this height threshold for successional-stage classification since the age of secondary forest introduces additional uncertainty as different previous land use and land management technics alter the rate of successional regrowth and thus the canopy structure recovery (Jakovac *et al.*, 2021). For example, abandoned areas may have greater regrowth when compared with areas of the same age that have ongoing land use, e.g. grazing, that arrests succession (Jakovac *et al.*, 2015; Jakovac *et al.*, 2021). From our classification, in the ES stage (average height < 8.5 m) there are more pixels concentrated in young forest (less than 10 years old) but also older secondary forests which did not achieve a mean canopy height taller than 8.5 m (SI Figure 4.1). In contrast, in the LS stages areas, we found young secondary forests with mean canopy heights taller than 8.5 m (SI Figure 4.1). This pattern is likely driven by previous land use and land cover before the area was classified as a secondary forest, which can interfere with the recovery of these secondary forests (Wandelli & Fearnside, 2015; Jakovac *et al.*, 2021). However, these incidents represented a small proportion of the data meaning the mean age of secondary forests in an ES stage was 7.4 years and 6.5 years in unburned areas and burned areas, respectively, while in LS stage it was 13.8 and 11.1 years respectively (SI Table 4.1). Overall, forests classified as ES stage according to their canopy height are younger than LS stage forests in our dataset. An example of CHMs in ES and LS unburned and burned is demonstrated on Figure 4.3.

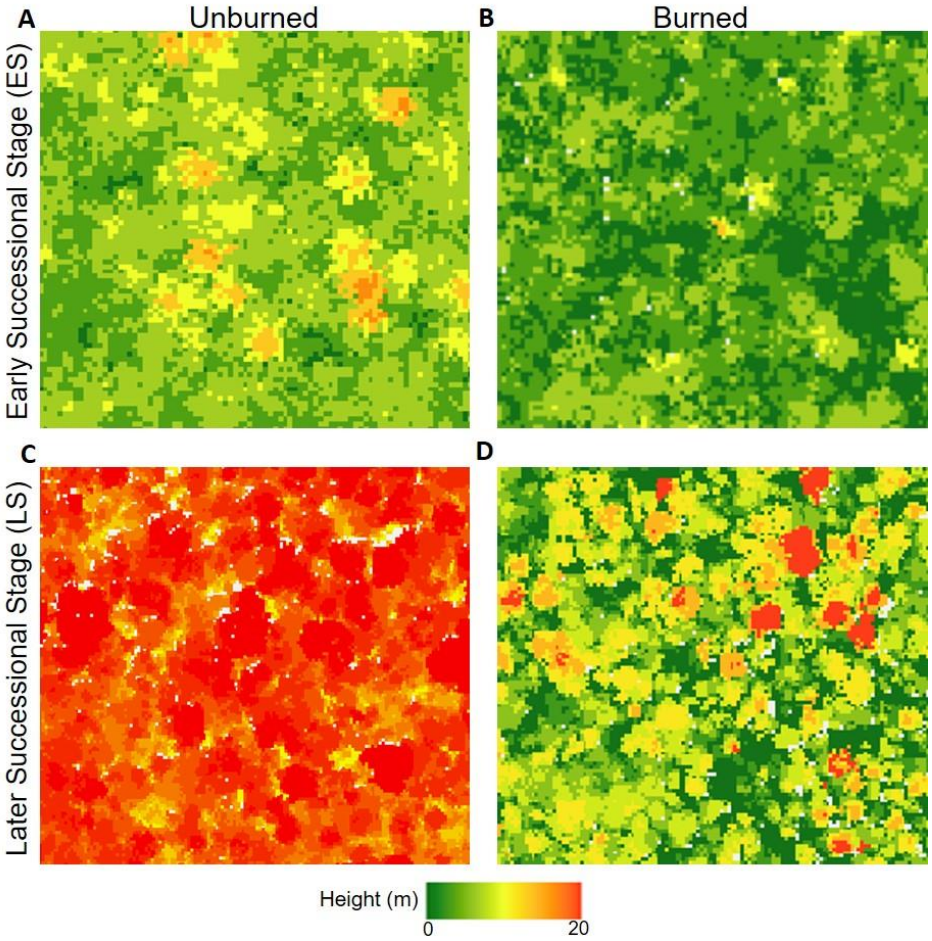

Figure 4.3. Examples of CHM of (A) early successional stage forest unburned, (B) early successional stage burned, (C) later successional stage forest unburned and (D) later successional stage forest burned.

4.3.4 Data Analysis

To evaluate differences between unburned and burned areas for each lidar metric, addressing our research question i, we used Mann-Whitney U tests for non-normally distributed data and *t*-tests for the normally distributed data.

A linear mixed effect model was fitted to analyse differences between unburned and burned areas in the different successional stages, addressing our question ii. Burned status, successional stage and their interaction were included as fixed effects and lidar sites (ID) was included as random effect. We applied a squared root transformation on maximum and mean canopy height and LAHV, and natural logarithmic transformation on openness at 5 m and roughness to normalise the data.

To evaluate the recovery of the canopy structure metrics over time (question iii) and differences in recovery rates between ES and LS stages (question iv), we analysed the LiDAR metrics as a chronosequence. We applied an additional linear mixed effect model using only the burned area data. The time since the last fire (YSLF), the successional stage and their interaction were included as fixed effects and the lidar site ID was again included as a random effect variable. We used this model to predict the recovery time for burned forests to reach the mean values of unburned areas for each lidar metric. All linear mixed effect models were undertaken using the *lme4* package (Bates *et al.*, 2018) in R statistical software v4.1.2 (R Core Team, 2020).

4.4 Results

4.4.1 Impacts of fire on secondary forests

Fire negatively affects canopy structure of secondary forests, with a more degraded state for all metrics in burned forests compared to unburned secondary forests ($p<0.001$) (SI Figure 4.2). Compared to unburned areas, burned areas had lower canopy heights (mean and maximum), LAI, and LAHV; and higher values of openness (at both 5 m and 10 m) and roughness. These patterns were consistent even when we divided the forests into ES and LS stages (Figure 4.3, Table 4.1). We only found one instance when unburned and burned forests did not significantly differ, with roughness being equivalent in LS forests irrespective of burning status ($p>0.05$; Figure 4.4-E).

Although fire impacted all metrics in both ES and LS forests (except roughness in LS), the magnitude of the observed differences varied by successional stage. This is showed by a significant interaction in our models between burning status and successional stage for all metrics analysed ($p<0.001$), except by the LAI ($p>0.05$; Figure 4.4). When analysed by the overall means of each metric, a large difference was observed in the percentage change in openness at 5 m, with 115% more openness in burned than unburned areas in ES stage, but only 32% more openness in a LS stage. This pattern was also found in the other metrics. Maximum and mean height was 22% and 33% lower in burned areas compared to unburned areas in ES stage forests, but only 8% and 14% in LS stage, respectively. Roughness was 25% higher in burned areas compared to unburned areas in ES stage forests and 10%

higher in LS stage forests. LAI and LAHV was 36% and 49% lower in burned than unburned areas in ES stage forests and only 18% and 24% lower in LS stages, respectively (Figure 4.4).

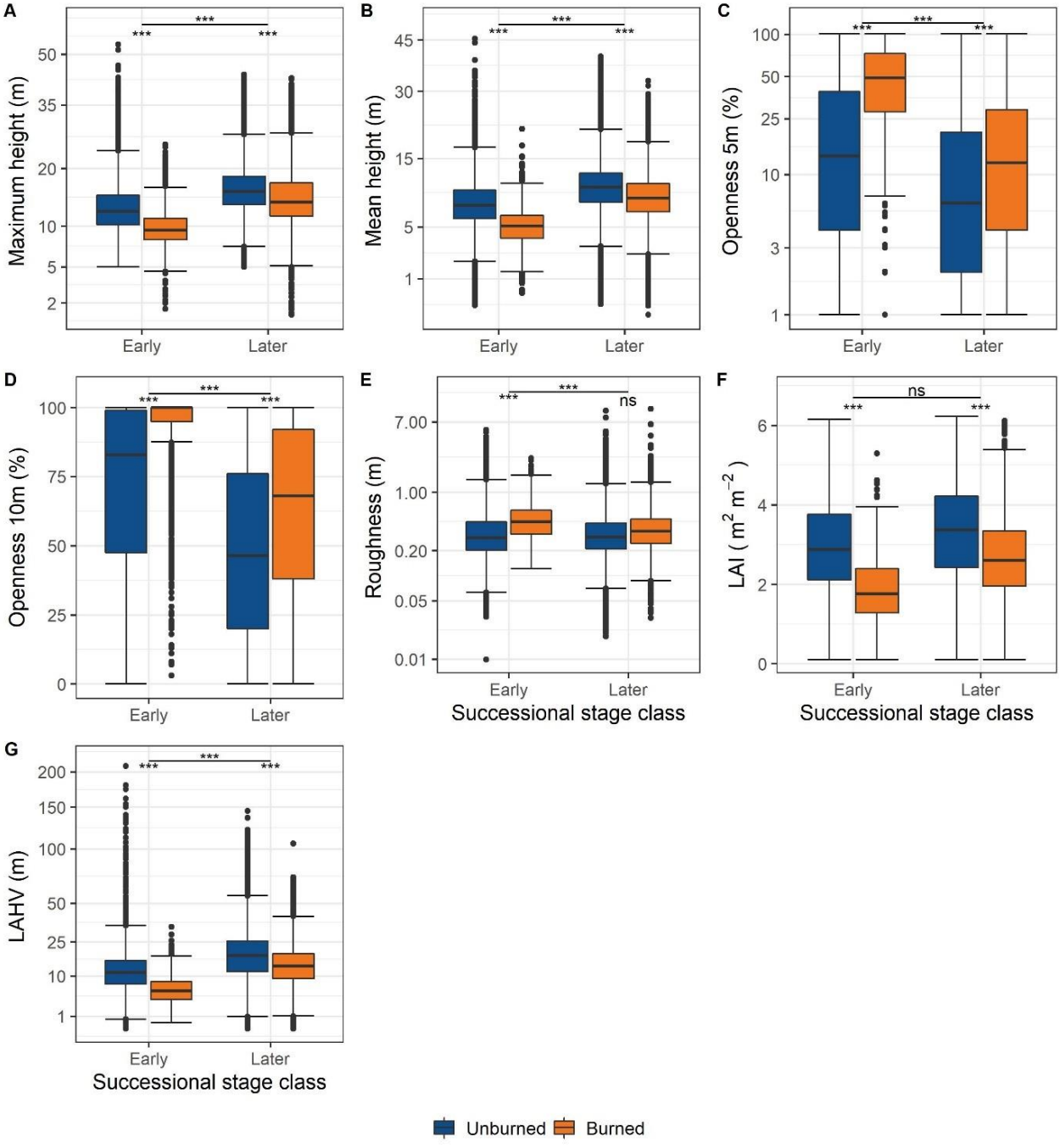

Figure 4.4. Boxplots for the canopy metrics (A) Maximum height (m), (B) Mean height (m), (C) Openness at 5 m (%), (D) Openness at 10 m (%), (E) Roughness (m), (F) Leaf Area Index (m^2 m^{-2}) and (G) Leaf Area Height Volume (m). Boxplots are divided into unburned (blue) and burned (orange) categories and grouped by the forest successional stage: Early (left), Later (right). The Y-axis is square root transformed for maximum height, mean height and LAHV; and natural log transformed for openness

at 5 m and roughness. Asterisks represent significant differences between unburned and burned categories for each successional stage and the interaction effect from the mixed effects model. Significance levels: *p<0.05, **p<0.01, ***p<0.001; ns, non-significant relationships.

Table 4.1. Parameter estimates ± standard error for canopy metrics analysed as fixed effects in the mixed effects models for forest successional stage (ES and LS), status of the forest (Unburned and Burned) and their interaction. Lidar flight site ID was included as a random effect and the coefficient represents the variance between levels. Asterisks represent the significance level of each variable: *p<0.05; **p<0.01; ***p<0.001. Successional stages and forest status coefficients represent comparisons between categories (ES and LS; Unburned and Burned, respectively). Total (conditional) R^2 represents the proportion of variance explained by our model and fixed effect (marginal) R^2 represents the variance explained by the fixed effect parameters.

	Intercept	Successional Stage (LS)	Forest Status (Burned)	Successional Stage (LS):Forest Status (Burned)	Flight ID	Fixed effect (marginal)R^2	Total (conditional) R^2
Sqrt. Maximum H.	3.41 ± 0.12***	0.78 ± 0.15***	-0.17 ± 0.01***	-0.27 ± 0.02***	0.09	0.29	0.48
Sqrt. Mean H.	2.63 ± 0.11***	0.72 ± 0.13***	-0.22 ± 0.02***	-0.16 ± 0.02***	0.07	0.24	0.39
Ln Openness 5m	-1.84 ± 0.29***	-0.94 ± 0.3**	0.4 ± 0.04***	-0.2 ± 0.04***	0.51	0.09	0.3
Openness 10m	0.78 ± 0.06***	-0.38 ± 0.07***	0.07 ± 0.01***	0.12 ± 0.01***	0.02	0.23	0.38
Ln Roughness	-1.15 ± 0.13***	-0.07 ± 0.15	0.15 ± 0.02***	-0.16 ± 0.02***	0.1	0.004	0.24
LAI	2.56 ± 0.42***	0.72 ± 0.48	-0.19 ± 0.04***	0.03 ± 0.05	0.7	0.06	0.41
Sqrt. LAHV	2.98 ± 0.39***	1.54 ± 0.45*	-0.29 ± 0.04***	-0.24 ± 0.05***	0.62	0.22	0.47

4.4.2 Recovery of secondary forests after fire

Our results show that the canopy structure of secondary forests becomes more similar to that of nearby unburned forests with the same successional stage with time after fire. In the ES stage, maximum canopy height ($p<0.001$), mean canopy height ($p<0.001$), openness at 5 m ($p<0.01$), openness at 10 m ($p<0.001$) and LAHV ($p<0.05$) could recover over time to the unburned state (Figure 4.5, Table 4.2, indicate in YSLF (ES) column). However, in the LS stage secondary forests, only maximum canopy height ($p<0.01$), openness at 5 m ($p<0.05$) and roughness ($p<0.001$) could recover to the unburned state (Figure 4.5, Table 4.2, indicate in YSLF (LS) column).

Early and later successional stage secondary forests also have different rates of recovery for some canopy structure metrics. According to the adjusted linear models, maximum canopy height and openness at 5 m have a faster recovery rate in ES stages, reaching the unburned state in 12 and 14 years, respectively (Figure 4.5, Table 4.2 indicated in YSLF (ES) column, Table 4.3), while LS stages take 19 and 29 years to recover these metrics to the unburned state, respectively (Figure 4.5, Table 4.2 indicated in YSLF (LS) column, Table 4.3). The mean canopy height and openness at 10 m also has significantly different rates of recovery between successional stages (Table 4.2, indicated in YSLF:Successional Stage (LS) column). However, these metrics do not have a significant rate of recovery in LS stages. Instead, only forests in ES stages have significant rates of recovery for these metrics, requiring 20 years for mean canopy height to reach the unburned state and 17 years for openness at 10 m. In ES stage forests, LAHV could recover to the unburned state in 40 years. Whilst in LS stage forest, we also found that roughness could reach the unburned state, but only 70 years after fire (Table 4.3). Overall, recovery rates of different forest structure metrics are highly variable and dependent on the successional stage.

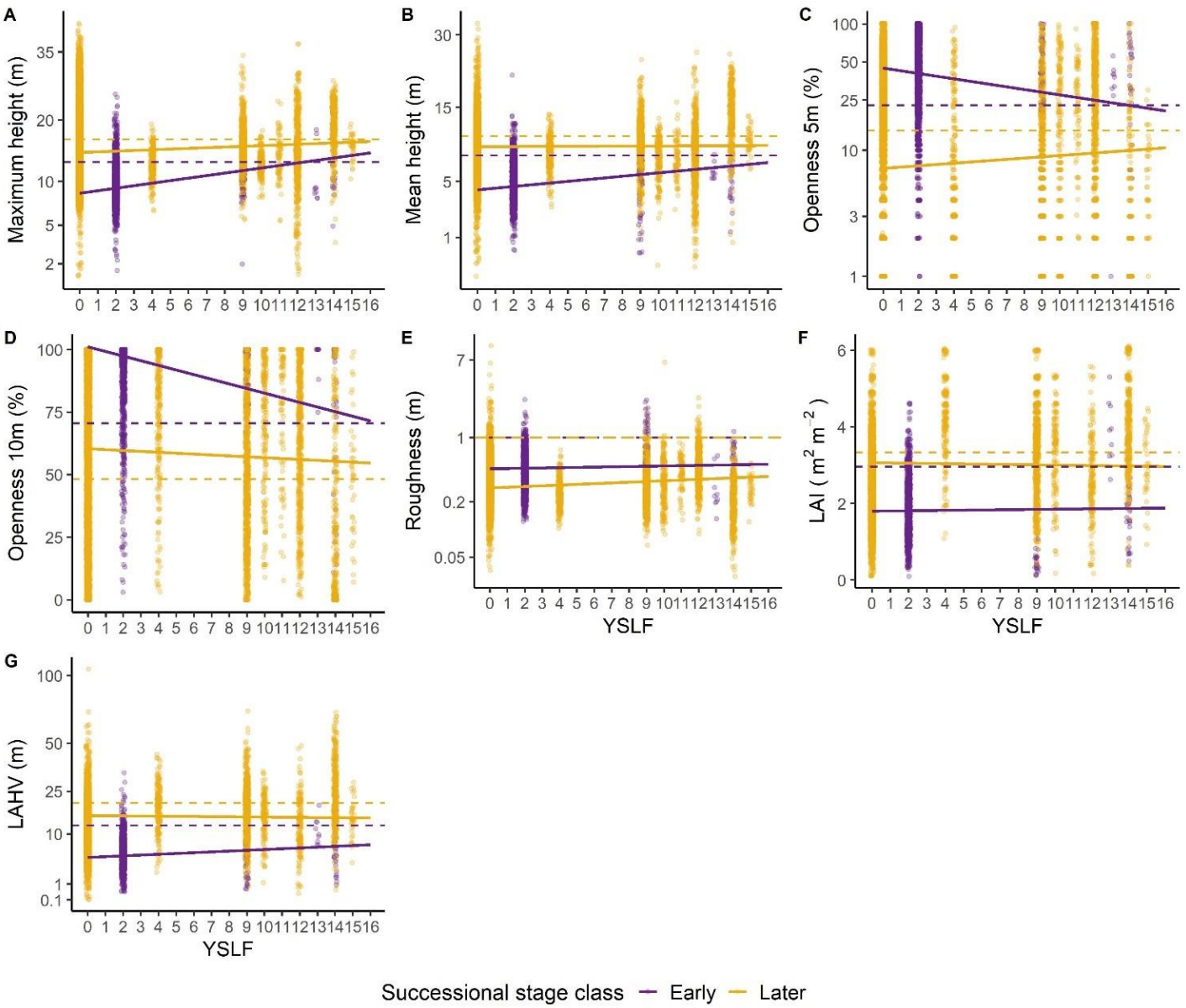

Figure 4.5. Recovery of canopy structure metrics with the year since last fire (YSLF). (A) Maximum height (m), (B) Mean height (m), (C) Openness at 5 m (%), (D) Openness at 10 m (%), (E) Roughness (m), (F) Leaf Area Index (m^2 m^{-2}) and (G) Leaf Area Height Volume (m). The y-axis is square root transformed for maximum height, mean height and LAHV; and natural log transformed for openness at 5 m and roughness. Purple lines indicate forests in an early successional stage and yellow lines forests in a later successional stage. Dashed lines refer to mean values of unburned areas for each successional stage.

Table 4.2. Parameter estimates ± standard error for canopy metrics analysed as fixed effects in the mixed effects models for year since last fire (YSLF). Model estimates are provided for both successional stages (ES and LS). Successional Stage (LS) represents the difference in the intercept and YSLF: Successional Stage (LS) represent the difference in the slope of the line in later successional stage forests compared to early successional stage forests. Lidar flight site ID was included as a random effect and the coefficient represents the variance between levels. Asterisks represent the significance level of each variable: *p<0.05; **p<0.01; ***p<0.001. Total (conditional) R^2 represents the proportion of variance explained by our model and fixed effect (marginal) R^2 represents the variance explained by the fixed effect parameters.

	Intercept (ES)	Intercept (LS)	YSLF (ES)	YSLF (LS)	LS	YSLF:Successional Stage (LS)	Flight ID	Fixed effect (marginal) R^2	Total (conditional) R^2
Sqrt. Maximum H.	2.92 ± 0.24***	3.78 ± 0.13***	0.05 ± 0.01***	0.01 ± 0.005**	0.87 ± 0.28**	-0.04 ± 0.01***	0.17	0.14	0.42
Sqrt. Mean H.	2.05 ± 0.23***	3.01 ± 0.12***	0.04 ± 0.01***	0.002 ± 0.005	0.95 ± 0.26***	-0.04 ± 0.01***	0.15	0.2	0.5
Ln Openness 5m	-0.8 ± 0.53	-2.6 ± 0.27***	-0.05 ± 0.02**	0.02 ± 0.01*	-1.83 ± 0.6**	0.07 ± 0.02***	0.82	0.16	0.5
Openness 10m	1.01 ± 0.11***	0.6 ± 0.06***	-0.02 ± 0.004***	-0.004 ± 0.002	-0.41 ± 0.13**	0.01 ± 0.005**	0.04	0.15	0.45
Ln Roughness	-0.78 ± 0.19***	-1.26 ± 0.1***	0.01 ± 0.01	0.02 ± 0.004***	-0.48 ± 0.22*	0.01 ± 0.008	0.11	0.09	0.4
LAI	1.80 ± 0.48***	3.07 ± 0.3***	0.005 ± 0.01	-0.01 ± 0.01	1.26 ± 0.55*	-0.01 ± 0.02	0.67	0.12	0.53
Sqrt. LAHV	2.15 ± 0.45***	3.96 ± 0.25***	0.03 ± 0.01*	-0.01 ± 0.01	1.81 ± 0.52**	-0.04 ± 0.02	0.58	0.2	0.52

Table 4.3. Recovery of canopy metrics by forest successional stage and time to recover to the mean unburned state. Recovery times are predicted from mixed effects models (Table 4.2).

	Early Stage		Later Stage	
	Does it recover?	How long?	Does it recover?	How long?
Maximum Height	√	12	√	19
Mean Height	√	20	X	NA
Openness at 5m	√	14	√	29
Openness at 10m	√	17	X	NA
Roughness	X	NA	√	70
LAI	X	NA	X	NA
LAHV	√	40	X	NA

4.5 Discussion

Secondary forests are highly susceptible to fire, especially because of their drier understory and high abundance of pioneer species with low wood density that are more likely to die after fire (Berenguer *et al.*, 2021). Repeated burning of secondary forests can reduce carbon stocks by more than 50% (Zarin *et al.*, 2005; Wandelli & Fearnside, 2015). However, uncertainty remains regarding how fires affects the vertical structure of secondary forests, and how successional stage affects their resistance and resilience to fire. By analysing airborne lidar data on nearby burned and unburned secondary rainforests with different post-fire ages, we show that the vertical structure of secondary forests is vulnerable to fire, but that these impacts are dependent on successional stage. Recovery rates, however, vary among attributes, with maximum height and a closed canopy recovering faster than mean height, roughness and biomass. Overall, ES stage forests show more potential for faster recovery than LS stage forests despite experiencing greater changes in their canopy structure post-fire.

4.5.1 Impacts of fire on secondary forests

We found that the canopy structure of ES stage forests is more affected by fires based on the overall mean of each metric, which has important implications for forest recovery. Canopy gaps at 5 m height presented the highest difference between ES and LS stages, when compared differences of burned and unburned areas, where ES stages had 83% more gaps than LS stage forests. This pattern is consistent for canopy height, roughness and leaf area height volume (LAHV). Early successional stage forests are probably less resistant to fire because these forests have a greater dominance of pioneer species with low wood density (Park *et al.*, 2005; d'Oliveira & Ribas, 2011; Berenguer *et al.*, 2018a), which have greater propensity to die within the first years after a fire (Barlow *et al.*, 2003a; Brando *et al.*, 2012; Berenguer *et al.*, 2021). The higher frequency of canopy gaps in our studied forests can be attributed to contagiousness, which is the tendency of new canopy gaps to form nearby to previous gaps (Jansen *et al.*, 2008; Hunter *et al.*, 2015). This contagiousness is driven by how fire changes interrelated microclimatic factors such as humidity, temperature buffering, and wind exposure (De Frenne *et al.*, 2021). Following changes in the microclimate, these areas are prone to more intense and recurrent fires that may cause more damage to the forest structure, with declines of more than 50% of small, medium and large basal areas plants (Prestes *et al.*, 2020). LAI was the only metric analysed which was equally affected in both ES and LS forest stages. We hypothesise that this result may be driven by the equivalent spread of fire over the vertical profile, burning leaves and branches equally in ES and LS stages, since the difference in mean canopy height was only 2 m before burning. Moreover, the drop of leaves may be a stress reaction of trees after fire which may not differ between successional stages (Karavani *et al.*, 2018). However, LAI may also not be a good metric to evaluate the vertical effects of fire in canopy structure because LAI does not differentiate between leaves and branches of different heights in the vertical profile and also because of the saturation of the LAI, a well-known problem in optical remote sensing data (Huete *et al.*, 2002; Galvão *et al.*, 2011).

4.5.2 Recovery of secondary forest after fire

Different attributes of the vertical canopy structure have different potential to recover after fire. Fire, and recurrent fire in understory vegetation affect the forests by changing species composition and forest structure (Prestes *et al.*, 2020). Following fire, the understory regrows quickly in some forests, causing a rapid closure of the canopy at 5 m height (d'Oliveira & Ribas, 2011). The presence of pioneer species in secondary forests, e.g., *Cecropia* sp. and *Miconia* sp. (Mesquita *et al.*, 2001; Zambiazi *et al.*, 2021), allows the canopy to recover quickly owing to their fast growth rates. We found that maximum canopy height could recover quickly, probably because only one single tree is required to grow to the top of the canopy. This can happen more easily in secondary forests because the open environment allows light-dependent pioneer species to recruit (Laurance *et al.*, 2006b). In contrast, LAI was not able to recover within the timeframe of this study (16 years). This finding is likely related to an intense reduction in leaf and branch density across the whole vertical strata caused by fire, which does not show a tendency to recover over time, potentially because of damage to the stems that then leads trees to die. On other hand, this finding may just be a limitation of lidar-derived LAI at detecting differences over time as stated in section 4.1. Further studies are necessary to determine more precisely the role of LAI in detecting the effects of fire on the vertical forest structure.

Although maximum height and openness at 5 m recovered in both ES and LS stage secondary forests, ES stage forests recovered faster. For example, the recovery of openness at 5 m in LS stages takes more than double the length of time to recover than in ES stage forests (29 vs 14 years, respectively). This emphasises the low resilience of LS forest compared to ES. This is probably related to a greater dominance of nitrogen fixing species in ES stages (Batterman *et al.*, 2013; Poorter *et al.*, 2021), increasing the soil fertility and providing a suitable environment for low wood density tree species with higher specific leaf area (Quesada *et al.*, 2012; Poorter *et al.*, 2021). These species regrow faster and consequently decrease canopy openness faster in ES forests. A lower density of stems in ES forests (Feldpausch *et al.*, 2007) is also likely to increase the rate of canopy closure as competition for resources is reduced. Secondary forests have a large density of low wood density trees and are highly vulnerable to drought conditions (Phillips *et al.*, 2009a; Feldpausch *et al.*, 2016;

Berenguer *et al.*, 2021), which typically co-occur with fire, and therefore the potential for regrowth is likely to be higher when competition for water is reduced.

The recovery of mean canopy height after burning to an unburned forest state is likely to be more challenging for a LS stage forest because for this recovery to happen, LS forests would need to achieve a higher number of trees close to 10 m height than ES forests. However, tree mortality after fires probably prevents this recovery within the timeframe of this study (Silva *et al.*, 2018). Meanwhile, for forests in ES stages, mean canopy height in the unburned state is shorter (8 m). Consequently, recovery can happen within two decades as a lower density of stems need to regrow after mortality to attain this mean canopy height of 8 m. Whilst our results suggest ES stage forests recover faster after burning, this is explained by both a faster growth rate and a shorter height to grow when compared with LS forests.

Biomass is particularly slow to recover after disturbance events since it is predominantly driven by the abundance of large trees (Poorter *et al.*, 2021) and secondary forests lose biomass through self-thinning as dense even-aged regrowing stems compete (Feldpausch *et al.*, 2007). In our study, we used the LAHV metric, which is closely related to biomass (de Almeida *et al.*, 2019a), and found that it was also slow to recover after fire. Forests in a LS stage have greater biomass and could not recover within the timeframe of our analysis. In contrast, ES stage forests are populated by low wood density tree species that have lower biomass and faster growth rates (Poorter *et al.*, 2021). Therefore, these forests have greater resilience to recover any reductions in biomass within approximately four decades after fire.

Although ES stage forests have greater potential to recover most canopy attributes, canopy roughness could only recover in LS secondary forests. ES stages may not recover canopy roughness during the study period due to post-fire recruitment and competition among dense even-aged individuals where canopy recovery occurs but is dominated by many individuals of the same height (Feldpausch *et al.*, 2007; Prestes *et al.*, 2020). Recovery of canopy roughness in LS is particularly slow, taking on average 70 years. This is because canopy roughness results from a heterogeneous mix of gaps dynamic and tree size, form, and age classes that require time to develop, and that are often lacking secondary forests experiencing severe or multiple disturbances that create structural homogeneity (Poorter *et al.*, 2021).

Even with some uncertainties in the dataset about burned areas owing to a coarse spatial resolution, our results were consistent with the literature, showing ES stage forests more vulnerable to fire effects (Brando *et al.*, 2012; Berenguer *et al.*, 2021). However, it is likely that many understory fires in these secondary forests were underestimated since the coarse resolution of the product is not suited to detect small fires. The use of a higher spatial resolution in the burned area products would support a more precise estimation of the impacts of fire on the vertical canopy structure of secondary forests.

4.5.3 Implications of burning secondary forests

Secondary forests in Amazonia play an important role in biodiversity conservation and mitigation of carbon emissions (Pan *et al.*, 2011; Chazdon *et al.*, 2016; Lennox *et al.*, 2018; Rozendaal *et al.*, 2019). An increased frequency of fire in these secondary forests, however, threatens their potential to regrow. We show that fire disturbances during secondary forest regrowth can delay the regeneration of vertical structure for decades because they are unable to fully recover from fires. Later successional stage forests have low resilience because the damage caused to their vertical structure is rarely recovered within two decades. The recovery of vertical structure and heterogeneity has important implications for flora and fauna biodiversity ensuring a sufficiently complex canopy structure for species coexistence and a microclimate that supports subcanopy specialists (Lindenmayer & Laurance, 2017). Policies that mitigate against fire, therefore, should be implemented in secondary forest to facilitate successful forest regeneration. These policies are increasingly important as forest succession progresses because of their declining resilience to recover. Mitigation of fires in secondary forests is likely to be critical if they are to continue to provide their wide array of ecological services.

4.6 Conclusions

In this study, we investigate the impacts of fire on the structure of secondary forests of different successional stages and their ability to recover. Secondary forests of all successional stages that experienced fire were more degraded than unburned forest

areas. Roughness was the only canopy metric that did not differ between unburned and burned areas in secondary forests, but only in later successional stages. Secondary forests in the early successional stage experienced more negative impacts on canopy structure from fire than later successional stages, except for leaf area index (LAI), which did not experience different impacts between early and later successional stages. Recovery rates were highly variable among the canopy metrics and depended on the successional stage of the forest. Overall, early successional stage forests have more potential for a faster recover than later successional stage forests despite experiencing greater changes in canopy structure post-fire. To improve our findings, we recommend future studies to develop lidar-based equations for secondary forests, as well as more acquisitions of field-base data that integrates with lidar measurements over larger patches of secondary forests. In addition, more lidar time series will help to confirm the temporal patterns indicated by our chronosequences. Fire management policies need to be introduced in secondary forests in ES and LS stages, assuring protection for vulnerable ES stage forests and sufficient time for LS forest to regenerate and provide key ecosystem services.

Chapter 5: Synthesis and Conclusions

Jamaraquá Community, National Forest of Tapajós, PA, Brazil

5.1 Summary of key findings

The research presented in this thesis investigates the effects of historical and recent fires on the dynamics and structure of Amazonian forests. The main aims of this thesis are to understand the long-term and short-term legacies of fire in both old-growth and secondary Amazonian forests. This thesis focuses on changes in biomass and vertical canopy structure as these are important for maintaining the carbon sink and microclimate of tropical forests.

My first empirical chapter (Chapter 2) focuses on the effects of historical fires on the response of forests to drought, using PyC as a proxy. This chapter reveals that forests that experienced historical fires potentially have a greater resilience to drought. The subsequent empirical chapters (Chapters 3 and 4) focus on the effects of recent fires in old-growth and secondary Amazonian forests. These chapters show that forests are negatively affected by fire. However, the extent of damage and recovery is highly variable, depending on fire reoccurrence, carbon stocks and forest successional stage.

In the next paragraphs I present the key findings of this thesis.

5.1.1 Chapter 2: Past fires enhance Amazon forest drought resistance

Forest productivity and rates of tree mortality are sensitive to drought and fire. Understanding whether past disturbances increase the resilience of forest to modern disturbances is critical in predicting how these forests will respond to a greater frequency and intensity of fire and drought. To understand the legacy of historical fires on Amazonian forests responses to drought, I first investigated the relationship of PyC with physicochemical soil properties and wood density, because soil PyC has the capacity to improve soil fertility, accelerating forest stem turnover. The results showed a strong positive correlation between soil PyC and soil fertility, clay and silt, and a negative correlation between soil PyC and wood density and sand. Secondly, I investigated if there is an association between soil PyC and aboveground carbon dynamics. The result of the linear mixed model analysis shows there are no significant relationships between soil PyC and forest dynamics in the analysed forest plots. However, when analysing the relationship for forest censuses that had experienced a

severe drought, my results show that the impact of drought is significantly greater in forest with low concentrations of soil PyC. These findings support the hypothesis that soil PyC increases soil fertility and water holding capacity in the soil, potentially affording a higher resistance to drought where soil PyC is abundant, whilst also favouring the establishment of species associated with historical disturbances, such as fire and drought.

5.1.2 Chapter 3: Fire reoccurrence increase recovery time of canopy structure in Amazonian primary forests

In recent decades, fire frequency has increased in Amazonia, bringing uncertainties about the future of this forest. Understanding changes in not only aboveground biomass, but also in the vertical canopy structure caused by fires and fire reoccurrence is important to evaluate the time for the forest to recover and its impacts on the global carbon balance. To investigate the effects of fire and fire reoccurrences on the canopy structure of primary forests, I compared vertical structure metrics derived from lidar data of unburned and burned areas across Amazonia. The results show that forests that experienced repeated fires are more dissimilar to the unburned forests than areas that only experienced one fire event. Repeated fires have a greater impact on forest structure and increases the time to recover to the unburned state. Fires create a condition whereby a drier and hotter microclimate increases the likelihood of new fire events, generating a positive feedback cycle where forests have an insufficient fire-free time to fully recovery, leading to losses in carbon stocks, reductions in biodiversity and altered regional climates.

5.1.3 Chapter 4: Resistance and resilience of canopy structure to fire depends on successional stage in Amazonian secondary forests

Secondary forests act as large carbon sink and play an important role in biodiversity conservation and forest fragment connectivity. However, fire also threatens the regrowth of secondary forests, and can have varying impacts on different successional stages. To understand the effects of fires on secondary forests, I used a range of canopy structure metrics derived from airborne lidar data across the South-Eastern

region of Brazilian Amazon. I investigated if the effects of fire on secondary forests differ by successional stage, if the canopy structure can recover after fire and if the rate of recovery between early and later successional stages is different. The results show that fires negatively affect canopy structure of secondary forest in early and later successional stages, however, forests in early successional stage have more potential for a faster recovery. The results also show that later successional stages have a very low resilience because their vertical structure was scarcely able to recover within two decades.

5.2 Implications of fire for the Amazonian forest carbon sink

The results from this thesis suggest that historical fires can increase forest resilience to drought by either increasing soil fertility and/or changing species composition. Therefore, forests that experienced historical fires may be less affected by drought and still act as a carbon sink, while forests that did not experience historical fires are more prone to becoming a carbon source during drought years. This result highlights that historical events in Amazonian forests may play an important role in determining how forests respond to modern disturbances. As our knowledge of historical disturbances advances, it is important to consider their effects and add them into models that predict the response of forests to fires and droughts, because areas with historical fires may have different carbon sink rates. Failure to include these data may result in less accurate predictions of how the terrestrial carbon sink will respond to drought in the future and thus the amount of carbon dioxide removed from the atmosphere by tropical forest vegetation.

Nowadays, forests are still experiencing fires and at a much higher frequency than in the past (Aragão *et al.*, 2018; Silva Junior *et al.*, 2018), leading to degradation of Amazonian forests. My results show that forests that experienced one fire event decrease their carbon stocks and can take almost one decade to recover to an unburned state. In addition, the reoccurrence of fires aggravates the loss in carbon stocks and has a strong role in slowing down recovery rates of these forests. Forests with low carbon stocks have experienced more negative impacts of fire than forests with high carbon stocks. These findings highlight the urgency of forest management and identify important areas for prioritisation. Areas that have already been burned

need to be protected to avoid any reoccurrences of fire because the repeated burning intensifies the damage caused to carbon stocks. To also maintain carbon stores, it is necessary to prioritise protection of forests with low carbon stocks, as fire has a greater impact on biomass in these forests. New legislations, implantation of active management and an improved and greater monitoring of illegal actives that are related to fire in Amazonian forests are potentially critical for maintaining the carbon sequestration potential of these forests.

This thesis also focuses on the impacts of fire in secondary forests. Whilst I did not analyse aboveground carbon density (ACD) directly, I did analyse the metric leaf area height volume (LAHV), which is closely related to ACD. Secondary forests, as also observed in primary forests, show a decrease in carbon stocks after fire. Secondary forests in early and later successional stages experienced significant declines in LAHV after fire. However, later successional stage forests have a lower potential to recover to an unburned state. Fire occurrences in secondary forests, especially in later successional stages may release the carbon sequestered during the regrowth of these forests, as they are unable to recover their biomass stock after fire. Therefore, when aiming to conserve the carbon sink of secondary forests, we should prioritise later successional forests to stay in a fire-free condition since these forests cannot easily recover lost biomass. Changes in species composition are also common after fires, driven by tree mortality and consecutive growth of pioneer species that have lower wood density (Mata *et al.*, 2022). Since species with low wood density typically store less carbon, forests will have lower carbon stocks with a greater density of pioneer species (Baker *et al.*, 2004). These tree species with low wood density, however, have faster growth rates. This fast growth may allow faster carbon accumulation with positive results for carbon sink, at least in the initial years until they reach saturation. Shifts in community mean wood density should thus also be considered when modelling the Amazonian carbon sink to more accurately predict how carbon sequestration will change in the future.

5.3 Implications of fire on Amazonian forest structure and biodiversity

Although assessing the impact of historical fires on the structure of Amazonian forests was beyond the scope of my research, my results do suggest long-term successional

changes in species composition. Areas with higher concentration of soil PyC had community-level low wood density, indicating a shift towards earlier successional species. This indicates that over long time periods, some species, particularly with high wood density could be more vulnerable to extinction, especially as the frequency of fire events in Amazonian forests is increasing (Aragão *et al.*, 2018; Berenguer *et al.*, 2018b; Silva Junior *et al.*, 2018).

Modern day fires increase tree mortality. As trees die, more gaps form in the forest canopy, altering the microclimate and consequently leaving a forest that is more vulnerable to the reoccurrence of fire (Prestes *et al.*, 2020). Forests that experienced the reoccurrence of fires need longer to recover their canopy structure. In secondary forests, both early and later successional stages experienced negative impacts of fire on the vertical canopy structure. However, early successional stages show faster recovery in the canopy attributes studied. Some canopy attributes, such as mean height and leaf area index (LAI), did not recover after fire during the studied regrowth interval, but did recover in later successional stages. When the frequency of canopy gaps increases in both primary and secondary forests in later successional stages, a shift in species composition is likely to occur as the microclimate of the forest changes and shade tolerant species cannot compete with pioneer species. Closing canopy gaps is likely to be important to allow more shade tolerant species to re-establish themselves (Laurance *et al.*, 2006a). Active management should therefore focus on closing the canopy, such as management of lianas (Finlayson *et al.*, 2022), supplementary planting (Philipson *et al.*, 2020), reduced logging (Milodowski *et al.*, 2021), among others. Preventing fire from reoccurring is also likely to be important to recover the canopy and provide the shade conditions needed to allow shade tolerant species to grow.

The drier microclimate created by changes in forest structure after fire is also likely to increase in the drought susceptibility of the forest. In drought periods, big trees are more likely to die (Phillips *et al.*, 2010; Rowland *et al.*, 2015). Since big trees act as keystone species (Lindenmayer & Laurance, 2017), their loss may have cascading impacts on the whole ecosystem. Changes to the hydrological regime, nutrient cycles and the distribution and abundance of conspecifics and heterospecifics (Lindenmayer & Laurance, 2017) are all potential consequences of the loss of these large trees. If fire leads to more frequent droughts, there may also be changes in the phenology and

reproductive cycles of many tree species (Rowland *et al.*, 2018). These shifts may reduce the evolutionary fitness of these trees, leaving them vulnerable to extinction. Changes in the forest structure caused by fire may also put other life forms in danger, such as epiphytes that are unlikely to survive in drier environments and without the presence of big trees (Lindenmayer & Laurance, 2017). Many animals and insects that depend on large trees and need complex canopy structures to survive may also decline (Lindenmayer & Laurance, 2017). It is therefore vital to introduce management actions that protect these areas from fire and guarantee their ecosystem services such as biodiversity conservation and climate change mitigation are kept intact.

5.4 Perspectives and challenges

The results from this thesis provide an insightful direction for the future of Amazonian forests under the increasing risk of degradation by fire. Several research challenges and opportunities for future research were identified during the development of this thesis, which I outline in this section.

In my first empirical chapter (Chapter 2), the PyC dataset, used as a proxy of historical fires, had some limitations. This dataset does not inform when the PyC was formed (e.g., 30 or 3000 years ago), and neither whether it originated from one large fire or several smaller fires, which would affect the vegetation in different ways. Further analysis including radiocarbon dating will help to address the knowledge gap and allow us to better understand the legacy effect of fire on vegetation. In my analysis of the impacts of fire reoccurrence in primary forests (Chapter 3), I was unable to investigate the influence of the time between fire reoccurrences owing to a lack of replication across fire interval periods. This is an important variable that should be addressed in future research, since previous studies have shown that forests burned in subsequent years are more impacted (Brando *et al.*, 2014). Moreover, I was unable to investigate the effects of fire reoccurrences on the canopy structure of secondary forests since my dataset did not provide enough areas that experienced more than one fire event. Therefore, the effect of fire reoccurrence on the vertical canopy structure of secondary forests and its impacts for forest regrowth still needs to be investigated in future research. Investigating the impacts of drought on modern day fires and its effects on forest structure and recovery from fire is another important area of research, but was

beyond the scope of this thesis. I recommend further research on this topic as it is known that drought exacerbates the occurrence of fire (Aragão *et al.*, 2018; Silva *et al.*, 2018; Silva Junior *et al.*, 2019), which may aggravate the impact of fire on carbon storage and forest structure.

In the chapters where I investigate the effect of recent fires on Amazonian forests (Chapters 3 and 4), the burned area data that I used was the MCD64A1 product from the MODIS sensor with a spatial resolution of 500 m, available from November 2000. This product has some uncertainties because its coarse spatial resolution leads to considerable underestimation of burned areas (Randerson *et al.*, 2012; Giglio *et al.*, 2018) and struggles to detect small burns. However, when compared with other burned area products with better spatial resolution, MCD64A1 shows a good performance (Pessôa *et al.*, 2020). A new burned area product using Landsat images was launched in May 2022 covering a period from 1985 to the present and with a spatial resolution of 30 m (Alencar *et al.*, 2022). This is a very promising new dataset, allowing an understanding of the effects of recent fires over a longer time series than MCD64A1 and also with a higher spatial resolution, thus decreasing uncertainties.

The empirical chapters developed in this thesis also have spatial limitations. Field plot inventories used in chapter 2 are mainly areas of 1 ha, which in total covered an area of 108 ha. Whilst this represents a relatively large number of plots, it remains less than 0.001% of the total area of the Amazon Basin. To better estimate forest dynamics, larger forest plots, with higher re-censusing frequency are needed. Larger forest plots have recently been established in some parts of the Amazon, but are too limited in number to provide a good spatial coverage of the whole of Amazonia. An effort to establish research plots with better distribution across the Amazon Basin would help improve our understanding of forest dynamics across all different climatic and edaphic conditions in the basin. Moreover, more field data combined with lidar measurements will guarantee better estimations of biomass and other forest attributes as well as lidar time series that could confirm the temporal patterns indicated by my results.

Besides, in chapter 4, my research focuses only on the south-eastern region of the Amazon forest because it is where the highest concentration of secondary forests is found. I recommend future research to address the effect of fire on canopy structure of secondary forests in other regions of the Amazon, as fire impacts and recovery rates may change in different climatic and edaphic conditions (Heinrich *et al.*, 2021).

Moreover, this thesis is only focused on Amazonian forests. Understanding the impacts of fire and the recovery after fire is crucial not only in the Amazon but also in all other tropical forests. More studies that follow the similar methodologies to this thesis, should be undertaken in Asian and African tropical forests providing better estimates of impacts of fire in tropical forests and its implications for the global carbon cycling and biodiversity conservation. Analyses that use similar methods could also reveal important information about the differences in ecology between tropical forest regions and highlight differences in long-term adaptations to fire.

In this thesis, I focus on aboveground carbon and forest structure. Further investigation into the impacts of fire on other forest attributes, such as eco-physiology, species diversity, impacts on animal communities, soil carbon, among others, will reveal the full impacts of fire on the whole forest ecosystem. Additionally, I only use soil analyses in chapter 2, since few airborne lidar sites overlap areas of permanent forest inventory plots with soil analyses, thereby preventing the inclusion of these variables in the analysis of chapters 3 and 4.

Finally, the results presented in this thesis have temporal limitations as they mainly focus on the impact of historical and recent fires in Amazonian forests. Further and more detailed investigations of how the frequency and intensity of fires affects forest aboveground biomass and vertical canopy structure and its effects on the global carbon and hydrological cycles and biodiversity are needed. Furthermore, my analyses focus on fire under current climatic conditions. Under future climate change, it is predicted that the Amazon will experience higher temperatures and drier conditions (IPCC, 2022). Since these conditions exacerbate the effects of fire on Amazonian forests (Aragão *et al.*, 2018), the impacts of fire on these forests is likely to change over time. Development of models that can predict how fire will change with time will be necessary if we wish to fully understand how the Amazon forest may change in the future.

5.5 Conclusion

The Amazon forest is the most biodiverse forest on Earth and has great importance for regulating carbon and hydrological global cycles. Despite tropical rainforest being an ecosystem with historically infrequent fires, forest degradation can transform these

forests into a fire prone environment. The advance of deforestation, degradation, and more frequent and intense droughts in recent decades, has increased the threat of fire in Amazonian forests. In the research developed in this thesis, I address the effects of fire on Amazonian forests from past to present. I found that historical fires may still be having an influence on current forest dynamics during drought years, by fires having added PyC to the soil that improves soil fertility and water holding capacity, whilst also favouring the establishment of species associated with historical disturbances. When studying the impacts of modern fires, I show they have large negative impacts on both old-growth and secondary forests. Modern fires affect carbon storage and canopy structure, with their effects more intense when fire reoccurs. Secondary forests have a low resilience when found in later successional stages, accentuating the importance of protecting these areas. Overall, impacts of fire on the carbon stocks and canopy structure of forests can take many decades to fully recover, with some parameters showing no recovery. This has substantial implications for the global carbon cycle and biodiversity. Implementation of forest conservation and monitoring and acting against illegal activities that produce forest fires is vital for the long-term future of the Amazon forest and its contribution to the planet.

Appendix 1: Co-authored publications

Some co-authored research has been developed during my PhD. The following papers have been published or are in preparation for submission. The abstracts of these papers are presented below.

21st Century drought-related fires counteract the decline of Amazon deforestation carbon emissions

Luiz E.O.C. Aragão, Liana O. Anderson, Marisa G. Fonseca, Thais M. Rosan, Laura B. Vedovato, Fabien H. Wagner, Camila V.J. Silva, Celso H.L. Silva Junior, Egidio Arai, Ana P. Aguiar, Jos Barlow, Erika Berenguer, Merritt N. Deeter, Lucas G. Domingues, Luciana Gatti, Manuel Gloor, Yadvinder Malhi, Jose A. Marengo, John B. Miller, Oliver L. Phillips & Sassan Saatchi. Nature Communications, 2018, 9, 536.

Abstract

Tropical carbon emissions are largely derived from direct forest clearing processes. Yet, emissions from drought-induced forest fires are, usually, not included in national-level carbon emission inventories. Here we examine Brazilian Amazon drought impacts on fire incidence and associated forest fire carbon emissions over the period 2003–2015. We show that despite a 76% decline in deforestation rates over the past 13 years, fire incidence increased by 36% during the 2015 drought compared to the preceding 12 years. The 2015 drought had the largest ever ratio of active fire counts to deforestation, with active fires occurring over an area of 799,293 km^2. Gross emissions from forest fires (989 ± 504 Tg CO2 $year^{-1}$) alone are more than half as great as those from old-growth forest deforestation during drought years. We conclude that carbon emission inventories intended for accounting and developing policies need to take account of substantial forest fire emissions not associated to the deforestation process.

Author contributions

L.E.O.C.A. and L.O.A. designed the research with additional input from M.G.F. L.O.A., M.G.F., F.H.W., C.S, C.H.L.S.J., L.V., T.M.R., E.A. and M.N.D. prepared the database and processed remote sensing data. L.O.A., M.G.F., M.N.D., F.H.W., C.H.L.S.J. and

L.E.O.C.A. analysed the data, with input from L.G.D. and L.G. L.E.O.C.A., L.O.A., M.G.F., A.P.A., J.B., E.B., L.G.D., L.G., M.G., Y.M., J.A.M., O.P., S.S., M.N.D. and J.B.M. analysed and interpreted the results. L.E.O.C.A. and L.O.A. wrote the manuscript, with input from all authors.

Deforestation-Induced Fragmentation Increases Forest Fire Occurrence in Central Brazilian Amazonia

Celso H. L. Silva Junior, Luiz E. O. C. Aragão, Marisa G. Fonseca, Catherine T. Almeida, Laura B. Vedovato & Liana O. Anderson. Forests, 2018, 9(6), 305.

Abstract

Amazonia is home to more than half of the world's remaining tropical forests, playing a key role as reservoirs of carbon and biodiversity. However, whether at a slower or faster pace, continued deforestation causes forest fragmentation in this region. Thus, understanding the relationship between forest fragmentation and fire incidence and intensity in this region is critical. Here, we use MODIS Active Fire Product (MCD14ML, Collection 6) as a proxy of forest fire incidence and intensity (measured as Fire Radiative Power—FRP), and the Brazilian official Land-use and Land-cover Map to understand the relationship among deforestation, fragmentation, and forest fire on a deforestation frontier in the Brazilian Amazonia. Our results showed that forest fire incidence and intensity vary with levels of habitat loss and forest fragmentation. About 95% of active fires and the most intense ones (FRP > 500 megawatts) were found in the first kilometre from the edges in forest areas. Changes made in 2012 in the Brazilian main law regulating the conservation of forests within private properties reduced the obligation to recover illegally deforested areas, thus allowing for the maintenance of fragmented areas in the Brazilian Amazonia. Our results reinforce the need to guarantee low levels of fragmentation in the Brazilian Amazonia in order to avoid the degradation of its forests by fire and the related carbon emissions.

Author contributions

C.H.L.S.J. and L.E.O.C.A. led in the design of the experiment. C.H.L.S.J. performed data analysis. C.H.L.S.J., L.E.O.C.A., M.G.F., C.T.A., L.B.V. and L.O.A. interpreted

the results. C.H.L.S.J., M.G.F. and C.T.A. wrote the paper with significant contributions from all authors.

Taking the pulse of Earth's tropical forests using networks of highly distributed plots

ForestPlots.net. This article is attributed collectively as ForestPlots.net et al. A list with all authors in alphabetical order first by country of institution and secondly by family name can be found here:
https://www.sciencedirect.com/science/article/pii/S0006320720309071, Biological Conservation, 2021, v. 260.

Abstract

Tropical forests are the most diverse and productive ecosystems on Earth. While better understanding of these forests is critical for our collective future, until quite recently efforts to measure and monitor them have been largely disconnected. Networking is essential to discover the answers to questions that transcend borders and the horizons of funding agencies. Here we show how a global community is responding to the challenges of tropical ecosystem research with diverse teams measuring forests tree-by-tree in thousands of long-term plots. We review the major scientific discoveries of this work and show how this process is changing tropical forest science. Our core approach involves linking long-term grassroots initiatives with standardized protocols and data management to generate robust scaled-up results. By connecting tropical researchers and elevating their status, our Social Research Network model recognises the key role of the data originator in scientific discovery. Conceived in 1999 with RAINFOR (South America), our permanent plot networks have been adapted to Africa (AfriTRON) and Southeast Asia (T-FORCES) and widely emulated worldwide. Now these multiple initiatives are integrated via forestplots.net cyber-infrastructure, linking colleagues from 54 countries across 24 plot networks. Collectively these are transforming understanding of tropical forests and their biospheric role. Together we have discovered how, where and why forest carbon and biodiversity are responding to climate change, and how they feedback on it. This long-term pan-tropical collaboration has revealed a large long-term carbon sink and its trends, as well as making clear which drivers are most important, which forest

processes are affected, where they are changing, what the lags are, and the likely future responses of tropical forests as the climate continues to change. By leveraging a remarkably old technology, plot networks are sparking a very modern revolution in tropical forest science. In the future, humanity can benefit greatly by nurturing the grassroots communities now collectively capable of generating unique, long-term understanding of Earth's most precious forests.

Author contributions

All authors have contributed to ForestPlots.net-associated networks by leading, collecting or supporting field data acquisition, or implementing and funding network development, data management, analyses and outputs. O.L.P. wrote the manuscript with initial contributions from S.L.L., M.J.S. contributed new analyses, M.J.S., G.L.P. and A.L. helped prepare the figures, and all authors reviewed the manuscript with many suggesting valuable edits. O.L.P., T.R.B., G.L.-G. and S.L.L. conceived ForestPlots.net. R.B., T.R.B., T.F., D.G., E.G., E.H., W.H., A.E.-M., A.L., S.L.L., K.M., Y.M., G.C.P., O.L.P., B.S-M., L.Q., and M.J.P.S have contributed tools, funding or management to its development since.

Forest Fragmentation and Fires in the Eastern Brazilian Amazon–Maranhão State, Brazil

Celso H. L. Silva-Junior, Arisson T. M. Buna, Denilson S. Bezerra , Ozeas S. Costa, Jr., Adriano L. Santos, Lidielze O. D. Basson, André L. S. Santos, Swanni T. Alvarado, Catherine T. Almeida, Ana T. G. Freire, Guillaume X. Rousseau, Danielle Celentano, Fabricio B. Silva, Maria S. S. Pinheiro, Silvana Amaral, Milton Kampel, Laura B. Vedovato, Liana O. Anderson & Luiz E. O. C. Aragão. Fire, 2022, 5, 77.

Abstract

Tropical forests provide essential environmental services to human well-being. In the world, Brazil has the largest continuous area of these forests. However, in the state of Maranhão, in the eastern Amazon, only 24% of the original forest cover remains. We integrated and analyzed active fires, burned area, land use and land cover, rainfall, and surface temperature datasets to understand forest fragmentation and forest fire dynamics from a remote sensing approach. We found that forest cover in the

Maranhão Amazon region had a net reduction of 31,302 km2 between 1985 and 2017, with 63% of losses occurring in forest core areas. Forest edges extent was reduced by 38%, while the size of isolated forest patches increased by 239%. Forest fires impacted, on average, around 1031 ± 695 $km^2\,year^{-1}$ of forest edges between 2003 and 2017, the equivalent of 60% of the total burned forest in this period. Our results demonstrated that forest fragmentation is an important factor controlling temporal and spatial variability of forest fires in the eastern Amazon region. Thus, both directly and indirectly, forest fragmentation can compromise biodiversity and carbon stocks in this Amazon region.

Author contributions

Data curation, C.H.L.S.-J.; Formal analysis, C.H.L.S.-J.; Methodology, C.H.L.S.-J.; Writing- original draft, C.H.L.S.-J., A.T.M.B. and D.S.B.; Writing-review and editing, O.S.C.J., A.L.S., L.O.D.B., A.L.S.S., S.T.A., C.T.A., A.T.G.F., G.X.R., D.C., F.B.S., M.S.S.P., S.A., M.K., L.B.V., L.O.A. and L.E.O.C.A. All authors have read and agreed to the published version of the manuscript.

Environmental and Human Controls on Soil Pyrogenic Carbon in Amazonia

Lidiany C.S. Carvalho, Michael I. Bird, Oliver L. Phillips, A. Junqueira, Ben H. Marimon-Junior, Carlos A. Quesada, Beatriz S. Marimon, Luiz E.O.C. Aragão, Gustavo Saiz, Laura B. Vedovato, Luciana Pereira, Edmar A. de Oliveira, E.N.H. Coronado, R. Herrera, C. Flores-Negron, C.P. Paz, E.M.O. Mendoza, L.A. Padilla, R.S. Thomas & Ted R. Feldpausch (*in preparation to be submitted to Nature*)

Abstract

Soils can store more C than atmosphere and vegetation combined and even modest changes in this major pool of C have the potential to significantly impact concentration of atmospheric CO2. Soil organic carbon (SOC) is compound for hundreds of different organic materials, ranging from more labile to stable forms of C with different turnover times. Fire derived C (also called pyrogenic carbon – PyC) is potentially the most stable C fraction of SOC with great mean residence time and strong capacity to act as a long-term C sink in geological C cycle scale. Besides the importance of soil PyC to

understand the global C carbon budget, the present understanding of SOC stocks and cycling has generally focused on labile fractions of C in the topsoil above 0.3 m and much less is known about the mechanisms that control variations in PyC concentration. Here we present results from the first analysis of drivers of PyC for whole-soil-profile (0-100 cm) coupled with spatial and temporal heterogeneity in fire and land use, vegetation, climate and pedogenesis at Amazon Basin scale. Our results demonstrate that different drivers are related with PyC variation, depending on soil depth. Fire and land use, climate, pedogenesis and vegetation are important in determining variations in PyC in the Amazon Basin. At soil surface (0-30 cm), variations of PyC can be explained by combination of Clay% in soil, wood density and precipitation, while the PyC deposited at deeper soil layer (50-100 cm) is associated with archaeological sites distribution in the Amazonia and lower precipitation during the Holocene. These results suggest that PyC at 50-100 cm depth may represent old pools of PyC derived from middle-late Holocene anthropogenic fires and the PyC at soil surface is driven by factors that represent proxies of PyC decomposition and stabilization on soil.

Appendix 2: Supporting Information of Chapter 2

SI Figure 2.1. Principal component analysis of Total P, pH and the exchangeable cations K, Ca and Mg used to construct the soil fertility variable.

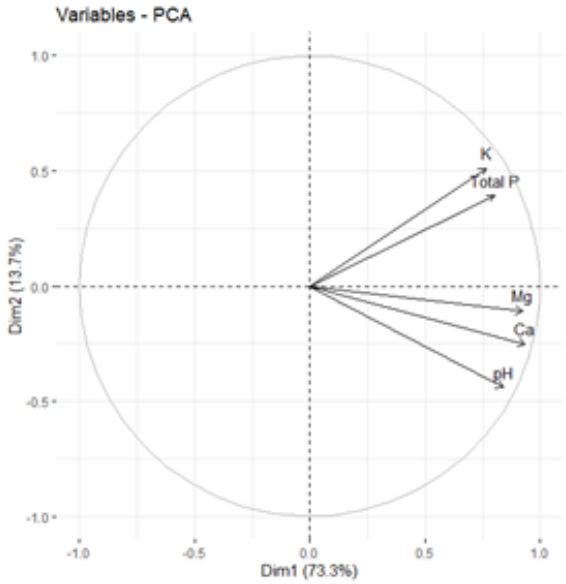

SI Figure 2.2. Spline correlograms describing spatial autocorrelation for the residual of the models related to AGC gain (A), AGC loss (B) and AGC net change (C) predicted by soil PyC. The black line represent the estimate and grey shade represents 95% confidence interval using 1000 bootstrap resamples.

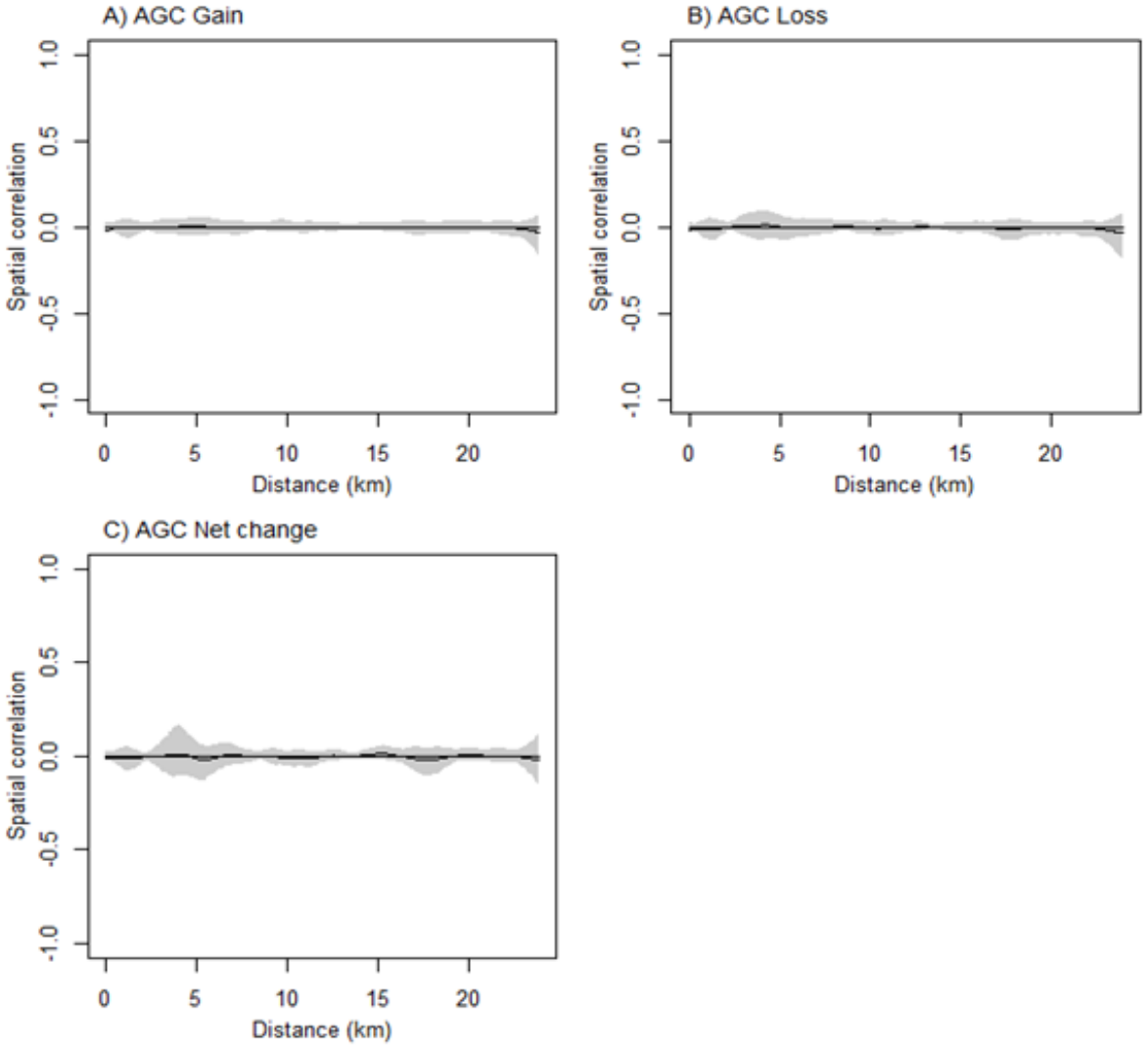

SI Figure 2.3. Spline correlograms describing spatial autocorrelation for the residual of the best model after model selection to predict AGC gain (A), AGC loss (B) and AGC net change (C) in census that experienced a severe drought (see methods). The black line represent the estimate and grey shade represents 95% confidence interval using 1000 bootstrap resamples.

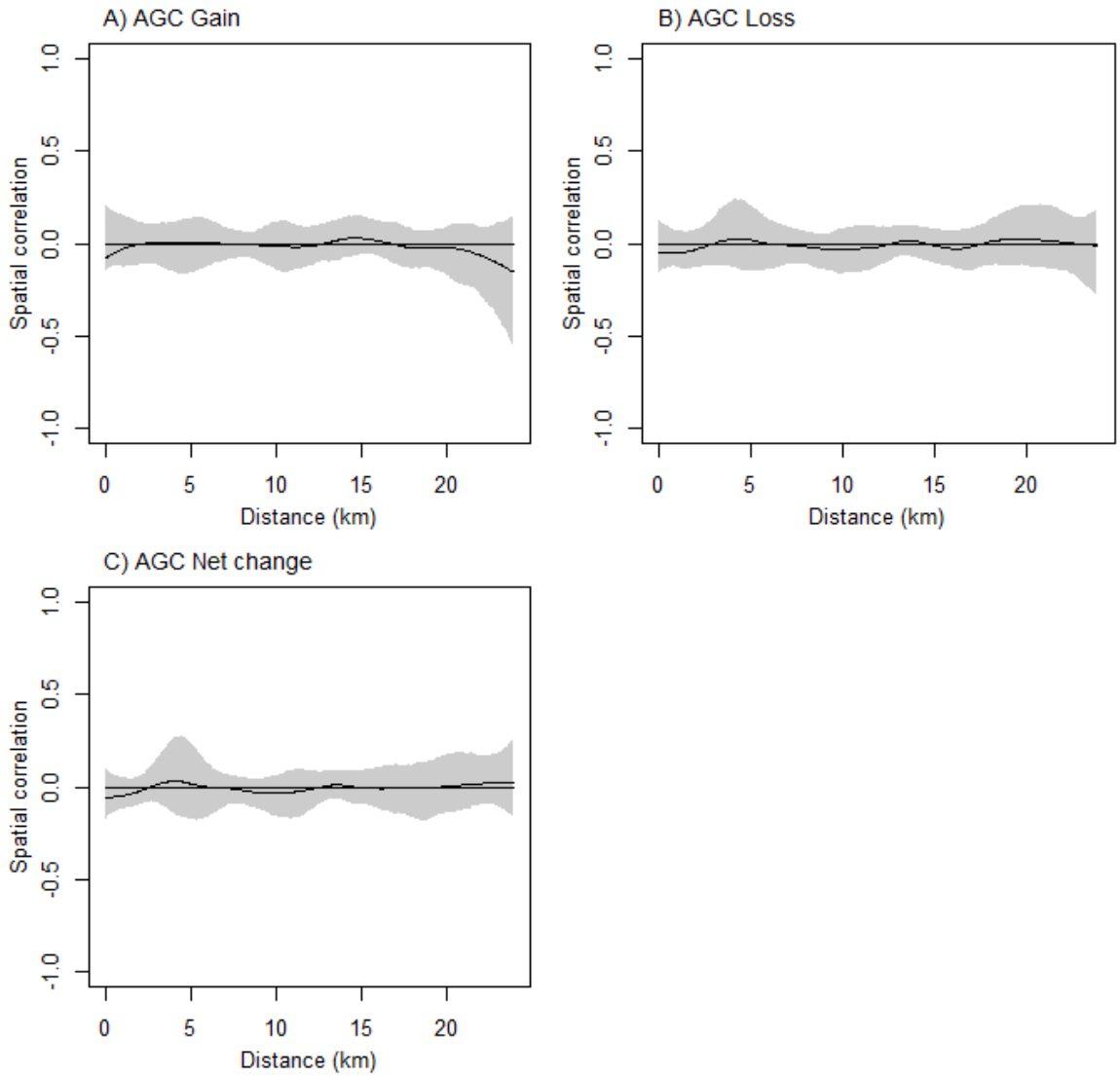

SI Table 2.1. Variables loadings on soil fertility variable (PC1) and values of the others axis (PC2, PC3, PC4, PC5).

	PC1 (73.3%)	PC2 (13.7%)	PC3 (6.9%)	PC4 (4.4%)	PC5 (1.7%)
pH	0.840	-0.441	0.025	0.301	0.097
Total P	0.801	0.393	-0.447	0.068	0.008
Ca	0.935	-0.252	0.011	-0.082	-0.234
Mg	0.926	-0.108	0.040	-0.328	0.147
K	0.765	0.512	0.379	0.097	-0.006

SI Table 2.2. Generalized Mixed Model (GLMM) to predict AGC gain, AGC loss and AGC net change with log PyC as fixed factor and Plot code nested in Plot cluster as random effect. AGC loss is squared transformed to ensure a normal distribution of fitted residuals.

	Intercept	Log PyC	Plot code: Plot cluster	Fixed effect (marginal) R^2	Total (conditional) R^2
AGC gain	3.35 ± 0.4***	0.18 ± 0.13	0.29	0.01	0.41
AGC loss	1.5 ± 0.26***	0.02 ± 0.08	0.14	0.00	0.13
AGC net change	0.65 ± 0.74	0.07 ± 0.24	0.54	0.00	0.09

Note: Coefficient estimates ± the SE are presented for each fixed effect. Total (conditional) R^2 represents the total variation explained by the model and is partitioned into the variation explained by the fixed effects (marginal R^2) and fixed plus random-effects (conditional R^2). Asterisks represent the significance level of each variable: *p<0.05; **p<0.01; ***p<0.001.

SI Table 2.3. Model selection to predict AGC Gain, AGC Loss and AGC Net Change for census classified as severe drought. The predictors variables were MCWD anomalies (MCWD Anom), soil PyC (PyC), Non-PyC Organic Carbon (OC), soil fertility (Fert) and wood density (WD) as fixed effects and plot code nested in plot cluster as random effect. MCWD Anom, PyC and OC were log transformed and AGC Loss was squared root transformed to ensure a normal distribution of fitted residuals. All independent variables are standardized. All models tested are presented and the best model was selected based on the Akaike Information Criterion corrected for sample size (AICc). The optimal model for AGC Gain, AGC Loss and AGC Net Change is highlighted in bold. ΔAICc values represent the difference in the AICc for each model compared to the optimal model.

Model	**AGC Gain**		**AGC Loss**		**AGC Net Change**	
	AICc	ΔAICc	AICc	ΔAICc	AICc	ΔAICc
MCWD Anom *PyC + MCWD Anom *OC + MCWD Anom * Fert + PyC * Fert +PyC *WD	162.2	29.5	146.2	34.1	277.8	29.4
MCWD Anom *PyC + MCWD Anom *OC + MCWD Anom * Fert + PyC * Fert + WD	157.3	24.6	140.9	28.8	274.8	26.4
MCWD Anom *PyC + MCWD Anom *OC + PyC * Fert + WD	151.8	19.1	136	23.9	272.6	24.2
MCWD Anom *PyC + MCWD Anom *OC + Fert + WD	147.2	14.5	129.2	17.1	267.9	19.5
MCWD Anom *PyC + MCWD Anom *OC + WD	142.2	9.5	124	11.9	265.1	16.7
MCWD Anom *PyC + OC + WD	138.1	5.4	117.9	5.8	261.6	13.2
MCWD Anom *PyC + WD	**132.7**	**0**	**112.1**	**0**	259.1	10.7
MCWD Anom *PyC	135.1	2.4	116.1	4	257.1	8.7

MCWD Anom + PyC +WD	134.2	1.5	112.3	0.2	-	-
MCWD Anom + PyC	-	-	-	-	255.9	7.5
MCWD Anom	-	-	-	-	251.9	3.5
Null	-	-	-	-	**248.4**	0

SI Table 2.4. Generalized Mixed Model (GLMM) to predict AGC gain and AGC loss with log Non-PyC Organic Carbon (OC) and MCWD anomalies (MCWD Anom) as fixed factor and Plot code nested in Plot cluster as random effect. AGC loss is squared transformed to ensure a normal distribution of fitted residuals.

	Intercept	MCWD Anom	OC	OC:MCWD Anom	Plot code: Plot cluster	Fixed effect (marginal) R^2	Total (conditional) R^2
AGC gain	2.59 ± 0.11***	-0.10 ± 0.09	-0.00± 0.09	-0.13 ± 0.09	0.42	0.03	0.66
AGC loss	1.60 ± 0.11***	-0.03 ± 0.11	-0.19 ± 0.15	0.15 ± 0.15	0.37	0.04	0.62

Note: Coefficient estimates ± the SE are presented for each fixed effect. Total (conditional) R^2 represents the total variation explained by the model and is partitioned into the variation explained by the fixed effects (marginal R^2) and fixed plus random-effects (conditional R^2). Asterisks represent the significance level of each variable: *p<0.05; **p<0.01; ***p<0.001.

Appendix 3: Supporting Information of Chapter 3

SI Figure 3.1. Violin plots for the canopy metrics (A) maximum height, (B) Roughness, (C) Openness at 5 m, (D) Openness at 15 m and, (E) LAI Understory and (F) LAHV. Yellow violins represent areas with single fire events (B1) and red violins represent areas with multiple fire events (B2+). Significance levels on the bottom of the violin represent significative difference from 0 (unburned state) and significant levels on top of violins represent significant differences between reoccurrences groups. There is no signficant difference between groups when brackets are absent. Significance level: *p<0.05, **p<0.01, ***p<0.001; ns, non-significant relationships.

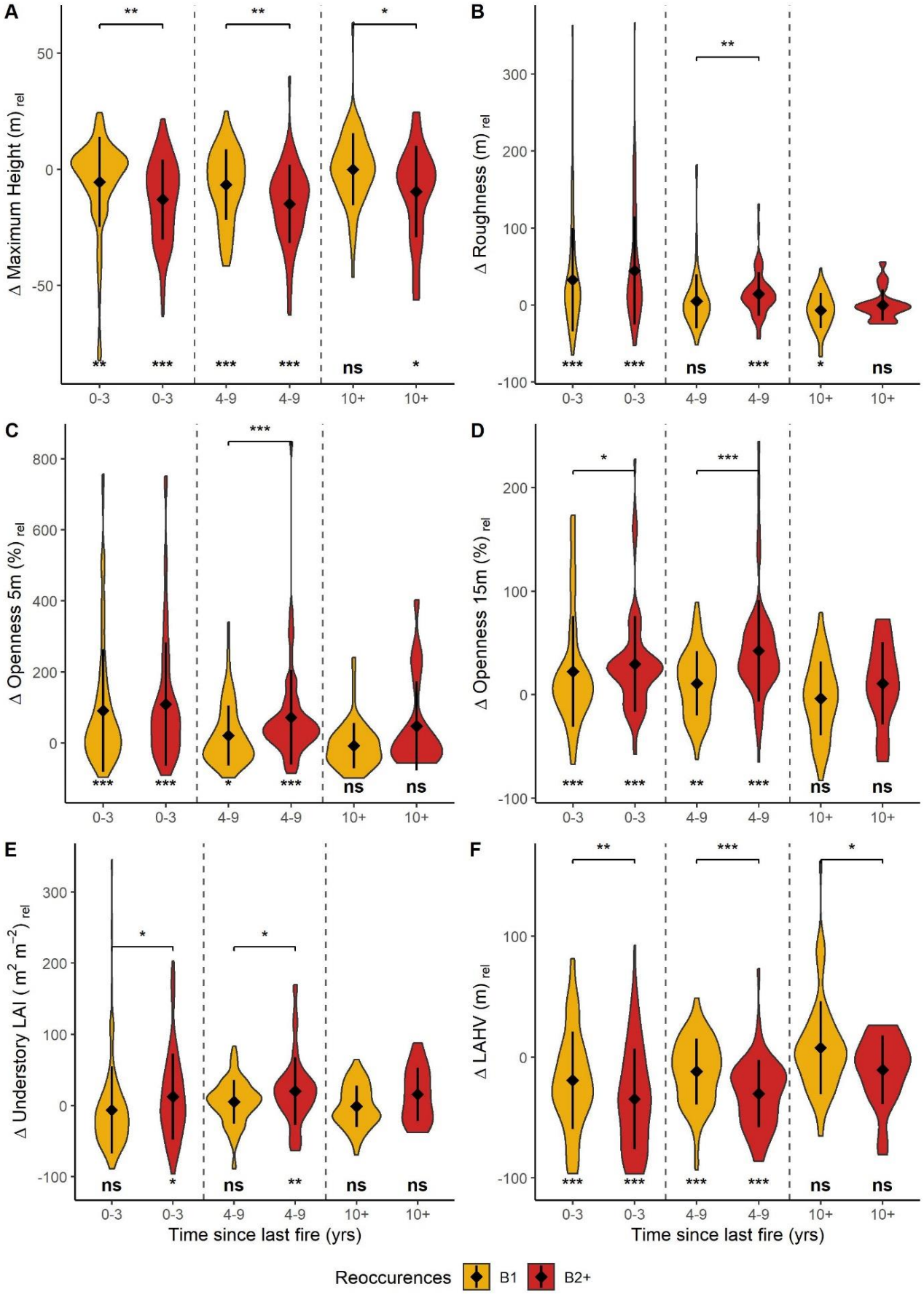
A
B
C
D
E
F
Δ Maximum Height (m) rel
Δ Roughness (m) rel
Δ Openness 5m (%) rel
Δ Openness 15m (%) rel
Δ Understory LAI (m2 m−2) rel
Δ LAHV (m) rel
0-3
4-9
10+
Time since last fire (yrs)
Reoccurences
B1
B2+

SI Figure 3.2. Violin plots for the canopy metrics (A) ACD, (B) maximum height, (C) Mean Height, (D) Roughness, (E) Openness at 5 m, (F) Openness at 10 m, (G) Openness at 15 m and, (H) LAI, (I) LAI Understory and (J) LAHV divided by forest with Low and High carbon stocks. Yellow violins represent areas with single fire events (B1) and red violins represent areas with multiple fire events (B2+). Significance levels on the bottom of the violin represent a significant difference from 0 (unburned state) and significant levels on top of the violins represent significant differences between reoccurrence groups. There is no signficant difference between groups when brackets are absent. Significance level: *p<0.05, **p<0.01, ***p<0.001; ns, non-significant relationships.

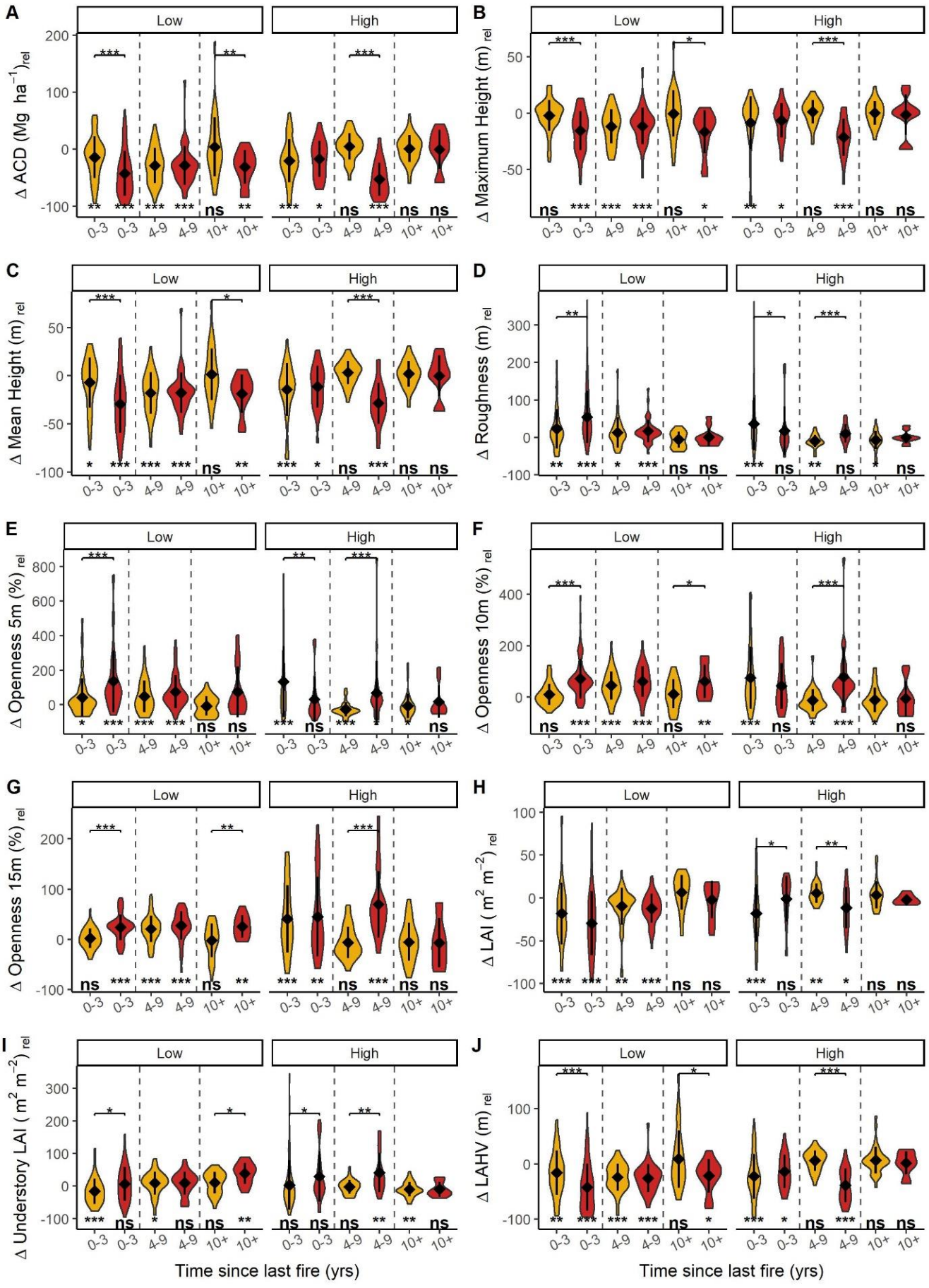
A
B
C
D
E
F
G
H
I
J
Low
High
Δ ACD (Mg ha^{-1})$_{rel}$
Δ Maximum Height (m) $_{rel}$
Δ Mean Height (m) $_{rel}$
Δ Roughness (m) $_{rel}$
Δ Openness 5m (%) $_{rel}$
Δ Openness 10m (%) $_{rel}$
Δ Openness 15m (%) $_{rel}$
Δ LAI (m^2 m^{-2}) $_{rel}$
Δ Understory LAI (m^2 m^{-2}) $_{rel}$
Δ LAHV (m) $_{rel}$
0-3
4-9
10+
Time since last fire (yrs)
Reoccurences
B1
B2+

SI Table 3.1. Percentage contributions to dimension 1-5 for each lidar metric to the principal component analysis for the different YSLF groups.

		Dimension 1			Dimension 2			Dimension 3			Dimension 4			Dimension 5		
	YSLF group	**0-3**	**4-9**	**+10**	**0-3**	**4-9**	**+10**	**0-3**	**4-9**	**+10**	**0-3**	**4-9**	**+10**	**0-3**	**4-9**	**+10**
	% Contribution	71.97	67.96	65.30	17.54	18.27	20.91	4.55	7.44	7.44	2.82	2.77	2.90	1.59	1.80	1.83
Metrics	Max H.	10.00	10.27	9.83	7.37	8.32	9.99	18.45	13.28	14.45	17.79	12.72	7.99	0.04	0.00	0.07
	Mean H.	13.14	13.79	14.07	2.18	1.87	2.30	1.74	2.15	2.85	1.61	2.71	2.06	0.58	2.19	2.54
	Openness 5m	10.71	8.90	8.79	5.93	11.90	14.19	10.11	10.81	6.16	12.56	23.91	18.45	13.19	0.22	1.45
	Openness 10m	12.34	12.66	12.70	0.24	0.08	0.05	14.03	6.21	9.32	1.58	0.77	4.94	14.00	41.84	40.95
	Openness 15m	11.39	12.88	13.13	7.15	3.25	3.61	0.02	0.19	0.05	0.04	0.56	0.09	0.55	6.60	8.40
	Roughness	8.49	6.11	6.01	12.69	23.72	23.18	14.89	11.85	8.64	2.49	0.40	1.05	56.33	20.68	18.73
	ACD	11.74	12.63	12.84	4.59	3.07	3.33	9.04	5.47	6.93	0.67	0.33	0.01	8.86	18.57	15.61
	LAI	9.54	6.55	6.36	13.20	23.42	22.24	0.18	6.58	4.87	24.05	20.52	20.87	5.54	5.75	8.22
	Understory LAI	0.32	2.98	2.74	46.49	24.13	20.66	31.16	41.74	45.46	3.54	11.93	12.72	0.79	1.86	3.66
	LAHV	12.33	13.22	13.53	0.16	0.25	0.45	0.39	1.71	1.27	35.68	26.15	31.81	0.10	2.29	0.37

Acronyms: YSLF: Years Since Last Fire, Max H.: Maximum Height, Mean H.: Mean Height, ACD: Aboveground Carbon Density, LAI: Leaf Area Index, Understory LAI: Leaf Area Index of Understory, LAHV: Leaf Area Height Volume.

SI Table 3.2. Parameters estimates ± standard error for the canopy metrics analysed as fixed effects in the linear mixed models for years since last fire (YSLF), Reoccurrences groups (B1 and B2+), Biomass groups (Low and High) and interaction of YSLF and Reoccurrence. Region was included as random effect and coefficient represents the variance between levels. Total (conditional) R^2 represents the proportion of variance explained by our model and fixed effect (marginal) R^2 represents the variance explained by the fixed effect parameters. Asterisks represent the significance level of each variable: *p<0.05; **p<0.01; ***p<0.001.

	Intercept	YSLF	Reoccurrences	Biomass	YSLF:Reoccurrences	Region	Fixed effect (marginal) R^2	Total (conditional) R^2
Δ ACD	-24.98 ± 3.62	1.63 ± 0.42***	-14.42 ± 5.14**	7.24 ± 3.44	-0.88 ± 0.80	0	0.12	0.12
Δ Maximum H.	-8.55 ± 3.11	0.444± 0.20*	-5.94 ± 2.39*	2.44 ± 1.72	-0.45 ± 0.38	15.18	0.07	0.12
Δ Mean H.	-16.47 ± 3.49*	1.05 ± 0.28***	-11.38 ± 3.38**	5.03 ± 2.38	-0.14 ± 0.53	10.88	0.12	0.13
Δ Openness 5m	101.82 ± 22.58*	-8.10 ± 1.61***	26.94 ± 19.15	-8.05 ± 13.65	1.59 ± 3.02	657.5	0.09	0.12
Δ Openness 10m	51.36 ± 19.07	-3.55 ± 0.91***	27.01 ± 10.71*	-4.23 ± 7.76	0.92 ± 1.69	872.3	0.08	0.2
Δ Openness 15m	15.29 ± 13.28	-2.1 ± 0.52***	14.85 ± 6.07*	12.18 ± 4.41**	1.07 ± 0.96	496.3	0.08	0.27
Δ Roughness	33.18 ± 4.82	-3.15 ± 0.56***	16.80 ± 6.86*	-4.89 ± 4.6	-1.64 ± 1.08	0	0.13	0.13
Δ LAI	-21.25 ± 2.87	1.82 ± 0.34***	-3.64 ± 4.04	6.41 ± 2.73	-0.16 ± 0.63	0	0.12	0.12
Δ Understory LAI	-2.11 ± 10.03	0.37 ± 0.60	18.93 ± 7.10**	4.18 ± 5.09	0.01 ± 1.12	172.7	0.03	0.1
Δ LAHV	-26.82 ± 3.68	2.17 ± 0.43***	-12.09 ± 5.18*	8.03 ± 3.5	-0.69 ± 0.81	0	0.14	0.14

SI Table 3.3. Summary of standardised major axis regression between lidar metrics for different treatments and YSLF groups. Significance level: *p<0.05, **p<0.01, ***p<0.0001; ns, non-significant relationships. The grey box denotes invalid correlations where x and y variables are the same. Correlation coefficient (r^2) and significant value (p) for SMA analysis and slope. The metrics showed are Aboveground Carbon Density (ACD), Mean height (Mean H.), Openness at 5m (Open 5m), Openness at 10m (Open 10m), Openness at 15m (Open 15m), Leaf Area Index (LAI), Understory Leaf Area Index of (Under LAI) and Leaf Area Height Volume (LAHV). The treatment groups (Treat.) are unburned (Unb.), single fire event (B1) and multiple fire events (B2+).

Bivariate relationship (y vs x -axis)		Treat.	Intercept			Slope			r2			p			Difference in slope and elevation						
			YSLF group			YSLF group			YSLF group			YSLF group			Treat.	YSLF group					
			0-3	4-9	10+	0-3	4-9	10+	0-3	4-9	10+	0-3	4-9	10+		0-3		4-9		10+	
																B1	B2+	B1	B2+	B1	B2+
ACD	Max H.	Unb.	-1.20	-1.20	-1.20	0.40	0.40	0.40	0.86	0.86	0.86	***	***	***	Unb.	*	***	ns	ns	ns	ns
		B1	-2.81	-1.92	-1.47	0.44	0.43	0.41	0.88	0.93	0.92	***	***	***	B1		**		ns		ns
		B2+	-4.14	-1.71	-0.90	0.51	0.40	0.40	0.91	0.87	0.94	***	***	***	B2+						
	Mean H.	Unb.	0.29	0.29	0.29	0.48	0.48	0.48	0.98	0.98	0.98	***	***	***	Unb.	ns	ns	ns	ns	ns	ns
		B1	0.15	0.21	0.20	0.49	0.48	0.48	1.00	1.00	1.00	***	***	***	B1		**		ns		ns
		B2+	0.32	0.23	0.13	0.48	0.49	0.49	0.99	0.99	1.00	***	***	***	B2+						
	Rough.	Unb.	1.81	1.81	1.81	-5.66	-5.66	-5.66	0.13	0.13	0.13	***	***	***	Unb.	ns	***	**	ns	ns	ns
		B1	2.76	-2.14	0.25	-6.07	-7.95	-6.76	0.36	0.33	0.12	***	***	**	B1		***		**		ns
		B2+	3.22	1.73	-5.34	-4.00	-4.54	-9.45	0.72	0.21	0.08	***	***	ns	B2+						
	Open 5m	Unb.	12.83	12.83	12.83	-15.66	-15.66	-15.66	0.28	0.28	0.28	***	***	***	Unb.	ns	***	ns	***	ns	ns
		B1	13.51	11.98	13.27	-13.56	-15.93	-18.40	0.71	0.54	0.27	***	***	***	B1		***		***		ns
		B2+	10.56	9.55	11.36	-9.36	-8.69	-14.33	0.85	0.62	0.54	***	***	***	B2+						
	Open 10m	Unb.	14.09	14.09	14.09	-12.39	-12.39	-12.39	0.63	0.63	0.63	***	***	***	Unb.	***	ns	**	***	ns	**
		B1	15.61	12.87	13.93	-14.69	-10.42	-12.30	0.86	0.86	0.79	***	***	***	B1		***		ns		*
		B2+	13.92	12.28	11.78	-12.57	-9.70	-9.12	0.94	0.86	0.85	***	***	***	B2+						
		Unb.	12.34	12.34	12.34	-9.21	-9.21	-9.21	0.86	0.86	0.86	***	***	***	Unb.	***	***	***	ns	ns	*

	Open 15m	B1	13.10	11.57	12.06	-11.44	-7.92	-8.67	0.91	0.91	0.91	***	***	***	B1		ns		ns		ns
		B2+	13.08	11.96	11.23	-11.62	-8.56	-7.47	0.87	0.86	0.93	***	***	***	B2+						
	LAI	Unb.	0.45	0.45	0.45	2.06	2.06	2.06	0.20	0.20	0.20	***	***	***	Unb.	ns	**	**	ns	ns	ns
		B1	1.29	-3.85	-0.96	2.47	2.82	2.36	0.55	0.40	0.14	***	***	**	B1		***		***		ns
		B2+	1.88	0.75	-4.94	1.59	1.54	3.08	0.66	0.46	0.32	***	***	**	B2+						
	Under LAI	Unb.	18.83	18.83	18.83	-10.12	-10.12	-10.12	0.12	0.12	0.12	***	***	***	Unb.	ns	**	ns	ns	ns	ns
		B1	16.26	16.72	19.47	-11.97	-8.39	-10.84	0.00	0.18	0.42	ns	***	***	B1		***		ns		ns
		B2+	-0.62	15.54	17.64	7.08	-8.15	-9.75	0.16	0.05	0.63	***	ns	***	B2+						
	LAHV	Unb.	3.54	3.54	3.54	0.12	0.12	0.12	0.73	0.73	0.73	***	***	***	Unb.	***	***	***	ns	ns	*
		B1	2.75	2.11	3.10	0.16	0.15	0.13	0.84	0.90	0.74	***	***	***	B1		ns		ns		ns
		B2+	2.27	2.52	1.49	0.17	0.14	0.16	0.87	0.82	0.92	***	***	***	B2+						
Maximum Height	Mean H.	Unb.	4.09	4.09	4.09	1.20	1.20	1.20	0.84	0.84	0.84	***	***	***	Unb.	ns	***	ns	ns	ns	ns
		B1	6.82	5.02	4.05	1.11	1.12	1.18	0.88	0.92	0.92	***	***	***	B1		***		ns		ns
		B2+	9.00	5.08	2.76	0.91	1.20	1.20	0.92	0.85	0.92	***	***	***	B2+						
	Rough.	Unb.	7.47	7.47	7.47	-14.25	-14.25	-14.25	0.00	0.00	0.00	ns	ns	ns	Unb.	ns	***	ns	ns	ns	ns
		B1	12.81	-0.72	4.03	-13.51	-18.63	-16.59	0.11	0.14	0.01	***	***	ns	B1		***		*		ns
		B2+	14.58	8.62	-9.06	-7.56	-11.35	-22.10	0.53	0.02	0.00	***	ns	ns	B2+						
	Open 5m	Unb.	35.25	35.25	35.25	-39.62	-39.62	-39.62	0.08	0.08	0.08	***	***	***	Unb.	*	***	ns	***	ns	ns
		B1	37.07	32.40	36.12	-30.93	-37.39	-45.85	0.48	0.34	0.11	***	***	**	B1		***		**		ns
		B2+	28.48	28.07	30.33	-17.88	-21.32	-35.10	0.70	0.36	0.38	***	***	**	B2+					ns	
	Open 10m	Unb.	38.30	38.30	38.30	-30.88	-30.88	-30.88	0.37	0.37	0.37	***	***	***	Unb.	ns	***	***	ns		ns
		B1	41.98	34.46	37.52	-33.67	-24.44	-29.89	0.64	0.72	0.63	***	***	***	B1		***		ns		ns
		B2+	35.04	35.58	31.73	-24.10	-25.07	-23.11	0.81	0.62	0.75	***	***	***	B2+					ns	
	Open 15m	Unb.	34.08	34.08	34.08	-23.10	-23.10	-23.10	0.68	0.68	0.68	***	***	***	Unb.	*	ns	***	ns		*
		B1	36.26	31.41	33.45	-25.96	-18.68	-21.98	0.83	0.83	0.82	***	***	***	B1		ns		ns		ns
		B2+	33.99	35.14	29.72	-22.94	-22.44	-17.31	0.84	0.76	0.85	***	***	***	B2+					ns	
	LAI	Unb.	4.03	4.03	4.03	5.20	5.20	5.20	0.06	0.06	0.06	***	***	***	Unb.	ns	***	ns	ns		ns
		B1	9.63	-4.68	1.31	5.46	6.63	5.72	0.31	0.30	0.04	***	***	ns	B1		***		**		ns
		B2+	11.94	6.33	-7.58	3.02	3.86	7.07	0.49	0.36	0.21	***	***	*	B2+					ns	
	Under	Unb.	50.03	50.03	50.03	-25.21	-25.21	-25.21	0.11	0.11	0.11	***	***	***	Unb.	ns	***	*	ns		ns

	LAI	B1	42.97	43.18	51.94	-26.66	-19.49	-27.48	0.02	0.16	0.36	ns	***	***	B1		***		ns		ns
		B2+	6.86	41.58	43.13	13.93	-19.04	-21.19	0.09	0.03	0.64	**	ns	***	B2+						
	LAHV	Unb.	12.09	12.09	12.09	0.31	0.31	0.31	0.47	0.47	0.47	***	***	***	Unb.	*	ns	ns	ns	ns	ns
		B1	12.63	9.68	11.25	0.37	0.35	0.31	0.64	0.78	0.54	***	***	***	B1		ns		ns		ns
		B2+	12.68	10.67	5.66	0.32	0.37	0.40	0.70	0.68	0.82	***	***	***	B2+						
Mean Height	Rough.	Unb.	2.87	2.87	2.87	-11.88	-11.88	-11.88	0.18	0.18	0.18	***	***	***	Unb.	ns	***	**	ns	ns	ns
		B1	5.24	-5.04	-0.08	-12.36	-16.58	-14.09	0.37	0.33	0.12	***	***	**	B1		***		**		ns
		B2+	5.99	3.05	-11.58	-8.44	-9.33	-19.62	0.74	0.23	0.10	***	***	ns	B2+						
	Open 5m	Unb.	25.96	25.96	25.96	-32.71	-32.71	-32.71	0.35	0.35	0.35	***	***	***	Unb.	*	***	ns	***	ns	ns
		B1	27.13	24.39	27.06	-27.65	-33.23	-38.36	0.72	0.54	0.28	***	***	***	B1		***		***		ns
		B2+	21.36	19.17	23.02	-19.53	-17.91	-29.49	0.87	0.64	0.57	***	***	***	B2+						
	Open 10m	Unb.	28.67	28.67	28.67	-26.05	-26.05	-26.05	0.69	0.69	0.69	***	***	***	Unb.	**	ns	***	***	ns	**
		B1	31.41	26.28	28.43	-29.94	-21.71	-25.58	0.87	0.87	0.79	***	***	***	B1		*		ns		*
		B2+	28.65	24.60	23.87	-26.62	-19.70	-18.78	0.95	0.86	0.87	***	***	***	B2+						
	Open 15m	Unb.	25.08	25.08	25.08	-19.62	-19.62	-19.62	0.87	0.87	0.87	***	***	***	Unb.	***	***	***	ns	ns	**
		B1	26.37	23.53	24.53	-23.43	-16.43	-18.03	0.92	0.91	0.91	***	***	***	B1		ns		ns		ns
		B2+	26.69	24.03	22.96	-24.45	-17.50	-15.82	0.87	0.86	0.93	***	***	***	B2+						
	LAI	Unb.	-0.03	-0.03	-0.03	4.34	4.34	4.34	0.24	0.24	0.24	***	***	***	Unb.	ns	***	**	*	ns	ns
		B1	2.24	-8.41	-2.58	5.03	5.84	4.91	0.55	0.39	0.14	***	***	**	B1		***		***		ns
		B2+	3.23	1.01	-10.79	3.32	3.18	6.40	0.67	0.45	0.32	***	***	**	B2+						
	Under LAI	Unb.	38.52	38.52	38.52	-21.14	-21.14	-21.14	0.11	0.11	0.11	***	***	***	Unb.	ns	***	ns	ns	ns	ns
		B1	32.77	34.22	39.81	-24.41	-17.40	-22.41	0.00	0.19	0.42	ns	***	***	B1		***		ns		ns
		B2+	-1.98	31.57	36.29	14.78	-16.84	-20.42	0.17	0.06	0.64	***	ns	***	B2+						
	LAHV	Unb.	6.46	6.46	6.46	0.26	0.26	0.26	0.76	0.76	0.76	***	***	***	Unb.	***	***	***	ns	ns	*
		B1	5.18	3.83	5.85	0.34	0.32	0.27	0.84	0.90	0.73	***	***	***	B1		ns		ns		ns
		B2+	3.98	4.58	2.66	0.35	0.30	0.32	0.87	0.83	0.93	***	***	***	B2+						
Roughness	Open 5m	Unb.	-1.95	-1.95	-1.95	2.80	2.80	2.80	0.88	0.88	0.88	***	***	***	Unb.	*	***	***	***	ns	ns
		B1	-1.86	-1.80	-1.97	2.50	2.09	2.88	0.63	0.82	0.84	***	***	***	B1		ns		ns		ns
		B2+	-1.82	-1.71	-1.91	2.34	1.91	2.29	0.88	0.63	0.54	***	***	***	B2+						
		Unb.	-2.18	-2.18	-2.18	2.25	2.25	2.25	0.48	0.48	0.48	***	***	***	Unb.	ns	***	***	ns	ns	ns

	Open 10m	B1	-2.14	-1.90	-2.07	2.48	1.36	2.01	0.52	0.38	0.26	***	***	***	B1		*		**		ns
		B2+	-2.66	-2.28	-2.00	3.11	2.08	1.50	0.74	0.34	0.20	***	***	*	B2+						
	Open 15m	Unb.	-1.88	-1.88	-1.88	1.71	1.71	1.71	0.17	0.17	0.17	***	***	***	Unb.	ns	***	***	ns	ns	**
		B1	-1.70	-1.74	-1.78	1.88	1.04	1.41	0.25	0.24	0.12	***	***	**	B1		***		**		ns
		B2+	-2.42	-2.17	-1.76	2.85	1.74	0.79	0.46	0.10	0.06	***	*	ns	B2+						
	LAI	Unb.	0.21	0.21	0.21	-0.36	-0.36	-0.36	0.61	0.61	0.61	***	***	***	Unb.	ns	ns	ns	ns	ns	ns
		B1	0.23	0.28	0.12	-0.40	-0.38	-0.34	0.68	0.50	0.62	***	***	***	B1		ns		ns		ns
		B2+	0.31	0.17	-0.02	-0.39	-0.33	-0.33	0.88	0.29	0.32	***	***	**	B2+						
	Under LAI	Unb.	-2.99	-2.99	-2.99	1.75	1.75	1.75	0.00	0.00	0.00	ns	ns	ns	Unb.	ns	ns	***	ns	ns	ns
		B1	0.86	-2.35	-2.84	-2.04	1.02	1.59	0.21	0.01	0.02	***	ns	ns	B1		ns		*		ns
		B2+	0.98	-2.85	-2.40	-1.79	1.61	1.00	0.50	0.00	0.03	***	ns	ns	B2+						
	LAHV	Unb.	-0.32	-0.32	-0.32	-0.02	-0.02	-0.02	0.41	0.41	0.41	***	***	***	Unb.	**	***	ns	*	ns	ns
		B1	0.01	-0.57	-0.44	-0.03	-0.02	-0.02	0.46	0.39	0.40	***	***	***	B1		***		**		ns
		B2+	0.24	-0.22	-0.62	-0.04	-0.03	-0.02	0.77	0.24	0.15	***	***	ns	B2+						
Open.5m	Open 10m	Unb.	-0.08	-0.08	-0.08	0.81	0.81	0.81	0.65	0.65	0.65	***	***	***	Unb.	***	***	*	***	ns	ns
		B1	-0.15	-0.05	-0.06	1.08	0.66	0.76	0.89	0.58	0.39	***	***	***	B1		***		***		ns
		B2+	-0.37	-0.30	-0.07	1.37	1.10	0.75	0.86	0.74	0.75	***	***	***	B2+						
	Open 15m	Unb.	0.02	0.02	0.02	0.62	0.62	0.62	0.30	0.30	0.30	***	***	***	Unb.	***	***	ns	**	ns	ns
		B1	0.03	0.02	0.05	0.85	0.50	0.53	0.60	0.41	0.23	***	***	***	B1		***		***		ns
		B2+	-0.25	-0.26	0.00	1.23	0.96	0.55	0.59	0.36	0.42	***	***	**	B2+						
	LAI	Unb.	0.77	0.77	0.77	-0.13	-0.13	-0.13	0.65	0.65	0.65	***	***	***	Unb.	***	***	**	***	ns	*
		B1	0.88	0.97	0.71	-0.17	-0.17	-0.11	0.72	0.50	0.61	***	***	***	B1		ns		ns		*
		B2+	0.92	1.04	1.07	-0.17	-0.19	-0.20	0.88	0.45	0.63	***	***	***	B2+						
	Under LAI	Unb.	-0.35	-0.35	-0.35	0.61	0.61	0.61	0.00	0.00	0.00	ns	ns	ns	Unb.	*	*	ns	*	ns	ns
		B1	1.12	-0.26	-0.30	-0.85	0.49	0.54	0.03	0.07	0.05	ns	*	ns	B1		ns		**		ns
		B2+	1.20	-0.66	-0.46	-0.77	0.91	0.71	0.36	0.03	0.33	***	ns	**	B2+						
	LAHV	Unb.	0.58	0.58	0.58	-0.01	-0.01	-0.01	0.52	0.52	0.52	***	***	***	Unb.	***	***	ns	***	ns	ns
		B1	0.80	0.59	0.54	-0.01	-0.01	-0.01	0.65	0.55	0.48	***	***	***	B1		***		***		*
		B2+	0.91	0.81	0.71	-0.02	-0.02	-0.01	0.83	0.51	0.61	***	***	***	B2+						
Open.10m		Unb.	0.13	0.13	0.13	0.79	0.79	0.79	0.78	0.78	0.78	***	***	***	Unb.	ns	***	ns	ns	ns	ns

	Open 15m	B1	0.16	0.11	0.13	0.80	0.79	0.75	0.84	0.90	0.90	***	***	***	B1		**		ns		ns
		B2+	0.09	0.03	0.05	0.91	0.90	0.85	0.86	0.75	0.78	***	***	***	B2+						
	LAI	Unb.	1.08	1.08	1.08	-0.16	-0.16	-0.16	0.36	0.36	0.36	***	***	***	Unb.	ns	**	***	ns	ns	*
		B1	0.96	1.64	1.15	-0.16	-0.28	-0.18	0.59	0.36	0.18	***	***	***	B1		*		**		ns
		B2+	0.96	1.23	1.67	-0.13	-0.17	-0.30	0.65	0.37	0.44	***	***	**	B2+						
	Under LAI	Unb.	-0.39	-0.39	-0.39	0.82	0.82	0.82	0.15	0.15	0.15	***	***	***	Unb.	ns	***	ns	ns	ns	ns
		B1	-0.05	-0.39	-0.45	0.82	0.82	0.88	0.00	0.29	0.50	ns	***	***	B1		*		ns		ns
		B2+	1.15	-0.38	-0.60	-0.56	0.88	1.03	0.11	0.15	0.67	***	**	***	B2+						
	LAHV	Unb.	0.84	0.84	0.84	-0.01	-0.01	-0.01	0.71	0.71	0.71	***	***	***	Unb.	***	***	***	***	ns	***
		B1	0.89	1.02	0.86	-0.01	-0.01	-0.01	0.75	0.85	0.68	***	***	***	B1		ns		ns		***
		B2+	0.93	1.01	1.15	-0.01	-0.01	-0.02	0.90	0.71	0.84	***	***	***	B2+						
Open.15m	LAI	Unb.	1.25	1.25	1.25	-0.22	-0.22	-0.22	0.19	0.19	0.19	***	***	***	Unb.	ns	***	***	ns	ns	ns
		B1	1.03	1.89	1.45	-0.22	-0.34	-0.26	0.39	0.33	0.09	***	***	*	B1		***		***		ns
		B2+	0.96	1.33	2.10	-0.14	-0.19	-0.39	0.38	0.35	0.20	***	***	*	B2+						
	Under LAI	Unb.	-0.71	-0.71	-0.71	1.10	1.10	1.10	0.21	0.21	0.21	***	***	***	Unb.	ns	***	ns	ns	ns	ns
		B1	-0.30	-0.64	-0.83	1.08	1.05	1.23	0.03	0.25	0.51	ns	***	***	B1		***		ns		ns
		B2+	1.18	-0.46	-0.80	-0.61	0.99	1.25	0.02	0.07	0.63	ns	*	***	B2+						
	LAHV	Unb.	0.92	0.92	0.92	-0.01	-0.01	-0.01	0.70	0.70	0.70	***	***	***	Unb.	**	ns	***	*	ns	***
		B1	0.92	1.15	1.01	-0.02	-0.02	-0.01	0.71	0.87	0.64	***	***	***	B1		ns		ns		*
		B2+	0.93	1.09	1.28	-0.01	-0.02	-0.02	0.74	0.75	0.80	***	***	***	B2+						
LAI	Under LAI	Unb.	-1.10	-1.10	-1.10	4.81	4.81	4.81	0.11	0.11	0.11	***	***	***	Unb.	ns	ns	***	ns	ns	ns
		B1	-1.49	0.59	-0.52	4.97	2.88	4.50	0.26	0.06	0.02	***	*	ns	B1		ns		*		ns
		B2+	-1.56	-2.31	0.82	4.42	4.73	3.15	0.61	0.15	0.03	***	**	ns	B2+						
	LAHV	Unb.	1.51	1.51	1.51	0.06	0.06	0.06	0.59	0.59	0.59	***	***	***	Unb.	ns	***	ns	***	ns	ns
		B1	0.58	2.20	1.70	0.07	0.05	0.05	0.74	0.53	0.53	***	***	***	B1		***		***		ns
		B2+	0.17	1.23	1.97	0.11	0.09	0.05	0.78	0.69	0.52	***	***	***	B2+						
Under LAI	LAHV	Unb.	1.50	1.50	1.50	-0.01	-0.01	-0.01	0.06	0.06	0.06	***	***	***	Unb.	ns	***	***	*	ns	ns
		B1	0.41	1.71	1.52	0.01	-0.02	-0.01	0.01	0.18	0.24	ns	***	***	B1		***		ns		ns
		B2+	0.39	1.59	1.66	0.03	-0.02	-0.02	0.20	0.01	0.49	***	ns	***	B2+						

SI Table 3.4. Number of significant different relationship in the SMA analysis between all lidar metrics by YSLF groups. B1 represents areas with single fire events and B2+ represents areas with multiple fire events

	Unburned vs B1			Unburned vs B2+			B1 vs B2+		
YSLF groups	0-3	4-9	10+	0-3	4-9	10+	0-3	4-9	10+
Number of significant relationships	20	25	0	36	17	11	31	21	6
% of significant relationships	44	56	0	80	38	24	69	47	13

SI Table 3.5. Mean values for each metric analysed separately by years since last fire (YSLF), number of fire events –single (B1) and multiple (B2+) and regions as defined in Heinrich *et al.* (2021).

Region	SE							SW							NE							NW						
Reoccurrens		B1			B2+				B1			B2+				B1			B2+				B1			B2+		
YSLF	Unb.	0-3	4-9	10+	0-3	4-9	10+	Unb.	0-3	4-9	10+	0-3	4-9	10+	Unb.	0-3	4-9	10+	0-3	4-9	10+	Unb.	0-3	4-9	10+	0-3	4-9	10+
ACD	66.1	56.7	46.5	66.1	31.1	36.4	56.7	96.3	131.6	104.1	90.9	132.2	*NA*	73.8	69.0	39.2	75.4	92.8	66.1	*NA*	*NA*	69.0	70.0	*NA*	79.1	*NA*	*NA*	*NA*
Max H.	22.3	22.6	19.4	22.5	17.9	18.7	20.3	27.5	29.6	28.1	27.1	30.1	*NA*	23.1	22.6	18.4	23.3	27.4	22.8	*NA*	*NA*	21.1	23.5	*NA*	21.7	*NA*	*NA*	*NA*
Mean H.	15.0	13.9	12.6	15.6	9.8	11.4	14.5	19.4	22.9	20.2	19.0	23.5	*NA*	16.1	16.2	11.5	17.3	19.3	14.2	*NA*	*NA*	14.9	16.2	*NA*	17.7	*NA*	*NA*	*NA*
Roughness	0.4	0.6	0.4	0.3	0.7	0.4	0.3	0.3	0.2	0.3	0.3	0.2	*NA*	0.3	0.3	0.5	0.2	0.3	0.6	*NA*	*NA*	0.4	0.4	*NA*	0.2	*NA*	*NA*	*NA*
Open. 5m	0.1	0.3	0.2	0.1	0.4	0.2	0.1	0.1	0.0	0.0	0.1	0.0	*NA*	0.1	0.1	0.4	0.0	0.1	0.2	*NA*	*NA*	0.2	0.2	*NA*	0.0	*NA*	*NA*	*NA*
Open. 10m	0.3	0.4	0.4	0.3	0.5	0.5	0.3	0.2	0.1	0.1	0.2	0.0	*NA*	0.3	0.2	0.5	0.2	0.2	0.3	*NA*	*NA*	0.3	0.3	*NA*	0.1	*NA*	*NA*	*NA*
Open 15m	0.5	0.5	0.6	0.5	0.7	0.7	0.5	0.3	0.1	0.3	0.3	0.1	*NA*	0.5	0.4	0.7	0.4	0.3	0.5	*NA*	*NA*	0.5	0.4	*NA*	0.2	*NA*	*NA*	*NA*
LAI	3.6	2.3	3.6	4.0	2.0	3.3	3.9	4.2	3.4	4.5	4.1	5.4	*NA*	4.4	3.5	2.3	4.6	3.5	3.0	*NA*	*NA*	3.8	4.1	*NA*	*NA*	*NA*	*NA*	*NA*
LAI Under	1.1	0.6	1.4	1.1	0.8	1.4	1.1	1.1	0.6	1.0	1.0	0.8	*NA*	1.4	0.9	0.9	1.3	0.7	1.0	*NA*	*NA*	0.7	0.9	*NA*	*NA*	*NA*	*NA*	*NA*
LAHV	34.5	26.1	29.3	39.0	16.9	23.3	36.2	47.9	52.5	53.5	48.1	82.1	*NA*	45.3	36.8	19.6	42.8	42.1	29.8	*NA*	*NA*	44.8	50.3	*NA*	*NA*	*NA*	*NA*	*NA*

Appendix 4: Supporting Information for Chapter 4

SI Figure 4.1. Frequency of secondary forest age by secondary forest successional stage. In (A) unburned areas in early successional stage, (B) burned areas in early successional stage, (C) unburned areas in later successional stage and (D) burned areas in later successional stage.

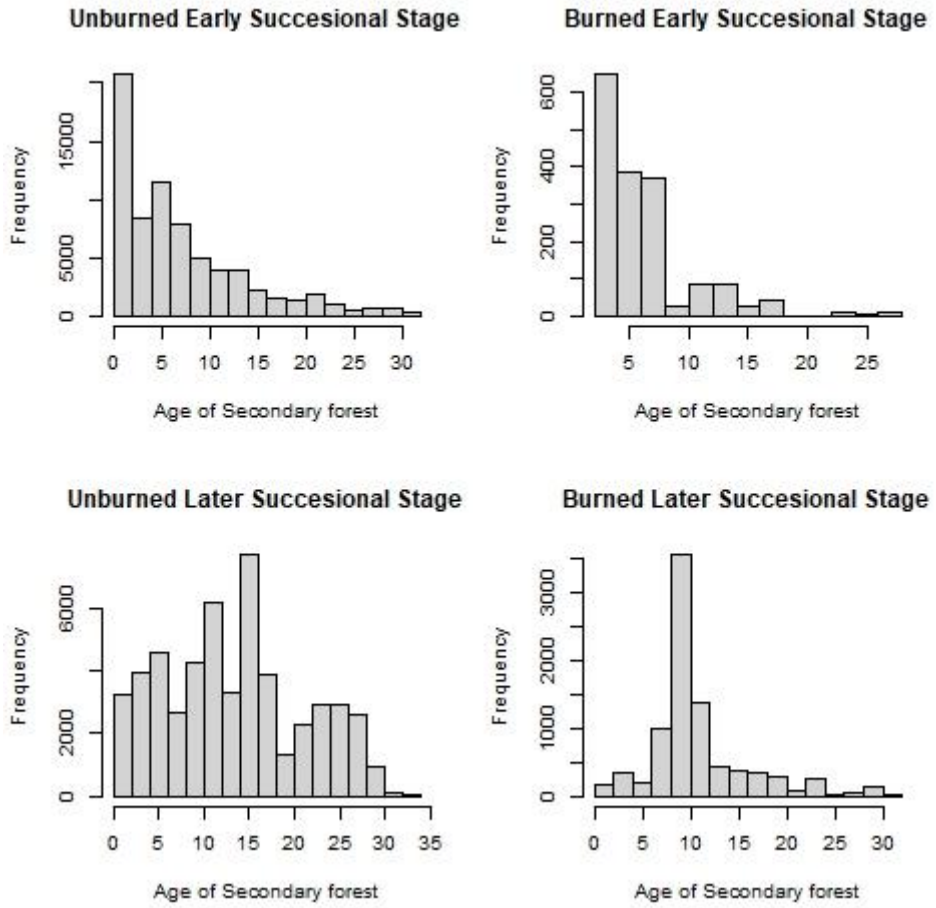

SI Figure 4.2. Boxplots for the canopy metrics (A) Maximum height, (B) Mean height, (C) Openness at 5 m, (D) Openness at 10 m, (E) Roughness, (F) Leaf Area Index and (G) Leaf Area Height Volume. Boxplots are divided into unburned (blue) and burned (orange) categories. Asterisks represent significant differences between unburned and burned categories. Significance levels: *p<0.05, **p<0.01, ***p<0.001; ns, non-significant relationships.

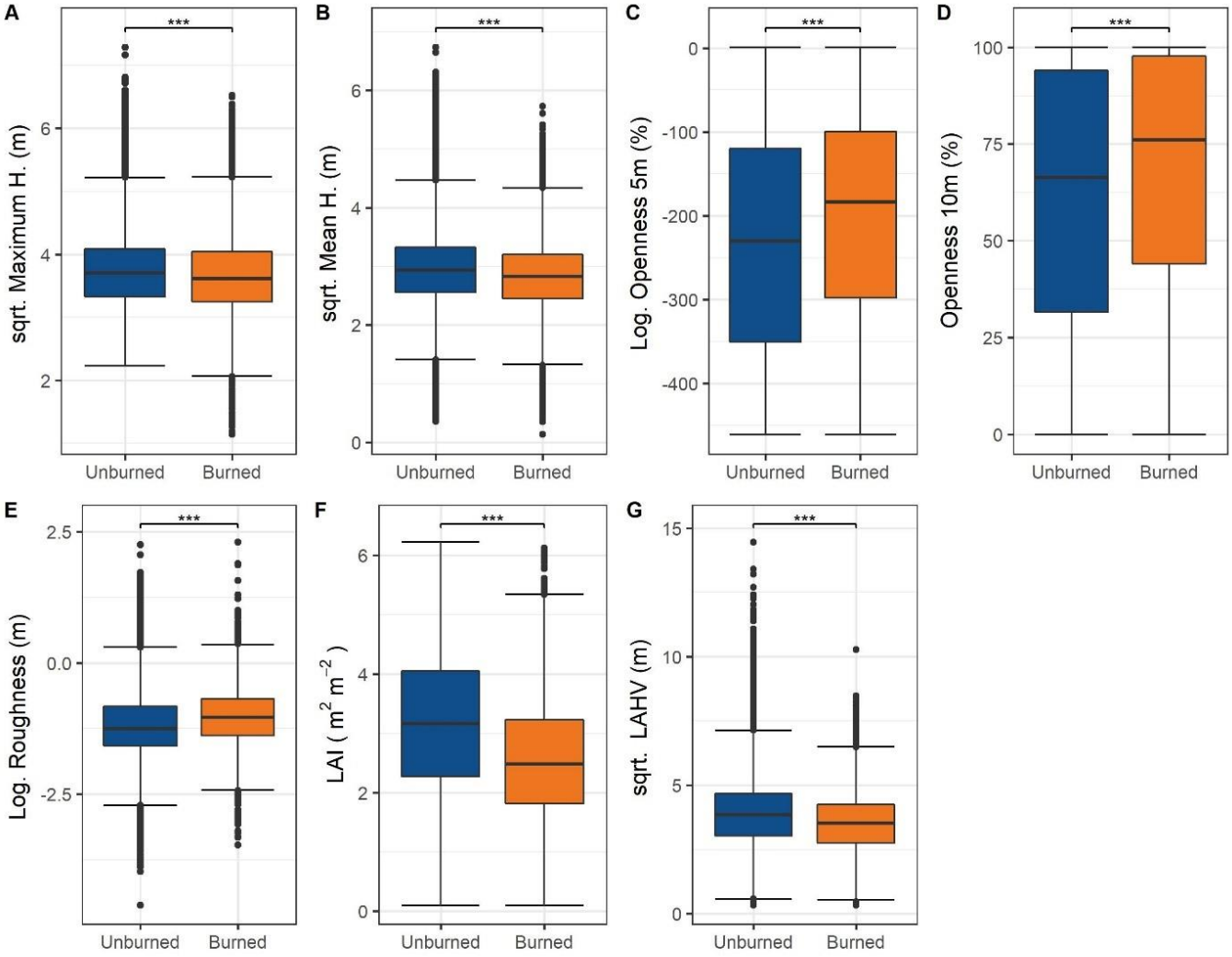

SI Figure 4.3 Coefficient estimates for each forest structure metric in early successional stage (blue) and later successional stage (orange) at zero years after the fire, predicted from linear mixed effects models (Table 4.2). Dots represent the coefficient mean and tails represent the 95% confidence interval of the mean.

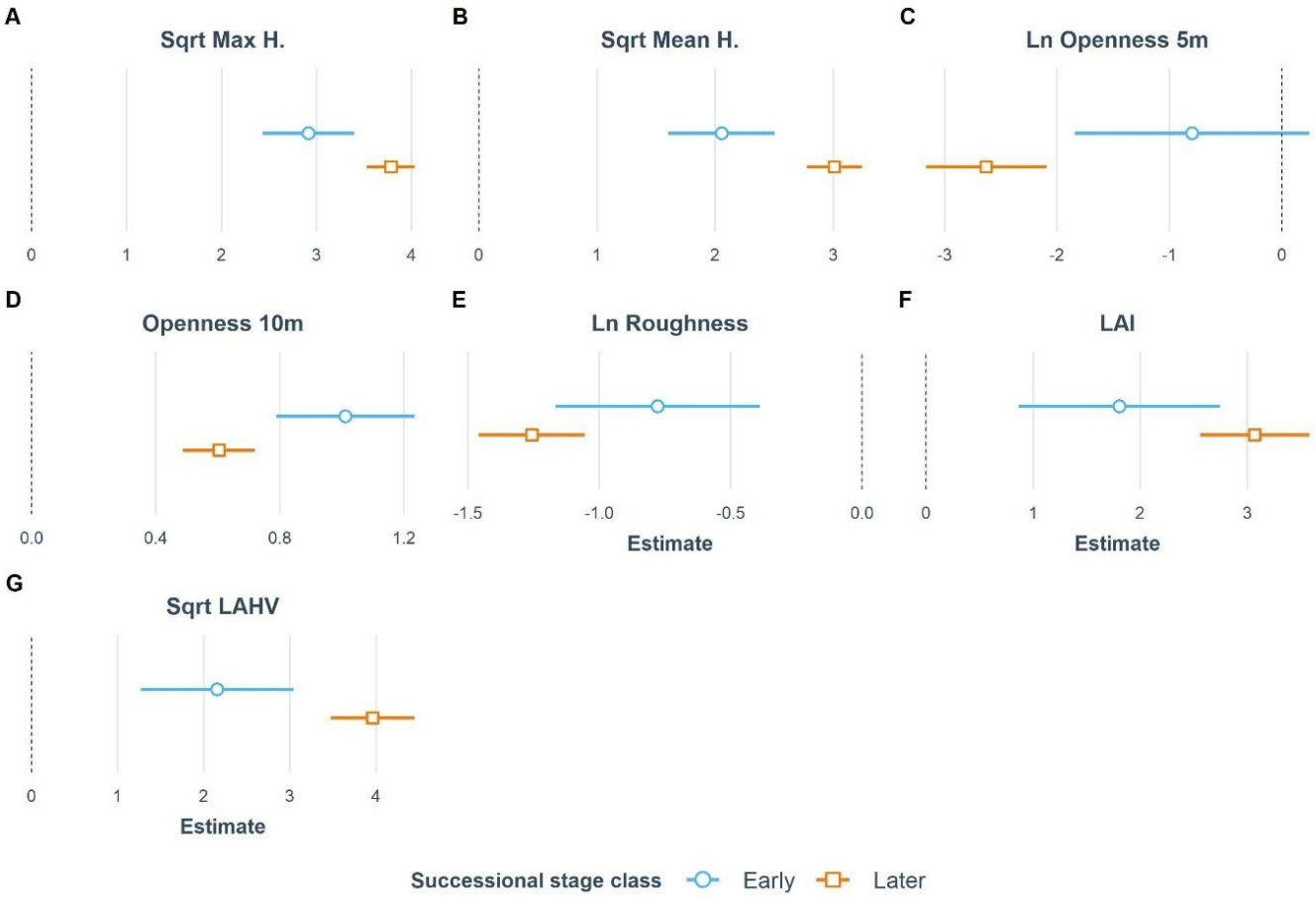

SI Table 4.1. Mean values of secondary forest age for each group of forest successional stage (Early Successional – ES and Later Successional – LS), for unburned and burned areas.

	ES		LS	
	Unburned	Burned	Unburned	Burned
Mean of Sec. For Age	7.4	6.51	13.85	11.13

References

Aleixo I, Norris D, Hemerik L, Barbosa A, Prata E, Costa F, Poorter L. 2019. Amazonian rainforest tree mortality driven by climate and functional traits. *Nature Climate Change* **9**(5): 384-388.

Alencar A, Nepstad D, Diaz MCV. 2006. Forest Understory Fire in the Brazilian Amazon in ENSO and Non-ENSO Years: Area Burned and Committed Carbon Emissions. *Earth Interactions* **10**(6): 1-17.

Alencar AAC, Arruda VLS, Silva WVd, Conciani DE, Costa DP, Crusco N, Duverger SG, Ferreira NC, Franca-Rocha W, Hasenack H, et al. 2022. Long-Term Landsat-Based Monthly Burned Area Dataset for the Brazilian Biomes Using Deep Learning. *Remote Sensing* **14**(11): 2510.

Alencar AAC, Solórzano LA, Nepstad DC. 2004. MODELING FOREST UNDERSTORY FIRES IN AN EASTERN AMAZONIAN LANDSCAPE. *ECOLOGICAL APPLICATIONS* **14**(sp4): 139-149.

Almeida, Stark SC, Schietti J, Camargo JLC, Amazonas NT, Gorgens EB, Rosa DM, Smith MN, Valbuena R, Saleska S, et al. 2019. Persistent effects of fragmentation on tropical rainforest canopy structure after 20 yr of isolation. *ECOLOGICAL APPLICATIONS* **29**(6): e01952.

Almeida DRAd, Nelson BW, Schietti J, Gorgens EB, Resende AF, Stark SC, Valbuena R. 2016. Contrasting fire damage and fire susceptibility between seasonally flooded forest and upland forest in the Central Amazon using portable profiling LiDAR. *Remote Sensing of Environment* **184**: 153-160.

Andersen H-E, Reutebuch SE, McGaughey RJ, d'Oliveira MV, Keller M. 2014. Monitoring selective logging in western Amazonia with repeat lidar flights. *Remote Sensing of Environment* **151**: 157-165.

Anderson K, Hancock S, Disney M, Gaston KJ. 2016. Is waveform worth it? A comparison of Li DAR approaches for vegetation and landscape characterization. *Remote Sensing in Ecology and Conservation* **2**(1): 5-15.

Anderson LO, Ribeiro Neto G, Cunha AP, Fonseca MG, Mendes de Moura Y, Dalagnol R, Wagner FH, de Aragão LEOeC. 2018. Vulnerability of Amazonian forests to repeated droughts. *Philosophical Transactions of the Royal Society B: Biological Sciences* **373**(1760): 20170411.

Aragão LE, Anderson LO, Fonseca MG, Rosan TM, Vedovato LB, Wagner FH, Silva CV, Junior CHS, Arai E, Aguiar AP. 2018. 21st Century drought-related fires counteract the decline of Amazon deforestation carbon emissions. *Nature Communications* **9**(1): 536.

Aragão LEOC, Malhi Y, Metcalfe DB, Silva-Espejo JE, Jimenez E, Navarrete D, Almeida S, Costa ACL, Salinas N, Phillips OL, et al. 2009. Above- and below-ground net primary productivity across ten Amazonian forests on contrasting soils. *Biogeosciences* **6**(12): 2759-2778.

Aragão LEOC, Malhi Y, Roman-Cuesta RM, Saatchi S, Anderson LO, Shimabukuro YE. 2007. Spatial patterns and fire response of recent Amazonian droughts. *Geophysical Research Letters* **34**(7).

Armenteras D, González TM, Retana J. 2013. Forest fragmentation and edge influence on fire occurrence and intensity under different management types in Amazon forests. *Biological Conservation* **159**: 73-79.

Ascough PL, Bird MI, Brock F, Higham TFG, Meredith W, Snape CE, Vane CH. 2009. Hydropyrolysis as a new tool for radiocarbon pre-treatment and the quantification of black carbon. *Quaternary Geochronology* **4**(2): 140-147.

Asner GP, Mascaro J. 2014. Mapping tropical forest carbon: Calibrating plot estimates to a simple LiDAR metric. *Remote Sensing of Environment* **140**: 614-624.

Avissar R, Werth D. 2005. Global hydroclimatological teleconnections resulting from tropical deforestation. *Journal of Hydrometeorology* **6**(2): 134-145.

Baker TR, Phillips OL, Malhi Y, Almeida S, Arroyo L, Di Fiore A, Erwin T, Killeen TJ, Laurance SG, Laurance WF, et al. 2004. Variation in wood density determines spatial patterns in Amazonian forest biomass. *GCB* **10**(5): 545-562.

Balch JK, Brando PM, Nepstad DC, Coe MT, Silvério D, Massad TJ, Davidson EA, Lefebvre P, Oliveira-Santos C, Rocha W. 2015. The susceptibility of southeastern Amazon forests to fire: insights from a large-scale burn experiment. *BioScience* **65**(9): 893-905.

Balch JK, Nepstad DC, Brando PM, Curran LM, Portela O, De Carvalho JR O, Lefebvre P. 2008. Negative fire feedback in a transitional forest of southeastern Amazonia. *Global Change Biology* **14**(10): 2276-2287.

Balch JK, Nepstad DC, Curran LM, Brando PM, Portela O, Guilherme P, Reuning-Scherer JD, de Carvalho O. 2011. Size, species, and fire behavior predict tree and liana mortality from experimental burns in the Brazilian Amazon. *Forest Ecology and Management* **261**(1): 68-77.

Barlow J, Lagan BO, Peres CA. 2003a. Morphological correlates of fire-induced tree mortality in a central Amazonian forest. *Journal of Tropical Ecology* **19**(3): 291-299.

Barlow J, Peres CA. 2008. Fire-mediated dieback and compositional cascade in an Amazonian forest. *Philos Trans R Soc Lond B Biol Sci* **363**(1498): 1787-1794.

Barlow J, Peres CA, Lagan BO, Haugaasen T. 2003b. Large tree mortality and the decline of forest biomass following Amazonian wildfires. *Ecology Letters* **6**(1): 6-8.

Barros-Rosa L, de Arruda PHZ, Machado NG, Pires-Oliveira JC, Eisenlohr PV. 2022. Fire probability mapping and prediction from environmental data: What a comprehensive savanna-forest transition can tell us. *Forest Ecology and Management* **520**: 120354.

Barros FdV, Bittencourt PR, Brum M, Restrepo-Coupe N, Pereira L, Teodoro GS, Saleska SR, Borma LS, Christoffersen BO, Penha D. 2019. Hydraulic traits explain differential responses of Amazonian forests to the 2015 El Niño-induced drought. *New Phytologist* **223**(3): 1253-1266.

Bartholomew D, Banin LF, Bittencourt PR, Suis MAF, Mercado LM, Nilus R, Burslem DF, Rowland LR. 2022. Differential nutrient limitation and tree height control leaf physiology, supporting niche partitioning in tropical dipterocarp forests. *Functional Ecology*.

Barton K. 2020. MuMIn: Multi-Model Inference. *Version* **1**(18): 439.

Bates D, Maechler M, Bolker B, Walker S, Christensen RHB, Singmann H, Dai B, Scheipl F, Grothendieck G, Green P. 2018. Package 'lme4'. *Version* **1**(17): 437.

Batterman SA, Hedin LO, van Breugel M, Ransijn J, Craven DJ, Hall JS. 2013. Key role of symbiotic dinitrogen fixation in tropical forest secondary succession. *Nature* **502**(7470): 224-227.

Bennett AC, McDowell NG, Allen CD, Anderson-Teixeira KJ. 2015. Larger trees suffer most during drought in forests worldwide. *Nature plants* **1**(10): 1-5.

Berenguer E, Gardner TA, Ferreira J, Aragão LEOC, Mac Nally R, Thomson JR, Vieira ICG, Barlow J. 2018a. Seeing the woods through the saplings: Using

wood density to assess the recovery of human-modified Amazonian forests. *Journal of Ecology* **106**(6): 2190-2203.

Berenguer E, Lennox GD, Ferreira J, Malhi Y, Aragão LEOC, Barreto JR, Del Bon Espírito-Santo F, Figueiredo AES, França F, Gardner TA, et al. 2021. Tracking the impacts of El Niño drought and fire in human-modified Amazonian forests. *Proceedings of the National Academy of Sciences* **118**(30): e2019377118.

Berenguer E, Malhi Y, Brando P, Cardoso Nunes Cordeiro A, Ferreira J, França F, Chesini Rossi L, Maria Moraes de Seixas M, Barlow J. 2018b. Tree growth and stem carbon accumulation in human-modified Amazonian forests following drought and fire. *Philosophical Transactions of the Royal Society B: Biological Sciences* **373**(1760): 20170308.

Bird MI, Wynn JG, Saiz G, Wurster CM, McBeath A. 2015. The Pyrogenic Carbon Cycle. *Annual Review of Earth and Planetary Sciences* **43**(1): 273-298.

Bittencourt PRL, Oliveira RS, da Costa ACL, Giles AL, Coughlin I, Costa PB, Bartholomew DC, Ferreira LV, Vasconcelos SS, Barros FV, et al. 2020. Amazonia trees have limited capacity to acclimate plant hydraulic properties in response to long-term drought. *Global Change Biology* **26**(6): 3569-3584.

BjØrnstad ON, Falck W. 2001. Nonparametric spatial covariance functions: estimation and testing. *Environmental and Ecological Statistics* **8**(1): 53-70.

Bonal D, Burban B, Stahl C, Wagner F, Hérault B. 2016. The response of tropical rainforests to drought—lessons from recent research and future prospects. *Annals of forest science* **73**(1): 27-44.

Bonini I, Rodrigues C, Dallacort R, Marimon Junior BH, Carvalho MAC. 2014. Rainfall and deforestation in the municipality of Colíder, southern Amazon. *Revista Brasileira de Meteorologia* **29**: 483-493.

Brando PM, Balch JK, Nepstad DC, Morton DC, Putz FE, Coe MT, Silvério D, Macedo MN, Davidson EA, Nóbrega CC. 2014. Abrupt increases in Amazonian tree mortality due to drought–fire interactions. *Proceedings of the National Academy of Sciences* **111**(17): 6347-6352.

Brando PM, Nepstad DC, Balch JK, Bolker B, Christman MC, Coe M, Putz FE. 2012. Fire-induced tree mortality in a neotropical forest: the roles of bark traits, tree size, wood density and fire behavior. *Global Change Biology* **18**(2): 630-641.

Brienen RJW, Phillips OL, Feldpausch TR, Gloor E, Baker TR, Lloyd J, Lopez-Gonzalez G, Monteagudo-Mendoza A, Malhi Y, Lewis SL, et al. 2015. Long-term decline of the Amazon carbon sink. *Nature* **519**(7543): 344-348.

Bullock EL, Woodcock CE, Souza Jr C, Olofsson P. 2020. Satellite-based estimates reveal widespread forest degradation in the Amazon. *Global Change Biology* **26**(5): 2956-2969.

Bush MB, Silman MR. 2007. Amazonian exploitation revisited: ecological asymmetry and the policy pendulum. *Frontiers in Ecology and the Environment* **5**(9): 457-465.

Bush MB, Silman MR, McMichael C, Saatchi S. 2008. Fire, climate change and biodiversity in Amazonia: a Late-Holocene perspective. *Philosophical Transactions of the Royal Society of London B Biological Sciences* **363**(1498): 1795-1702.

Carter JK, Schimid K, Waters L, Betzhold B, Hadley R, Mataosky R, Halleran J. 2012. *Lidar 101: An Introduction to Lidar Technology, Data, and Applications.*

Charleston, SC: National Oceanic and Atmospheric Administration (NOAA) Coastal Services Cente.

Chao K-J, Phillips OL, Monteagudo A, Torres-Lezama A, Vásquez Martínez R. 2009. How do trees die? Mode of death in northern Amazonia. *Journal of Vegetation Science* **20**(2): 260-268.

Chave J, Andalo C, Brown S, Cairns MA, Chambers JQ, Eamus D, Folster H, Fromard F, Higuchi N, Kira T, et al. 2005. Tree allometry and improved estimation of carbon stocks and balance in tropical forests. *Oecologia* **145**(1): 87-99.

Chave J, Coomes D, Jansen S, Lewis SL, Swenson NG, Zanne AE. 2009. Towards a worldwide wood economics spectrum. *Ecology Letters* **12**(4): 351-366.

Chazdon RL, Broadbent EN, Rozendaal DM, Bongers F, Zambrano AMA, Aide TM, Balvanera P, Becknell JM, Boukili V, Brancalion PH. 2016. Carbon sequestration potential of second-growth forest regeneration in the Latin American tropics. *Science Advances* **2**(5): e1501639.

Chazdon RL, Pearcy RW. 1991. The importance of sunflecks for forest understory plants. *BioScience* **41**(11): 760-766.

Chazdon RL, Peres CA, Dent D, Sheil D, Lugo AE, Lamb D, Stork NE, Miller SE. 2009. The potential for species conservation in tropical secondary forests. *Conservation Biology* **23**(6): 1406-1417.

Cheng C-H, Lehmann J, Thies JE, Burton SD. 2008. Stability of black carbon in soils across a climatic gradient. *Journal of Geophysical Research* **113**(G2).

Clark DB, Ferraz A, Clark DA, Kellner JR, Letcher SG, Saatchi S. 2019. Diversity, distribution and dynamics of large trees across an old-growth lowland tropical rain forest landscape. *PLOS ONE* **14**(11): e0224896.

Clement CR. 1999. 1942 and the Loss of Amazonian Crop Genetic Resources. I. The Relation between Domestication and Human Population Decline. *Economic Botany* **53**(2): 188-202.

Coelho de Souza F, Dexter KG, Phillips OL, Brienen RJW, Chave J, Galbraith DR, Lopez Gonzalez G, Monteagudo Mendoza A, Pennington RT, Poorter L, et al. 2016. Evolutionary heritage influences Amazon tree ecology. *Proceedings of the Royal Society B: Biological Sciences* **283**(1844).

Coomes DA, Kunstler G, Canham CD, Wright E. 2009. A greater range of shade-tolerance niches in nutrient-rich forests: an explanation for positive richness–productivity relationships? *Journal of Ecology* **97**(4): 705-717.

Coppola AI, Seidel M, Ward ND, Viviroli D, Nascimento GS, Haghipour N, Revels BN, Abiven S, Jones MW, Richey JE, et al. 2019. Marked isotopic variability within and between the Amazon River and marine dissolved black carbon pools. *Nature Communications* **10**(1): 4018.

Czimczik CI, Masiello CA. 2007. Controls on black carbon storage in soils. *Global Biogeochemical Cycles* **21**(3).

d'Oliveira MVN, Figueiredo EO, Papa DdA. 2014. Uso do LIDAR como Ferramenta para o Manejo de Precisão em Florestas Tropicais. *Embrapa Acre-Livro técnico* **132**: 1-132.

d'Oliveira MVN, Ribas LA. 2011. Forest regeneration in artificial gaps twelve years after canopy opening in Acre State Western Amazon. *Forest Ecology and Management* **261**(11): 1722-1731.

da Rocha HR, Goulden ML, Miller SD, Menton MC, Pinto LDVO, de Freitas HC, e Silva Figueira AM. 2004. Seasonality of water and heat fluxes over a tropical forest in eastern Amazonia. *ECOLOGICAL APPLICATIONS* **14**(sp4): 22-32.

da Silva Carvalho LC, Fearnside PM, Nascimento MT, Barbosa RI. 2018. Amazon soil charcoal: Pyrogenic carbon stock depends of ignition source distance and forest type in Roraima, Brazil. *Global Change Biology* **24**(9): 4122-4130.

Dalagnol R, Phillips OL, Gloor E, Galvão LS, Wagner FH, Locks CJ, Aragão LEOC. 2019. Quantifying Canopy Tree Loss and Gap Recovery in Tropical Forests under Low-Intensity Logging Using VHR Satellite Imagery and Airborne LiDAR. *Remote Sensing* **11**(7): 817.

Davies SJ, Abiem I, Salim KA, Aguilar S, Allen D, Alonso A, Anderson-Teixeira K, Andrade A, Arellano G, Ashton PS. 2021. ForestGEO: Understanding forest diversity and dynamics through a global observatory network. *Biological Conservation* **253**: 108907.

de Almeida DRA, Almeyda Zambrano AM, Broadbent EN, Wendt AL, Foster P, Wilkinson BE, Salk C, Papa DdA, Stark SC, Valbuena R, et al. 2020. Detecting successional changes in tropical forest structure using GatorEye drone-borne lidar. *Biotropica* **52**(6): 1155-1167.

de Almeida DRA, Stark SC, Chazdon R, Nelson BW, Cesar RG, Meli P, Gorgens EB, Duarte MM, Valbuena R, Moreno VS, et al. 2019a. The effectiveness of lidar remote sensing for monitoring forest cover attributes and landscape restoration. *Forest Ecology and Management* **438**: 34-43.

de Almeida DRA, Stark SC, Shao G, Schietti J, Nelson BW, Silva CA, Gorgens EB, Valbuena R, Papa DdA, Brancalion PHS. 2019b. Optimizing the Remote Detection of Tropical Rainforest Structure with Airborne Lidar: Leaf Area Profile Sensitivity to Pulse Density and Spatial Sampling. *Remote Sensing* **11**(1): 92.

De Faria BL, Marano G, Piponiot C, Silva CA, Dantas VdL, Rattis L, Rech AR, Collalti A. 2021. Model-Based Estimation of Amazonian Forests Recovery Time after Drought and Fire Events. *Forests* **12**(1): 8.

De Frenne P, Lenoir J, Luoto M, Scheffers BR, Zellweger F, Aalto J, Ashcroft MB, Christiansen DM, Decocq G, De Pauw K, et al. 2021. Forest microclimates and climate change: Importance, drivers and future research agenda. *Global Change Biology* **27**(11): 2279-2297.

de Melo Carvalho M, de Holanda Nunes Maia A, Madari B, Bastiaans L, Van Oort P, Heinemann A, Soler da Silva M, Petter F, Marimon Jr B, Meinke H. 2014. Biochar increases plant-available water in a sandy loam soil under an aerobic rice crop system. *Solid Earth* **5**(2): 939-952.

de Oliveira EA, Marimon-Junior BH, Marimon BS, Iriarte J, Morandi PS, Maezumi SY, Nogueira DS, Aragão LEOC, da Silva IB, Feldpausch TR. 2020. Legacy of Amazonian Dark Earth soils on forest structure and species composition. *Global Ecology and Biogeography* **29**(9): 1458-1473.

Denevan WM. 1992. *The native population of the Americas in 1492*. Madison: Univ. of Wis. Press.

Denevan WM. 1996. A Bluff Model of Riverine Settlement in Prehistoric Amazonia. *Annals of the Association of American Geographers* **86**(4): 654-681.

Denslow JS, Chaverri S LG, Vargas R O. 2019. Patterns in a species-rich tropical understory plant community. *Biotropica* **51**(5): 664-673.

Dent DH, Joseph Wright S. 2009. The future of tropical species in secondary forests: A quantitative review. *Biological Conservation* **142**(12): 2833-2843.

Detto M, Asner GP, Muller-Landau HC, Sonnentag O. 2015. Spatial variability in tropical forest leaf area density from multireturn lidar and modeling. *Journal of Geophysical Research: Biogeosciences* **120**(2): 294-309.

Doughty CE, Metcalfe DB, da Costa MC, de Oliveira AAR, Neto GFC, Silva JA, Aragão LEOC, Almeida SS, Quesada CA, Girardin CAJ, et al. 2014. The production, allocation and cycling of carbon in a forest on fertile terra preta soil in eastern Amazonia compared with a forest on adjacent infertile soil. *Plant Ecology & Diversity* **7**(1-2): 41-53.

Driscoll DA, Armenteras D, Bennett AF, Brotons L, Clarke MF, Doherty TS, Haslem A, Kelly LT, Sato CF, Sitters H, et al. 2021. How fire interacts with habitat loss and fragmentation. *Biological Reviews* **96**(3): 976-998.

Dubayah R, Blair JB, Goetz S, Fatoyinbo L, Hansen M, Healey S, Hofton M, Hurtt G, Kellner J, Luthcke S. 2020. The Global Ecosystem Dynamics Investigation: High-resolution laser ranging of the Earth's forests and topography. *Science of remote sensing* **1**: 100002.

Dubreuil V, Debortoli N, Funatsu B, Nédélec V, Durieux L. 2012. Impact of land-cover change in the Southern Amazonia climate: a case study for the region of Alta Floresta, Mato Grosso, Brazil. *Environmental Monitoring and Assessment* **184**(2): 877-891.

Duffy PB, Brando P, Asner GP, Field CB. 2015. Projections of future meteorological drought and wet periods in the Amazon. *Proceedings of the National Academy of Sciences* **112**(43): 13172-13177.

EBA. 2016. EBA—Estimativa de biomassa na Amazônia. Melhoria dos métodos de estimativa de biomassa e de modelos de estimativa de emissões por mudança de uso da terra.

Erickson CL 2008. Amazonia: The Historical Ecology of a Domesticated Landscape. In: Silverman H, Isbell WH eds. *The Handbook of South American Archaeology*. New York, NY: Springer New York, 157-183.

Esquivel-Muelbert A, Phillips OL, Brienen RJW, Fauset S, Sullivan MJP, Baker TR, Chao K-J, Feldpausch TR, Gloor E, Higuchi N, et al. 2020. Tree mode of death and mortality risk factors across Amazon forests. *Nature Communications* **11**(1): 5515.

Fearnside PM. 2012. Brazil's Amazon forest in mitigating global warming: unresolved controversies. *Climate Policy* **12**(1): 70-81.

Fearnside PM, Guimaraes WM. 1996. Carbon uptake by secondary forests in Brazilian Amazonia. *Forest Ecology and Management* **80**(1-3): 35-46.

Feldpausch TR, Banin L, Phillips OL, Baker TR, Lewis SL, Quesada CA, Affum-Baffoe K, Arets EJMM, Berry NJ, Bird M, et al. 2011. Height-diameter allometry of tropical forest trees. *Biogeosciences* **8**(5): 1081-1106.

Feldpausch TR, Carvalho L, Macario KD, Ascough PL, Flores CF, Coronado ENH, Kalamandeen M, Phillips OL, Staff RA. 2022. Forest Fire History in Amazonia Inferred From Intensive Soil Charcoal Sampling and Radiocarbon Dating. *Frontiers in Forests and Global Change* **5**.

Feldpausch TR, Lloyd J, Lewis SL, Brienen RJW, Gloor M, Mendoza AM, Lopez-Gonzalez G, Banin L, Abu Salim K, Affum-Baffoe K, et al. 2012. Tree height integrated into pantropical forest biomass estimates. *Biogeosci* **9**(8): 3381-3403.

Feldpausch TR, Phillips OL, Brienen RJW, Gloor E, Lloyd J, Lopez-Gonzalez G, Monteagudo-Mendoza A, Malhi Y, Alarcon A, Alvarez Davila E, et al. 2016. Amazon forest response to repeated droughts. *Global Biogeochemical Cycles* **30**(7): 964-982.

Feldpausch TR, Prates Clark CC, Fernandes ECM, Riha SJ. 2007. Secondary forest growth deviation from chronosequence predictions in central Amazonia. *Global Change Biology* **13**(5): 967-979.

Feldpausch TR, Riha SJ, Fernandes ECM, Wandelli EV. 2005. Development of forest structure and leaf area in secondary forests regenerating on abandoned pastures in central Amazônia. *Earth Interactions [available online at http://earthinteractions.org/]* **9**: 1-21.

Feldpausch TR, Rondon MA, Fernandes ECM, Riha SJ, Wandelli E. 2004. Carbon and nutrient accumulation in secondary forests regenerating on pastures in central Amazonia. *ECOLOGICAL APPLICATIONS* **14**: S164-S176.

Field CB, Behrenfeld MJ, Randerson JT, Falkowski P. 1998. Primary Production of the Biosphere: Integrating Terrestrial and Oceanic Components. *Science* **281**(5374): 237-240.

Finlayson C, Roopsind A, Griscom BW, Edwards DP, Freckleton RP. 2022. Removing climbers more than doubles tree growth and biomass in degraded tropical forests. *Ecology and Evolution* **12**(3): e8758.

ForestPlots.net, Blundo C, Carilla J, Grau R, Malizia A, Malizia L, Osinaga-Acosta O, Bird M, Bradford M, Catchpole D, et al. 2021. Taking the pulse of Earth's tropical forests using networks of highly distributed plots. *Biological Conservation* **260**: 108849.

França FM, Benkwitt CE, Peralta G, Robinson JPW, Graham NAJ, Tylianakis JM, Berenguer E, Lees AC, Ferreira J, Louzada J, et al. 2020. Climatic and local stressor interactions threaten tropical forests and coral reefs. *Philosophical Transactions of the Royal Society B: Biological Sciences* **375**(1794): 20190116.

Franklin JF, Shugart H, Harmon ME. 1987. Tree death as an ecological process. *BioScience*: 550-556.

Funk C, Peterson P, Landsfeld M, Pedreros D, Verdin J, Shukla S, Husak G, Rowland J, Harrison L, Hoell A, et al. 2015. The climate hazards infrared precipitation with stations—a new environmental record for monitoring extremes. *Scientific Data* **2**(1): 150066.

Fyllas NM, Patiño S, Baker TR, Bielefeld Nardoto G, Martinelli LA, Quesada CA, Paiva R, Schwarz M, Horna V, Mercado LM, et al. 2009. Basin-wide variations in foliar properties of Amazonian forest: phylogeny, soils and climate. *Biogeosciences* **6**(11): 2677-2708.

Galvão LS, dos Santos JR, Roberts DA, Breunig FM, Toomey M, de Moura YM. 2011. On intra-annual EVI variability in the dry season of tropical forest: A case study with MODIS and hyperspectral data. *Remote Sensing of Environment* **115**(9): 2350-2359.

Gatti LV, Basso LS, Miller JB, Gloor M, Gatti Domingues L, Cassol HLG, Tejada G, Aragão LEOC, Nobre C, Peters W, et al. 2021. Amazonia as a carbon source linked to deforestation and climate change. *Nature* **595**(7867): 388-393.

Gatti LV, Gloor M, Miller JB, Doughty CE, Malhi Y, Domingues LG, Basso LS, Martinewski A, Correia CS, Borges VF, et al. 2014. Drought sensitivity of Amazonian carbon balance revealed by atmospheric measurements. *Nature* **506**(7486): 76-80.

Gerwing JJ, Vidal E. 2002. Changes in liana abundance and species diversity eight years after liana cutting and logging in an eastern Amazonian forest. *Conservation Biology* **16**(2): 544-548.

Giglio L, Boschetti L, Roy DP, Humber ML, Justice CO. 2018. The Collection 6 MODIS burned area mapping algorithm and product. *Remote Sensing of Environment* **217**: 72-85.

Giglio L, Justice, C., Boschetti, L., Roy, D. 2015. MCD64A1 MODIS/Terra+Aqua Burned Area Monthly L3 Global 500m SIN Grid V006 [Data set].In DAAC NELP.

Giongo M, Koehler HS, do Amaral Machado S, Kirchner FF, Marchetti M. 2010. LiDAR: princípios e aplicações florestais. *Pesquisa Florestal Brasileira* **30**(63): 231-231.

Glaser B. 2007. Prehistorically modified soils of central Amazonia: a model for sustainable agriculture in the twenty-first century. *Philosophical Transactions of the Royal Society B: Biological Sciences* **362**(1478): 187-196.

Glaser B, Balashov E, Haumaier L, Guggenberger G, Zech W. 2000. Black carbon in density fractions of anthropogenic soils of the Brazilian Amazon region. *Organic Geochemistry* **31**(7): 669-678.

Glaser B, Haumaier L, Guggenberger G, Zech W. 2001. The 'Terra Preta' phenomenon: a model for sustainable agriculture in the humid tropics. *Naturwissenschaften* **88**(1): 37-41.

Glaser B, Lehmann J, Zech W. 2002. Ameliorating physical and chemical properties of highly weathered soils in the tropics with charcoal - a review. *Biology and Fertility of Soils* **35**(4): 219-230.

Goetz SJ, Hansen M, Houghton RA, Walker W, Laporte N, Busch J. 2015. Measurement and monitoring needs, capabilities and potential for addressing reduced emissions from deforestation and forest degradation under REDD+. *Environmental Research Letters* **10**(12): 123001.

Gorgens EB, Nunes MH, Jackson T, Coomes D, Keller M, Reis CR, Valbuena R, Rosette J, de Almeida DRA, Gimenez B, et al. 2021. Resource availability and disturbance shape maximum tree height across the Amazon. *Global Change Biology* **27**(1): 177-189.

Goulart AC, Macario KD, Scheel-Ybert R, Alves EQ, Bachelet C, Pereira BB, Levis C, Marimon Junior BH, Marimon BS, Quesada CA, et al. 2017. Charcoal chronology of the Amazon forest: A record of biodiversity preserved by ancient fires. *Quaternary Geochronology* **41**: 180-186.

Greenwood S, Ruiz-Benito P, Martínez-Vilalta J, Lloret F, Kitzberger T, Allen CD, Fensham R, Laughlin DC, Kattge J, Bönisch G, et al. 2017. Tree mortality across biomes is promoted by drought intensity, lower wood density and higher specific leaf area. *Ecology Letters* **20**(4): 539-553.

Harris NL, Brown S, Hagen SC, Saatchi SS, Petrova S, Salas W, Hansen MC, Potapov PV, Lotsch A. 2012. Baseline Map of Carbon Emissions from Deforestation in Tropical Regions. *Science* **336**(6088): 1573-1576.

Hassebo Y. 2012. Active remote sensing: LiDAR SNR improvements. *Remote Sens. Adv. Tech. Platf*.

Haugaasen T, Barlow J, Peres CA. 2003. Surface wildfires in central Amazonia: Short-term impact on forest structure and carbon loss. *Forest Ecology and Management* **179**: 321-331.

Heinrich VHA, Dalagnol R, Cassol HLG, Rosan TM, de Almeida CT, Silva Junior CHL, Campanharo WA, House JI, Sitch S, Hales TC, et al. 2021. Large carbon sink potential of secondary forests in the Brazilian Amazon to mitigate climate change. *Nature Communications* **12**(1): 1785.

Hubau W, Lewis SL, Phillips OL, Affum-Baffoe K, Beeckman H, Cuní-Sanchez A, Daniels AK, Ewango CEN, Fauset S, Mukinzi JM, et al. 2020. Asynchronous

carbon sink saturation in African and Amazonian tropical forests. *Nature* **579**(7797): 80-87.

Huete A, Didan K, Miura T, Rodriguez EP, Gao X, Ferreira LG. 2002. Overview of the radiometric and biophysical performance of the MODIS vegetation indices. *Remote Sensing of Environment* **83**(1): 195-213.

Hunter MO, Keller M, Morton D, Cook B, Lefsky M, Ducey M, Saleska S, de Oliveira Jr RC, Schietti J. 2015. Structural dynamics of tropical moist forest gaps. *PLOS ONE* **10**(7): e0132144.

Husson F, Josse J, Le S, Mazet J, Husson MF. 2016. Package 'FactoMineR'. *An R package* **96**: 698.

INPE 2021. Database of wildfires detected by satellites.

IPCC. 2006. (eds. Eggleston HS, Buendia, L., Miwa, K., Ngara, T. &, Tanabe K, eds. Chapter 4 Forest Land. In IPCC Guidelines for National Greenhouse Gas Inventories.

IPCC. 2022. Climate Change 2022: Impacts, Adaptation, and Vulnerability. Contribution of Working Group II to the Sixth Assessment Report of the Intergovernmental Panel on Climate Change[H.-O. Pörtner, D.C. Roberts, M. Tignor, E.S. Poloczanska, K. Mintenbeck, A. Alegría, M. Craig, S. Langsdorf, S. Löschke, V. Möller, A. Okem, B. Rama (eds.)]. Cambridge University Press.

Jakovac, Peña-Claros M, Kuyper T, Bongers F. 2015. Loss of secondary-forest resilience by land-use intensification in the Amazon. *Journal of Ecology* **103**(1): 67-77.

Jakovac CC, Junqueira AB, Crouzeilles R, Peña-Claros M, Mesquita RCG, Bongers F. 2021. The role of land-use history in driving successional pathways and its implications for the restoration of tropical forests. *Biological Reviews* **96**(4): 1114-1134.

Jansen PA, Meer PJVd, Bongers F. 2008. SPATIAL CONTAGIOUSNESS OF CANOPY DISTURBANCE IN TROPICAL RAIN FOREST: AN INDIVIDUAL-TREE-BASED TEST. *Ecology* **89**(12): 3490-3502.

John R, Dalling JW, Harms KE, Yavitt JB, Stallard RF, Mirabello M, Hubbell SP, Valencia R, Navarrete H, Vallejo M. 2007. Soil nutrients influence spatial distributions of tropical tree species. *Proceedings of the National Academy of Sciences* **104**(3): 864-869.

Johnson MO, Galbraith D, Gloor M, De Deurwaerder H, Guimberteau M, Rammig A, Thonicke K, Verbeeck H, Randow C, Monteagudo A, et al. 2016. Variation in stem mortality rates determines patterns of above-ground biomass in Amazonian forests: implications for dynamic global vegetation models. *Global Change Biology* **22**(12): 3996-4013.

Karavani A, Boer MM, Baudena M, Colinas C, Díaz-Sierra R, Pemán J, de Luis M, Enríquez-de-Salamanca Á, Resco de Dios V. 2018. Fire-induced deforestation in drought-prone Mediterranean forests: drivers and unknowns from leaves to communities. *Ecological Monographs* **88**(2): 141-169.

Kassambara A, Mundt F. 2017. Factoextra: extract and visualize the results of multivariate data analyses. *R package version* **1**(5): 337-354.

Kauffman JB. 1991. Survival by sprouting following fire in tropical forests of the eastern Amazon. *Biotropica* **23**(3): 219-224.

Koele N, Bird M, Haig J, Marimon-Junior BH, Marimon BS, Phillips OL, de Oliveira EA, Quesada CA, Feldpausch TR. 2017. Amazon Basin forest pyrogenic carbon stocks: First estimate of deep storage. *Geoderma* **306**: 237-243.

Langenbrunner B, Pritchard MS, Kooperman GJ, Randerson JT. 2019. Why Does Amazon Precipitation Decrease When Tropical Forests Respond to Increasing CO2? *Earth's Future* **7**(4): 450-468.

Laurance WF, Nascimento HEM, Laurance SG, Andrade A, Ribeiro J, Giraldo JP, Lovejoy TE, Condit R, Chave J, Harms KE, et al. 2006a. Rapid decay of tree-community composition in Amazonian forest fragments. *Proceedings of the National Academy of Sciences of the United States of America* **103**(50): 19010-19014.

Laurance WF, Nascimento HEM, Laurance SG, Andrade AC, Fearnside PM, Ribeiro JEL, Capretz RL. 2006b. Rain forest fragmentation and the proliferation of successional trees. *Ecology* **87**(2): 469-482.

Le Roux R, Wagner F, Blanc L, Betbeder J, Gond V, Dessard H, Funatzu B, Bourgoin C, Cornu G, Herault B, et al. 2022. How wildfires increase sensitivity of Amazon forests to droughts. *Environmental Research Letters* **17**(4): 044031.

Lefsky MA, Cohen WB, Parker GG, Harding DJ. 2002. Lidar remote sensing for ecosystem studies: Lidar, an emerging remote sensing technology that directly measures the three-dimensional distribution of plant canopies, can accurately estimate vegetation structural attributes and should be of particular interest to forest, landscape, and global ecologists. *BioScience* **52**(1): 19-30.

Lehmann J, Skjemstad J, Sohi S, Carter J, Barson M, Falloon P, Coleman K, Woodbury P, Krull E. 2008. Australian climate-carbon cycle feedback reduced by soil black carbon. *Nature Geoscience* **1**(12): 832-835.

Leitold V, Keller M, Morton DC, Cook BD, Shimabukuro YE. 2015. Airborne lidar-based estimates of tropical forest structure in complex terrain: opportunities and trade-offs for REDD+. *Carbon balance and management* **10**(1): 1-12.

Leitold V, Morton DC, Longo M, dos-Santos MN, Keller M, Scaranello M. 2018. El Niño drought increased canopy turnover in Amazon forests. *New Phytologist* **219**(3): 959-971.

Lennox GD, Gardner TA, Thomson JR, Ferreira J, Berenguer E, Lees AC, Mac Nally R, Aragão LEOC, Ferraz SFB, Louzada J, et al. 2018. Second rate or a second chance? Assessing biomass and biodiversity recovery in regenerating Amazonian forests. *Global Change Biology* **24**(12): 5680-5694.

Levis C, Costa FR, Bongers F, Pena-Claros M, Clement CR, Junqueira AB, Neves EG, Tamanaha EK, Figueiredo FO, Salomao RP, et al. 2017. Persistent effects of pre-Columbian plant domestication on Amazonian forest composition. *Science* **355**(6328): 925-931.

Liang B, Lehmann J, Solomon D, Kinyangi J, Grossman J, O'Neill B, Skjemstad JO, Thies J, Luizão FJ, Petersen J, et al. 2006. Black carbon increases cation exchange capacity in soils. *Soil Science Society of America Journal* **70**(5): 1719-1730.

Lindenmayer DB, Laurance WF. 2017. The ecology, distribution, conservation and management of large old trees. *Biological Reviews* **92**(3): 1434-1458.

Lindenmayer DB, Laurance WF, Franklin JF. 2012. Global Decline in Large Old Trees. *Science* **338**(6112): 1305-1306.

Llopart M, Reboita MS, Coppola E, Giorgi F, Da Rocha RP, De Souza DO. 2018. Land use change over the Amazon Forest and its impact on the local climate. *Water* **10**(2): 149.

Longo M, Keller M, dos-Santos MN, Leitold V, Pinage ER, Baccini A, Saatchi S, Nogueira EM, Batistella M, Morton DC. 2016. Aboveground biomass

variability across intact and degraded forests in the Brazilian Amazon. *Global Biogeochemical Cycles* **30**(11): 1639-1660.

Lopes AV, Chiang JCH, Thompson SA, Dracup JA. 2016. Trend and uncertainty in spatial-temporal patterns of hydrological droughts in the Amazon basin. *Geophysical Research Letters* **43**(7): 3307-3316.

Lopez-Gonzalez G, Lewis S, Burkitt M, Phillips O. 2011. ForestPlots.net: A web application and research tool to manage and analyse tropical forest plot data. *Journal of Vegetation Science* **22**: 610-613.

Lu D. 2006. The potential and challenge of remote sensing-based biomass estimation. *International Journal of Remote Sensing* **27**: 1297-1328.

Lu D, Chen Q, Wang G, Liu L, Li G, Moran E. 2016. A survey of remote sensing-based aboveground biomass estimation methods in forest ecosystems. *International Journal of Digital Earth* **9**(1): 63-105.

Major J, Lehmann J, Rondon M, Goodale C. 2010. Fate of soil-applied black carbon: downward migration, leaching and soil respiration. *Global Change Biology* **16**(4): 1366-1379.

Malhi Y, Girardin C, Metcalfe DB, Doughty CE, Aragão LEOC, Rifai SW, Oliveras I, Shenkin A, Aguirre-Gutiérrez J, Dahlsjö CAL, et al. 2021. The Global Ecosystems Monitoring network: Monitoring ecosystem productivity and carbon cycling across the tropics. *Biological Conservation* **253**: 108889.

Malhi Y, Roberts JT, Betts RA, Killeen TJ, Li WH, Nobre CA. 2008. Climate change, deforestation, and the fate of the Amazon. *Science* **319**(5860): 169-172.

MapBiomas 2021. MapBiomas Amazonia Project - Collection 3 of Amazonian Annual Land Cover & Land Use Map Series. *MapBiomas Amazonia Project is a multi-institutional initiative of RAISG to generate the annual land cover and land use maps using an automated classification of satellite images. The complete description of the project can be found at http://amazonia.mapbiomas.org/".*

Marengo JA, Espinoza JC. 2016. Extreme seasonal droughts and floods in Amazonia: causes, trends and impacts. *International Journal of Climatology* **36**(3): 1033-1050.

Massi KG, Bird M, Marimon BS, Marimon BH, Nogueira DS, Oliveira EA, Phillips OL, Quesada CA, Andrade AS, Brienen RJW, et al. 2017. Does soil pyrogenic carbon determine plant functional traits in Amazon Basin forests? *Plant Ecology* **218**(9): 1047-1062.

Mata S, Braga JMA, Moser P, Sartori RA, Sánchez-Tapia A, Sansevero JBB. 2022. Forever young: arrested succession in communities subjected to recurrent fires in a lowland tropical forest. *Plant Ecology* **223**(6): 659-670.

McDowell N, Allen CD, Anderson-Teixeira K, Brando P, Brienen R, Chambers J, Christoffersen B, Davies S, Doughty C, Duque A, et al. 2018. Drivers and mechanisms of tree mortality in moist tropical forests. *New Phytologist* **219**(3): 851-869.

McDowell NG. 2011. Mechanisms Linking Drought, Hydraulics, Carbon Metabolism, and Vegetation Mortality *Plant Physiology* **155**(3): 1051-1059.

McMichael C, Palace M, Bush M, Braswell B, Hagen S, Neves E, Silman M, Tamanaha E, Czarnecki C. 2014. Predicting pre-Columbian anthropogenic soils in Amazonia. *Proceedings of the Royal Society B: Biological Sciences* **281**(1777): 20132475.

McMichael CH, Correa-Metrio A, Bush MB. 2012. Pre-Columbian fire regimes in lowland tropical rainforests of southeastern Peru. *Palaeogeography, Palaeoclimatology, Palaeoecology* **342–343**(0): 73-83.

Meredith W, Ascough PL, Bird MI, Large DJ, Snape CE, Song J, Sun Y, Tilston EL. 2013. Direct evidence from hydropyrolysis for the retention of long alkyl moieties in black carbon fractions isolated by acidified dichromate oxidation. *Journal of Analytical and Applied Pyrolysis* **103**: 232-239.

Mesquita RCG, Ickes K, Ganade G, Williamson GB. 2001. Alternative successional pathways in the Amazon Basin. *Journal of Ecology* **89**(4): 528-537.

Metzger JP. 2003. Effects of slash-and-burn fallow periods on landscape structure. *Environmental Conservation* **30**(4): 325-333.

Milodowski DT, Coomes DA, Swinfield T, Jucker T, Riutta T, Malhi Y, Svátek M, Kvasnica J, Burslem DFRP, Ewers RM, et al. 2021. The impact of logging on vertical canopy structure across a gradient of tropical forest degradation intensity in Borneo. *Journal of Applied Ecology* **58**(8): 1764-1775.

Miranda AC, Miranda HS, Dias IdFO, Dias BFdS 1993. Soil and air temperatures during prescribed Cerrado fires in Central Brazil. 313-320.

Moura YMd, Balzter H, Galvão LS, Dalagnol R, Espírito-Santo F, Santos EG, Garcia M, Bispo PdC, Oliveira RC, Shimabukuro YE. 2020. Carbon Dynamics in a Human-Modified Tropical Forest: A Case Study Using Multi-Temporal LiDAR Data. *Remote Sensing* **12**(3): 430.

Nepstad DC, Tohver IM, Ray D, Moutinho P, Cardinot G. 2007. Mortality of large trees and lianas following experimental drought in an Amazon forest. *Ecology* **88**(9): 2259-2269.

Neves EG, Petersen JB, Bartone RN, Heckenberger MJ 2004. The timing of terra preta formation in the Central Amazon: archaeological data from three sites. *Amazonian Dark Earths: Explorations in Space and Time*: Springer, 125-134.

Neves EG, Petersen JB, Bartone RN, Silva CA 2003. Historical and socio-cultural origins of Amazonian dark earths. *Amazonian Dark Earths: Origins, Properties, and Management*: Kluwer Academic Publishers, 29-50.

Oliveira EA. 2017. *Efeito histórico de pertubações e do carbono pirogênico do solo na composição e estrutura das florestas na Amazônia.* Doutor em Biodiversidade e Conservação, Universidade do Estado de Mato Grosso Nova Xavantina-MT.

Oliveira RS, Costa FRC, van Baalen E, de Jonge A, Bittencourt PR, Almanza Y, Barros FdV, Cordoba EC, Fagundes MV, Garcia S, et al. 2019. Embolism resistance drives the distribution of Amazonian rainforest tree species along hydro-topographic gradients. *New Phytologist* **221**(3): 1457-1465.

Ordoñez JC, Van Bodegom PM, Witte JPM, Wright IJ, Reich PB, Aerts R. 2009. A global study of relationships between leaf traits, climate and soil measures of nutrient fertility. *Global Ecology and Biogeography* **18**(2): 137-149.

Pan Y, Birdsey RA, Fang J, Houghton R, Kauppi PE, Kurz WA, Phillips OL, Shvidenko A, Lewis SL, Canadell JG, et al. 2011. A large and persistent carbon sink in the world's forests. *Science* **333**(6045): 988-993.

Panisset JS, Libonati R, Gouveia CMP, Machado-Silva F, França DA, França JRA, Peres LF. 2018. Contrasting patterns of the extreme drought episodes of 2005, 2010 and 2015 in the Amazon Basin. *International Journal of Climatology* **38**(2): 1096-1104.

Paredes-Trejo F, Barbosa HA, Giovannettone J, Lakshmi Kumar TV, Thakur MK, de Oliveira Buriti C. 2021. Long-Term Spatiotemporal Variation of Droughts in the Amazon River Basin. *Water* **13**(3): 351.

Park A, Joaquin Justiniano M, Fredericksen TS. 2005. Natural regeneration and environmental relationships of tree species in logging gaps in a Bolivian tropical forest. *Forest Ecology and Management* **217**(2): 147-157.

Parra-Sanchez E, Banks-Leite C. 2022. Value of human-modified forests for the conservation of canopy epiphytes. *Biotropica* **n/a**(n/a).

Pausas JG, Keeley JE. 2009. A Burning Story: The Role of Fire in the History of Life. *BioScience* **59**(7): 593-601.

Paz-Rivera C, Putz FE. 2009. Anthropogenic soils and tree distributions in a lowland forest in Bolivia. *Biotropica* **41**(6): 665-675.

Pellegrini AFA, Refsland T, Averill C, Terrer C, Staver AC, Brockway DG, Caprio A, Clatterbuck W, Coetsee C, Haywood JD, et al. 2021. Decadal changes in fire frequencies shift tree communities and functional traits. *Nature Ecology & Evolution* **5**(4): 504-512.

Pessenda L, Valencia E, Aravena R, Telles E, Boulet R 1998. Paleoclimate studies in Brazil using carbon isotopes in soils In: Wasserman J, Silva-Filho E, Villas-Boas R eds. *Environmental Geochemistry in the Tropics*: Springer Berlin / Heidelberg, 7-16.

Pessôa ACM, Anderson LO, Carvalho NS, Campanharo WA, Junior CHLS, Rosan TM, Reis JBC, Pereira FRS, Assis M, Jacon AD, et al. 2020. Intercomparison of Burned Area Products and Its Implication for Carbon Emission Estimations in the Amazon. *Remote Sensing* **12**(23): 3864.

Petersen JB, Neves EG, Heckenberger MJ 2001. Chapter 3 - 'Gift from the past: Terra Preta and prehistoric Amerindian Occupation in Amazonia' [in] Unknown Amazon: culture in nature in ancient Brazil. In: McEwan C, Barreto C, Neves E eds. *Unknown Amazon: culture in nature in ancient Brazil*. London: British Museum Press, 86-107.

Philipson CD, Cutler MEJ, Brodrick PG, Asner GP, Boyd DS, Costa PM, Fiddes J, Foody GM, Heijden GMFvd, Ledo A, et al. 2020. Active restoration accelerates the carbon recovery of human-modified tropical forests. *Science* **369**(6505): 838-841.

Phillips OL, Aragao LE, Lewis SL, Fisher JB, Lloyd J, Lopez-Gonzalez G, Malhi Y, Monteagudo A, Peacock J, Quesada CA, et al. 2009a. Drought sensitivity of the Amazon rainforest. *Science* **323**(5919): 1344-1347.

Phillips OL, Baker T, Feldpausch T, Brienen R. 2009b. Field manual for establishment and remeasurement (RAINFOR).

Phillips OL, Baker TR, Arroyo L, Higuchi N, Killeen TJ, Laurance WF, Lewis SL, Lloyd J, Malhi Y, Monteagudo A, et al. 2004. Pattern and process in Amazon tree turnover, 1976-2001. *Philos Trans R Soc Lond B Biol Sci* **359**(1443): 381-407.

Phillips OL, Lewis SL, Baker TR, Chao KJ, Higuchi N. 2008. The changing Amazon forest. *Philosophical Transactions of the Royal Society of London B Biological Sciences* **363**(1498): 1819-1827.

Phillips OL, van der Heijden G, Lewis SL, Lopez-Gonzalez G, Aragao LE, Lloyd J, Malhi Y, Monteagudo A, Almeida S, Davila EA, et al. 2010. Drought-mortality relationships for tropical forests. *New Phytologist* **187**(3): 631-646.

Pivello V. 2011. *The Use of Fire in the Cerrado and Amazonian Rainforests of Brazil: Past and Present*.

Pontes-Lopes A. 2021. *Remote Sensing for monitoring fire-affected forests in the Central Amazon.* Doctorate in Remote Sensing, Instituto Nacional de Pesquisas Espaciais São José dos Campos.

Pontes-Lopes A, Silva CVJ, Barlow J, Rincón LM, Campanharo WA, Nunes CA, de Almeida CT, Silva Júnior CHL, Cassol HLG, Dalagnol R, et al. 2021. Drought-driven wildfire impacts on structure and dynamics in a wet Central Amazonian forest. *Proceedings of the Royal Society B: Biological Sciences* **288**(1951): 20210094.

Poorter L, Bongers F, Aide TM, Almeyda Zambrano AM, Balvanera P, Becknell JM, Boukili V, Brancalion PH, Broadbent EN, Chazdon RL, et al. 2016. Biomass resilience of Neotropical secondary forests. *Nature* **530**(7589): 211-214.

Poorter L, Craven D, Jakovac CC, Sande MTvd, Amissah L, Bongers F, Chazdon RL, Farrior CE, Kambach S, Meave JA, et al. 2021. Multidimensional tropical forest recovery. *Science* **374**(6573): 1370-1376.

Power M, Mayle F, Bartlein P, Marlon J, Anderson R, Behling H, Brown K, Carcaillet C, Colombaroli D, Gavin D, et al. 2012. Climatic control of the biomass-burning decline in the Americas after AD 1500. *The Holocene* **23**(1): 3-13.

Prestes NCCdS, Massi KG, Silva EA, Nogueira DS, de Oliveira EA, Freitag R, Marimon BS, Marimon-Junior BH, Keller M, Feldpausch TR. 2020. Fire Effects on Understory Forest Regeneration in Southern Amazonia. *Frontiers in Forests and Global Change* **3**(10).

Preston C, Schmidt M. 2006. Black (pyrogenic) carbon: a synthesis of current knowledge and uncertainties with special consideration of boreal regions. *Biogeosciences* **3**(4): 397-420.

Pugh TAM, Rademacher T, Shafer SL, Steinkamp J, Barichivich J, Beckage B, Haverd V, Harper A, Heinke J, Nishina K, et al. 2020. Understanding the uncertainty in global forest carbon turnover. *Biogeosciences* **17**(15): 3961-3989.

Quesada CA, Lloyd J, Schwarz M, Patiño S, Baker TR, Czimczik C, Fyllas NM, Martinelli L, Nardoto GB, Schmerler J, et al. 2010. Variations in chemical and physical properties of Amazon forest soils in relation to their genesis. *Biogeosciences* **7**(5): 1515-1541.

Quesada CA, Paz C, Oblitas Mendoza E, Phillips OL, Saiz G, Lloyd J. 2020. Variations in soil chemical and physical properties explain basin-wide Amazon forest soil carbon concentrations. *SOIL* **6**(1): 53-88.

Quesada CA, Phillips OL, Schwarz M, Czimczik CI, Baker TR, Patino S, Fyllas NM, Hodnett MG, Herrera R, Almeida S, et al. 2012. Basin-wide variations in Amazon forest structure and function are mediated by both soils and climate. *Biogeosciences* **9**(6): 2203-2246.

R Core Team 2020. R: A Language and Environment for Statistical Computing. R Foundation for Statistical Computing.

Randerson JT, Chen Y, van der Werf GR, Rogers BM, Morton DC. 2012. Global burned area and biomass burning emissions from small fires. *Journal of Geophysical Research: Biogeosciences* **117**(G4).

Rappaport DI, Morton DC, Longo M, Keller M, Dubayah R, dos-Santos MN. 2018. Quantifying long-term changes in carbon stocks and forest structure from Amazon forest degradation. *Environmental Research Letters* **13**(6): 065013.

Ray D, Nepstad D, Moutinho P. 2005. MICROMETEOROLOGICAL AND CANOPY CONTROLS OF FIRE SUSCEPTIBILITY IN A FORESTED AMAZON LANDSCAPE. *ECOLOGICAL APPLICATIONS* **15**(5): 1664-1678.

Rehn E, Rowe C, Ulm S, Woodward C, Bird M. 2021. A late-Holocene multiproxy fire record from a tropical savanna, eastern Arnhem Land, Northern Territory, Australia. *The Holocene* **31**(5): 870-883.

Reisser M, Purves RS, Schmidt MWI, Abiven S. 2016. Pyrogenic Carbon in Soils: A Literature-Based Inventory and a Global Estimation of Its Content in Soil Organic Carbon and Stocks. *Frontiers in Earth Science* **4**(80).

Requena Suarez D, Rozendaal DMA, De Sy V, Phillips OL, Alvarez-Dávila E, Anderson-Teixeira K, Araujo-Murakami A, Arroyo L, Baker TR, Bongers F, et al. 2019. Estimating aboveground net biomass change for tropical and subtropical forests: Refinement of IPCC default rates using forest plot data. *Global Change Biology* **25**(11): 3609-3624.

Richards PW. 1973. The tropical rain forest. *Scientific American* **229**(6): 58-68.

Ricklefs RE. 1977. Environmental heterogeneity and plant species diversity: a hypothesis. *The American Naturalist* **111**(978): 376-381.

Roberts J, Cabral OM, De Aguiar LF. 1990. Stomatal and boundary-layer conductances in an Amazonian terra firme rain forest. *Journal of Applied Ecology*: 336-353.

Rowland L, da Costa AC, Galbraith DR, Oliveira RS, Binks OJ, Oliveira AA, Pullen AM, Doughty CE, Metcalfe DB, Vasconcelos SS, et al. 2015. Death from drought in tropical forests is triggered by hydraulics not carbon starvation. *Nature* **528**(7580): 119-122.

Rowland L, da Costa ACL, Oliveira AAR, Almeida SS, Ferreira LV, Malhi Y, Metcalfe DB, Mencuccini M, Grace J, Meir P. 2018. Shock and stabilisation following long-term drought in tropical forest from 15 years of litterfall dynamics. *Journal of Ecology* **106**(4): 1673-1682.

Rozendaal DMA, Bongers F, Aide TM, Alvarez-Dávila E, Ascarrunz N, Balvanera P, Becknell JM, Bentos TV, Brancalion PHS, Cabral GAL, et al. 2019. Biodiversity recovery of Neotropical secondary forests. *Science Advances* **5**(3): eaau3114.

Rumpel C, Chaplot V, Planchon O, Bernadou J, Valentin C, Mariotti A. 2006. Preferential erosion of black carbon on steep slopes with slash and burn agriculture. *CATENA* **65**(1): 30-40.

Ryan MG, Phillips N, Bond BJ. 2006. The hydraulic limitation hypothesis revisited. *Plant, Cell & Environment* **29**(3): 367-381.

Saatchi S, Asefi-Najafabady S, Malhi Y, Aragao LE, Anderson LO, Myneni RB, Nemani R. 2013. Persistent effects of a severe drought on Amazonian forest canopy. *Proceedings of the National Academy of Sciences of the United States of America* **110**(2): 565-570.

Saiz G, Goodrick I, Wurster CM, Zimmermann M, Nelson PN, Bird MI. 2014. Charcoal re-combustion efficiency in tropical savannas. *Geoderma* **219-220**: 40-45.

Saiz G, Wynn J, Wurster C, Goodrick I, Nelson P, Bird M. 2015. *Pyrogenic carbon from tropical savanna burning: Production and stable isotope composition*.

Salati E, Vose PB 1986. The Water Cycle in Tropical Forests, with Special Reference to the Amazon. In: Marini-Bettòlo GB ed. *Studies in Environmental Science*: Elsevier, 623-648.

Salguero-Gómez R, Jones OR, Jongejans E, Blomberg SP, Hodgson DJ, Mbeau-Ache C, Zuidema PA, De Kroon H, Buckley YM. 2016. Fast–slow continuum and reproductive strategies structure plant life-history variation worldwide. *Proceedings of the National Academy of Sciences* **113**(1): 230-235.

Sanford RL, Jr., Saldarriaga J, Clark KE, Uhl C, Herrera R. 1985. Amazon rain-forest fires. *Science* **227**(4682): 53-55.

Santos GM, Gomes PRS, Anjos RM, Cordeiro RC, Turcq BJ, Sifeddine A, di Tada ML, Cresswell RG, Fifield LK. 2000. 14C AMS dating of fires in the central Amazon rain forest. *Nuclear Instr Meth Physics Res Sec B: Beam Inter Mat Atoms* **172**(1-4): 761-766.

Sato LY, Gomes VCF, Shimabukuro YE, Keller M, Arai E, dos-Santos MN, Brown IF. 2016. Post-Fire Changes in Forest Biomass Retrieved by Airborne LiDAR in Amazonia. *Remote Sensing* **8**(10): 839.

Schmidt MWI, Noack AG. 2000. Black carbon in soils and sediments: Analysis, distribution, implications, and current challenges. *Global Biogeochemical Cycles* **14**(3): 777-793.

Schnitzer SA, Dalling JW, Carson WP. 2000. The impact of lianas on tree regeneration in tropical forest canopy gaps: evidence for an alternative pathway of gap-phase regeneration. *Journal of Ecology* **88**(4): 655-666.

Scott AC, Glasspool IJ. 2006. The diversification of Paleozoic fire systems and fluctuations in atmospheric oxygen concentration. *Proc Natl Acad Sci U S A* **103**(29): 10861-10865.

Silva CA, Hudak AT, Vierling LA, Klauberg C, Garcia M, Ferraz A, Keller M, Eitel J, Saatchi S. 2017. Impacts of airborne lidar pulse density on estimating biomass stocks and changes in a selectively logged tropical forest. *Remote Sensing* **9**(10): 1068.

Silva CVJ, Aragao L, Barlow J, Espirito-Santo F, Young PJ, Anderson LO, Berenguer E, Brasil I, Foster Brown I, Castro B, et al. 2018. Drought-induced Amazonian wildfires instigate a decadal-scale disruption of forest carbon dynamics. *Philos Trans R Soc Lond B Biol Sci* **373**(1760): 20180043.

Silva CVJ, Aragão LEOC, Young PJ, Espirito-Santo F, Berenguer E, Anderson LO, Brasil I, Pontes-Lopes A, Ferreira J, Withey K, et al. 2020. Estimating the multi-decadal carbon deficit of burned Amazonian forests. *Environmental Research Letters* **15**(11): 114023.

Silva Junior, Aragão L, Anderson L, Fonseca M, Shimabukuro Y, Vancutsem C, Achard F, Beuchle R, Numata I, Silva C 2020a. Persistent collapse of biomass in Amazonian forest edges following deforestation leads to unaccounted carbon losses. Sci. Adv. 6, eaaz8360.

Silva Junior, Heinrich VHA, Freire ATG, Broggio IS, Rosan TM, Doblas J, Anderson LO, Rousseau GX, Shimabukuro YE, Silva CA, et al. 2020b. Benchmark maps of 33 years of secondary forest age for Brazil. *Scientific Data* **7**(1): 269.

Silva Junior CHL, Anderson LO, Silva AL, Almeida CT, Dalagnol R, Pletsch MAJS, Penha TV, Paloschi RA, Aragão LEOC. 2019. Fire Responses to the 2010 and 2015/2016 Amazonian Droughts. *Frontiers in Earth Science* **7**(97).

Silva Junior CHL, Aragão LEOC, Fonseca MG, Almeida CT, Vedovato LB, Anderson LO. 2018. Deforestation-Induced Fragmentation Increases Forest Fire Occurrence in Central Brazilian Amazonia. *Forests* **9**(6): 305.

Silveira MVF, Petri CA, Broggio IS, Chagas GO, Macul MS, Leite CCSS, Ferrari EMM, Amim CGV, Freitas ALR, Motta AZV, et al. 2020. Drivers of Fire Anomalies in the Brazilian Amazon: Lessons Learned from the 2019 Fire Crisis. *Land* **9**(12): 516.

Six J, Conant RT, Paul EA, Paustian K. 2002. Stabilization mechanisms of soil organic matter: Implications for C-saturation of soils. *Plant and Soil* **241**(2): 155-176.

Smith CC, Espírito-Santo FDB, Healey JR, Young PJ, Lennox GD, Ferreira J, Barlow J. 2020. Secondary forests offset less than 10% of deforestation-mediated carbon emissions in the Brazilian Amazon. *Global Change Biology* **26**(12): 7006-7020.

Soares CPB, Neto FP, Souza AL 2011. Biomassa e Carbono. In: UFV ed. *Dendrometria e Inventário Florestal*. Vicosa, 272.

Sørensen LH. 1972. Stabilization of newly formed amino acid metabolites in soil by clay minerals. *Soil Science* **114**(1): 5-11.

Souza AL, Soares CPB. 2013. *Florestas nativas: estrutura, dinamica e manejo*. Vicosa: UFV.

Spracklen D, Garcia-Carreras L. 2015. The impact of Amazonian deforestation on Amazon basin rainfall. *Geophysical Research Letters* **42**(21): 9546-9552.

Stark, Leitold V, Wu JL, Hunter MO, de Castilho CV, Costa FRC, McMahon SM, Parker GG, Shimabukuro MT, Lefsky MA, et al. 2012. Amazon forest carbon dynamics predicted by profiles of canopy leaf area and light environment. *Ecology Letters* **15**(12): 1406-1414.

Steininger MK. 2000. Secondary forest structure and biomass following short and extended land-use in central and southern Amazonia. *Journal of Tropical Ecology* **16**(5): 689-708.

Stephenson NL, van Mantgem PJ. 2005. Forest turnover rates follow global and regional patterns of productivity. *Ecology Letters* **8**(5): 524-531.

Sustainable-Landscapes. 2016. Sustainable landscapes.

Tang H, Dubayah R, Swatantran A, Hofton M, Sheldon S, Clark DB, Blair B. 2012. Retrieval of vertical LAI profiles over tropical rain forests using waveform lidar at La Selva, Costa Rica. *Remote Sensing of Environment* **124**: 242-250.

Ullrich A, Pfennigbauer M 2011. Echo digitization and waveform analysis in airborne and terrestrial laser scanning. *Photogrammetric Week*. 217-228.

Uriarte M, Schwartz N, Powers JS, Marín-Spiotta E, Liao W, Werden LK. 2016. Impacts of climate variability on tree demography in second growth tropical forests: the importance of regional context for predicting successional trajectories. *Biotropica* **48**(6): 780-797.

van Leeuwen M, Nieuwenhuis M. 2010. Retrieval of forest structural parameters using LiDAR remote sensing. *European Journal of Forest Research* **129**(4): 749-770.

Vasconcelos SSd, Fearnside PM, Graça PMLdA, Nogueira EM, Oliveira LCd, Figueiredo EO. 2013. Forest fires in southwestern Brazilian Amazonia: Estimates of area and potential carbon emissions. *Forest Ecology and Management* **291**: 199-208.

von Randow C, Manzi AO, Kruijt B, de Oliveira PJ, Zanchi FB, Silva RL, Hodnett MG, Gash JHC, Elbers JA, Waterloo MJ, et al. 2004. Comparative measurements and seasonal variations in energy and carbon exchange over forest and pasture in South West Amazonia. *Theoretical and Applied Climatology* **78**(1-3): 5-26.

Wagner W, Ullrich A, Melzer T, Briese C, Kraus K. 2004. *From single-pulse to full-waveform airborne laser scanners: Potential and practical challenges*: na.

Wandelli EV, Fearnside PM. 2015. Secondary vegetation in central Amazonia: Land-use history effects on aboveground biomass. *Forest Ecology and Management* **347**: 140-148.

Warton DI, Duursma RA, Falster DS, Taskinen S. 2012. smatr 3– an R package for estimation and inference about allometric lines. *Methods in Ecology and Evolution* **3**(2): 257-259.

Wilson JW. 1959. Analysis of the spatial distribution of foliage by two-dimensional point quadrats. *New Phytologist* **58**(1): 92-99.

Wright IJ, Reich PB, Westoby M, Ackerly DD, Baruch Z, Bongers F, Cavender-Bares J, Chapin T, Cornelissen JH, Diemer M. 2004. The worldwide leaf economics spectrum. *Nature* **428**(6985): 821-827.

Yang Y, Saatchi SS, Xu L, Yu Y, Choi S, Phillips N, Kennedy R, Keller M, Knyazikhin Y, Myneni RB. 2018. Post-drought decline of the Amazon carbon sink. *Nature Communications* **9**(1): 3172.

Zambiazi DC, Fantini AC, Piotto D, Siminski A, Vibrans AC, Oller DC, Piazza GE, Peña-Claros M. 2021. Timber stock recovery in a chronosequence of secondary forests in Southern Brazil: Adding value to restored landscapes. *Forest Ecology and Management* **495**: 119352.

Zarin DJ, Davidson EA, Brondizio E, Vieira ICG, Sa T, Feldpausch T, Schuur EA, Mesquita R, Moran E, Delamonica P, et al. 2005. Legacy of fire slows carbon accumulation in Amazonian forest regrowth. *Frontiers in Ecology and the Environment* **3**: 365-369.

Zhou T, Popescu S. 2019. waveformlidar: An R Package for Waveform LiDAR Processing and Analysis. *Remote Sensing* **11**(21): 2552.